

**Molecular Transformations Utilizing the Intrinsic
Functions of Intramolecular Ion Pairs as Bifunctional
Organic Base Catalysts**

分子内イオン対型分子に内在する二官能性有機塩基触媒の
機能を利用した分子変換反応の開発

TORII Masahiro

鳥居 雅弘

Department of Applied Chemistry, Graduate School of Engineering
Nagoya University

Contents

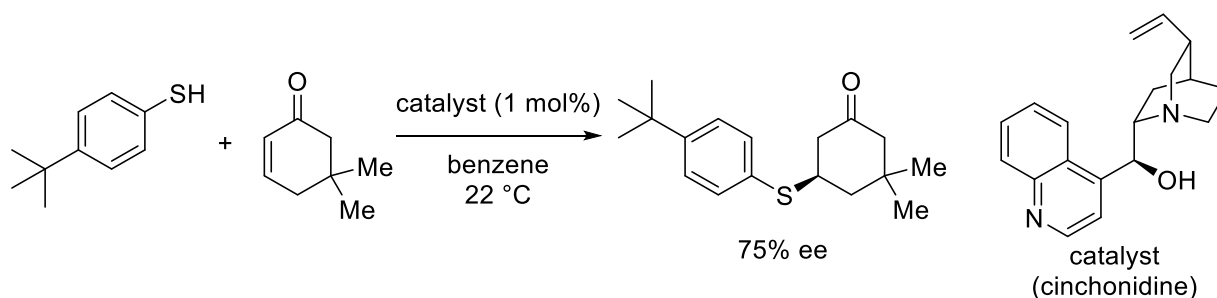
	Page
Chapter 1 General Introduction and Summary	1
Chapter 2 Chiral Ammonium Betaine-Catalyzed Asymmetric Mannich-Type Reaction of Oxindoles	21
Chapter 3 Stereoselective Aza-Henry Reaction of 3-Nitro Dihydro-2(3 <i>H</i>)-Quinolones with <i>N</i> -Boc Aldimines under the Catalysis of Chiral Ammonium Betaines	36
Chapter 4 Acridinium Betaines as a Single-Electron-Transfer Catalyst: Molecular Design and Application to the Dimerization of Oxindoles	52
Publication List	91
Acknowledgement	92

Chapter 1

General Introduction and Summary

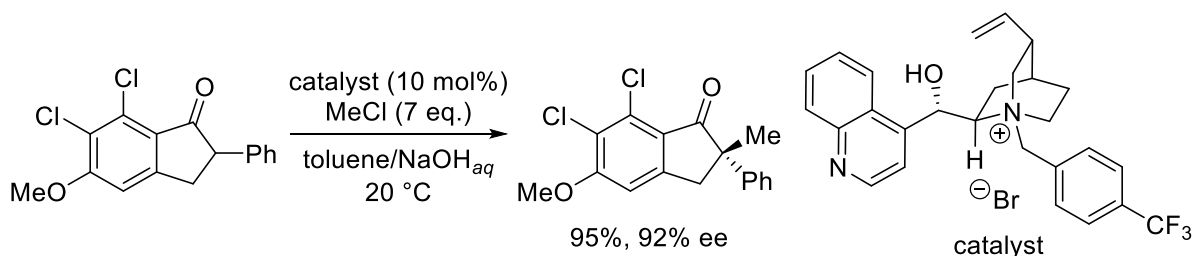
1.1 Chemistry of Asymmetric Catalysts

Controlling reactive species (such as enolate) generated from the deprotonation of the substrates have been considered as an important issue for the asymmetric reactions and catalytic activity. In the content, organic molecular catalysts, which are relatively easy to handle and do not use expensive rare metals have attracted attention as tool with low environmental burden in recent years. For example, chiral Brønsted base catalysis is a one typical tool of molecular transformations in the organic synthesis.¹ In 1981, Wynberg et al. first reported that natural cinchona-alkaloid effectively acts as an organic molecular catalyst in the conjugate addition reaction of aromatic thiols to cyclic ketones (Scheme 1).²



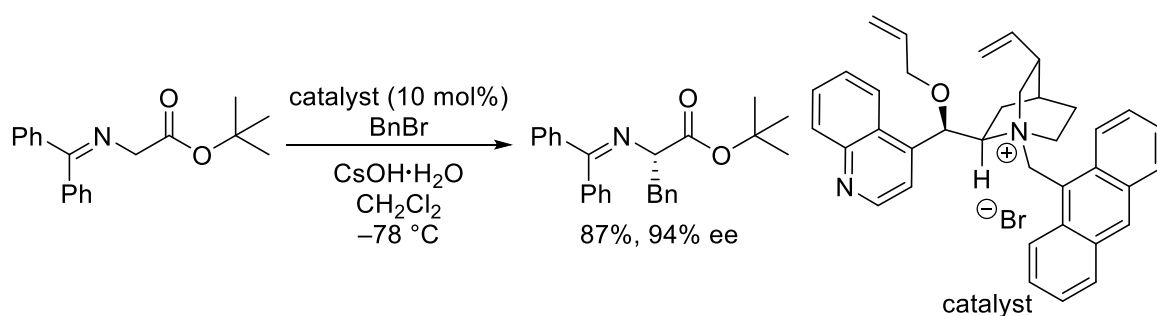
Scheme 1 First asymmetric reaction catalyzed by cinchona-alkaloid

As another approach of controlling reactive anionic species, phase-transfer reaction has been known as a method capable of precisely controlling a nucleophilic anion species. Especially, quaternary ammonium salts are established phase-transfer catalyst.³ In 1984, Merck first demonstrated the application of cinchona-alkaloid derived quaternary ammonium salt as excellent stereoselective phase-transfer catalyst (Scheme 2).⁴

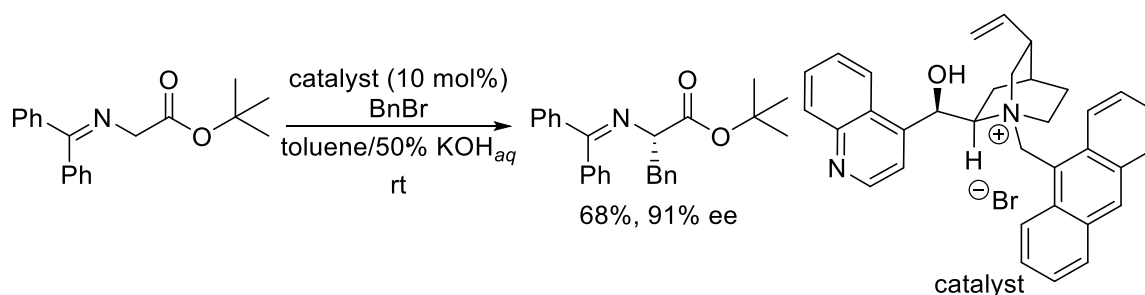


Scheme 2 Asymmetric phase-transfer alkylation reaction reported by Merck

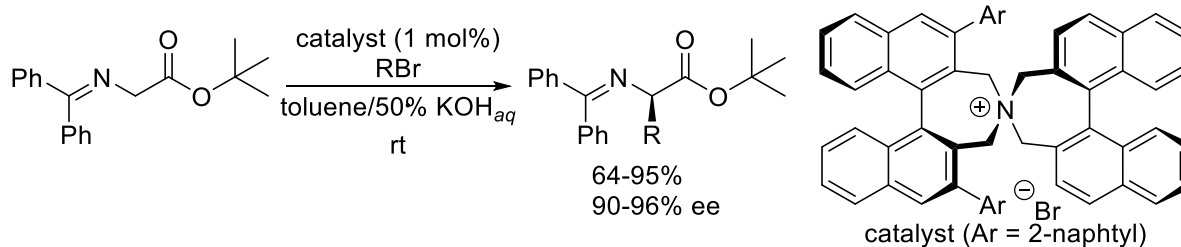
After 1990s, the chemistry of phase-transfer catalysis generated salient attention. Corey, Lygo, and Maruoka developed the asymmetric phase-transfer alkylation of Schiff bases.⁵⁻⁷ The product obtained was derivatized to natural and unnatural α -amino acid (Scheme 3-5).



Scheme 3 Asymmetric phase-transfer alkylation reaction reported by Corey



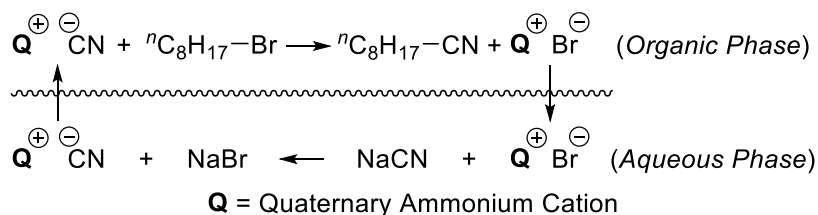
Scheme 4 Asymmetric phase-transfer alkylation reaction reported by Corey



Scheme 5 Asymmetric phase-transfer alkylation reaction reported by Maruoka

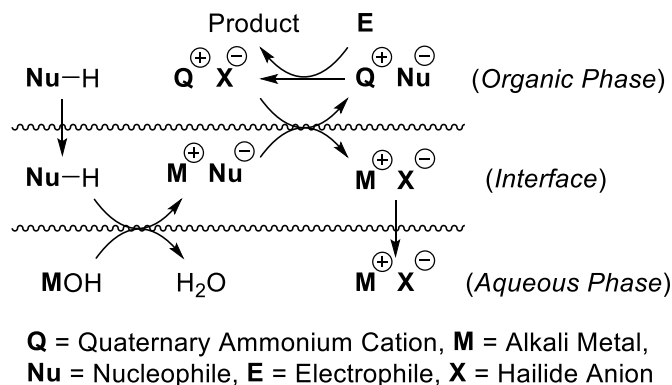
Mechanism of phase-transfer reaction has been proposed by Stark and Makosza. Stark suggested an extraction mechanism in 1971 (Figure 1)⁸. For example, a heterogeneous mixture of aqueous sodium cyanide and 1-bromooctane didn't react. However after the addition of a catalytic amount of quaternary ammonium bromide, the cyanation of 1-bromooctane proceeded. He proposed that the ion exchange between sodium cyanide and ammonium bromide occurred in aqueous phase. Then the organic-soluble ammonium cyanide transfers to organic phase and reacts with 1-bromooctane. Finally regenerated ammonium bromide gets transferred to aqueous phase.

Figure 1 Extraction Mechanism Proposed by Stark



On the other hand, Makosza suggested an interfacial mechanism (Figure 2)⁹. In a phase-transfer reaction, deprotonation of nucleophile was caused by metal hydroxide in interfacial area between organic phase and aqueous phase. Generated metal carboanion was extracted by phase-transfer catalysis to form ammonium carboanion in organic phase. Finally, ammonium carboanion reacts with electrophile to form product, and regenerate ammonium salt in organic phase.

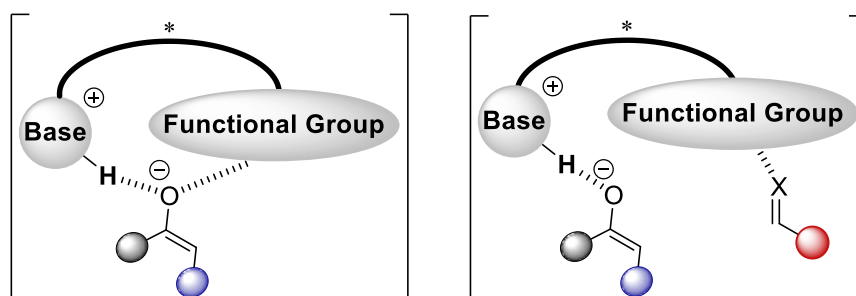
Figure 2 Interfacial Mechanism Proposed by Makosza



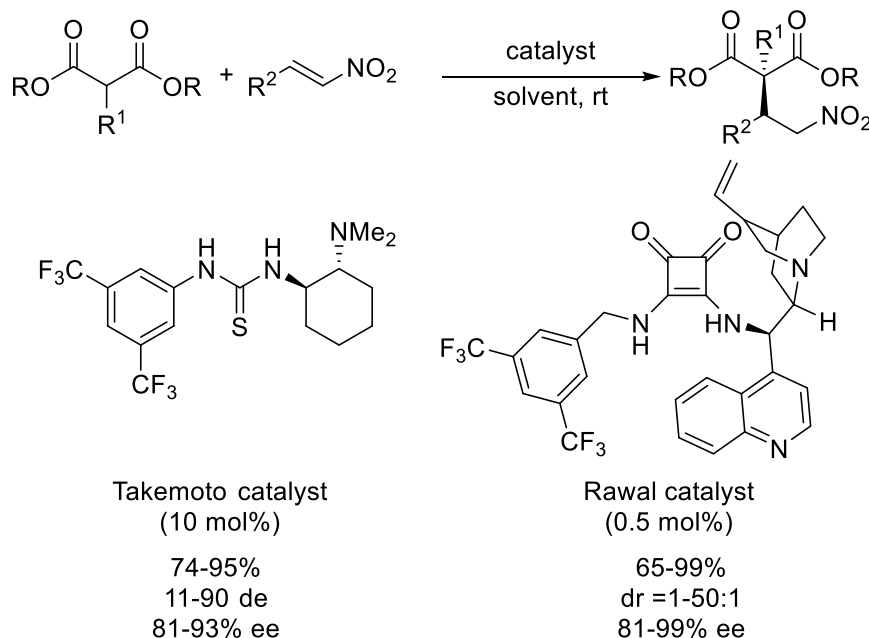
1.2 Bifunctional Base Catalyst

Bifunctional base catalysis has emerged as an important tool for controlling the reactivity and selectivity in such reactions. These catalysts generally comprises a base for the deprotonation of the substrate and a functional group for the substrate recognition (Figure 3).¹⁰

Figure 3 A model of bifunctional base catalyst

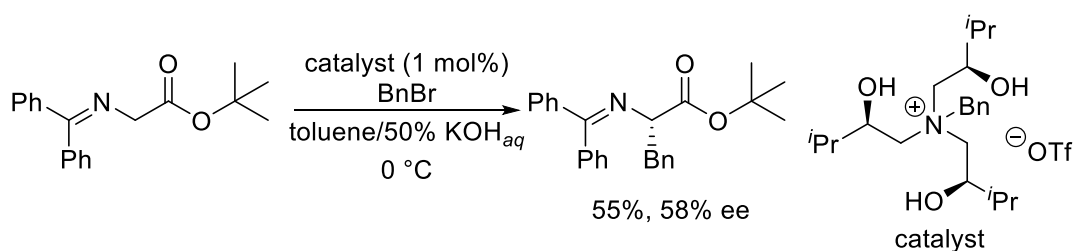


In 2003, Takemoto and co-workers reported a bifunctional thiourea catalyzed Michael addition of malonates to nitroolefins (Scheme 6). In this seminal work, the nitroolefin was bound to thiourea by dual hydrogen bonding, whereas the amine component of the catalyst was responsible for the deprotonation of malonate.¹¹ Subsequently, Rawal and co-workers developed a chiral squaramide based dual hydrogen bonding catalyst.¹²



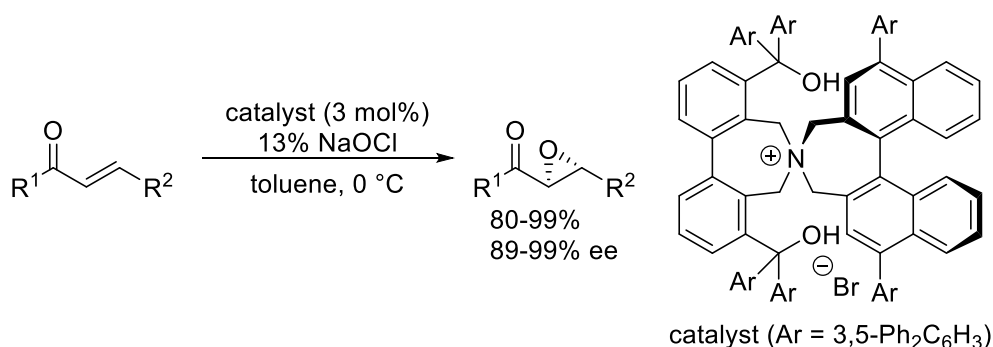
Scheme 6 Bifunctional base catalyzed enantioselective Michael reaction.

At the same time, Tanabe et al. reported asymmetric alkylation of Schiff base catalyzed a new bifunctional phase-transfer catalyst (Scheme 7).¹³



Scheme 7 Bifunctional quarter ammonium salt catalyzed enantioselective alkylation reaction.

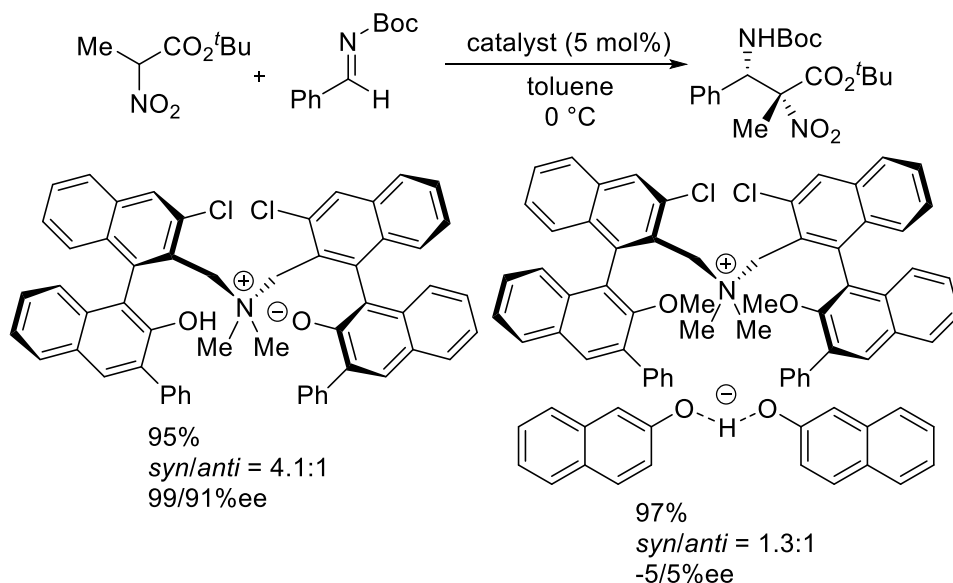
Maruoka et al. developed a high enantioselective epoxidation of α,β -unsaturated ketones catalyzed chiral quaternary ammonium salt possessing hydroxy group as a hydrogen donor (Scheme 8).¹⁴ They confirmed that hydroxy group of catalyst structure was essential for catalytic activity and enantioselectivity.



Scheme 8 Asymmetric Epoxidation catalyzed Bifunctional Ammonium Salt.

1.3.1 Intramolecular Ion Pairs Catalyst as Bifunctional Base Catalysis

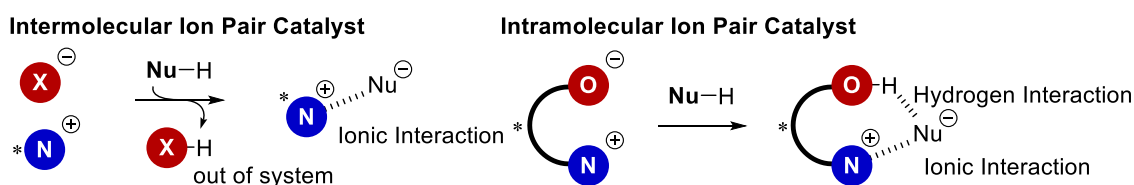
As described in the previous section, organic ion pair catalyst is generally an intermolecular ion pair salt. On the other hand, our research group has been interested in the catalysis of intramolecular ammonium salts called ammonium betaines. In 2008, our research group reported a stereoselective Mannich-type reaction of nitroesters using a newly developed intramolecular ion pair catalyst called ammonium betaine.¹⁵ Catalytic structure of the intramolecular ion pair was essential for stereoselectivity. However, the intermolecular ion pair salt showed catalytic activity but the Mannich product was obtained with diminished enantioselectivity (Scheme 9).



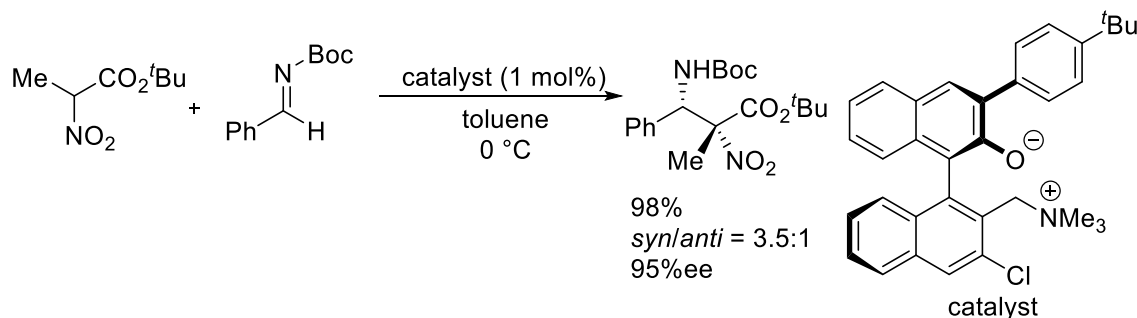
Scheme 9 Asymmetric Mannich-type reaction catalyzed chiral ammonium betaine.

The advantage of intramolecular ion pair structure lies in its ability to employ the cation unit and anion unit in the catalytic function. In general, when an intermolecular ion pair molecule acts as base catalysis, anion unit is out of catalytic system. In these catalytic systems, the reactive anion is recognized only through ionic interaction. Whereas an intramolecular ion pair acting as a base catalyst can recognize the reactive anion by cooperative function of hydrogen bonding and ionic interaction (Figure 4).

Figure 4 Inter. vs. Intramolecular ion pair catalyst

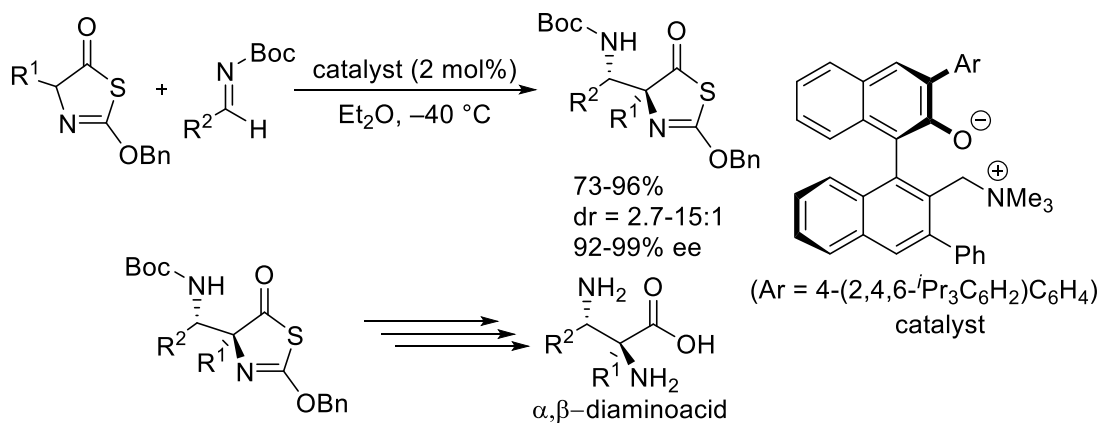


Following this work, a simplified C_1 -type chiral ion pair was developed as a highly stereoselective bifunctional base catalyst for the Mannich-type reaction of nitroester to imines (Scheme 10).¹⁶



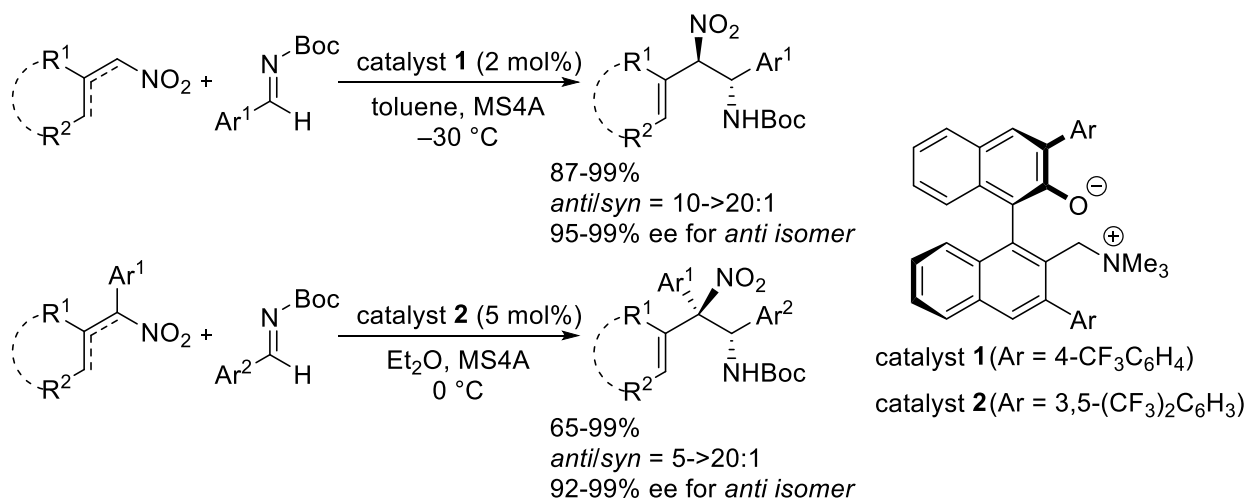
Scheme 10 Asymmetric Mannich-type reaction catalyzed chiral ammonium betaine.

The scope of chiral ammonium betaine as highly stereoselective catalyst was also explored with several other prochiral nucleophiles. In 2010, our group reported a stereoselective Mannich-type reaction of thiazole-5(4*H*)-one. The adduct was transformed easily to α,β -diaminoacid (Scheme 11).¹⁷



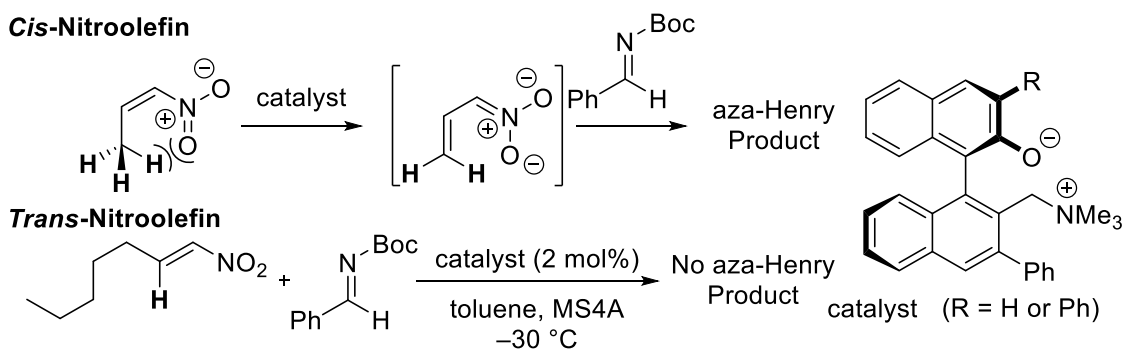
Scheme 11 Asymmetric Mannich-type reaction of thiazole-5(4*H*)-one

Subsequently, our group developed a new strategy for vinylous nitrate generation by chiral ammonium betaine. Several nitroolefin underwent a highly stereoselective aza-Henry reaction to afford the product in a good yield, high diastereo- and enantioselectivity (Scheme 12).¹⁸⁻¹⁹



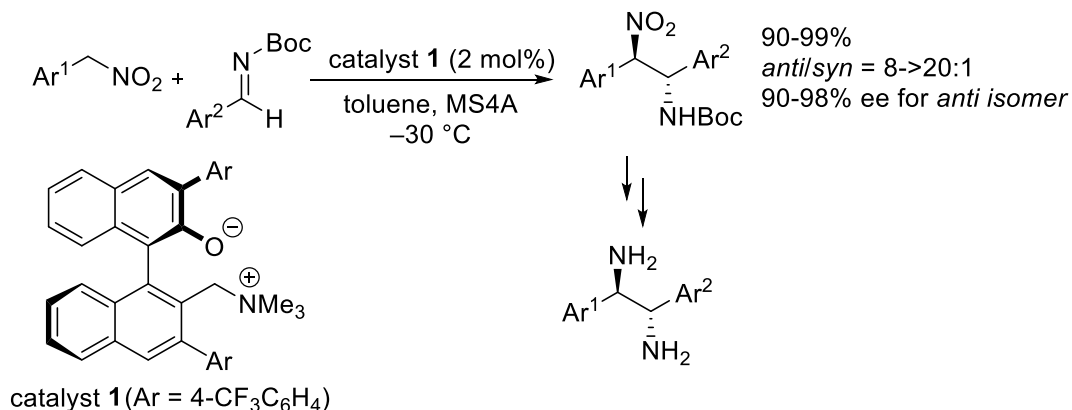
Scheme 12 Asymmetric aza-Henry reaction of nitroolefin

Due to the steric repulsion between nitro and methylene group, the betaine could only cause deprotonation of *cis*-nitroolefins. Whereas under the reaction conditions, the *trans*-nitroolefins remain unreacted (Scheme 13).



Scheme 13 Crucial difference of *cis*- and *trans*- nitroolefin as an aza-Henry reaction

A synthetically useful strategy for the synthesis of a well-established chiral reagent 1,2-diphenylenediamine was also developed. Under the optimized conditions, a chiral betaine catalyzed enantioselective aza-Henry reaction was achieved in gram scale. The adduct was further reduced to obtain the diamine in good yield (Scheme 14).²⁰

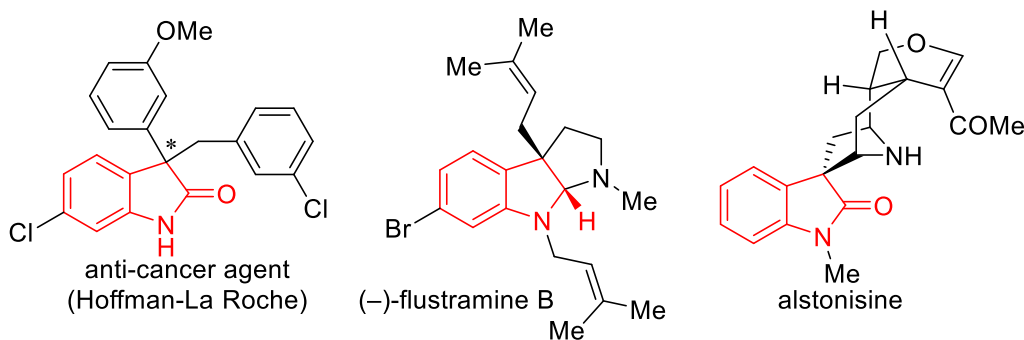


Scheme 14 Asymmetric aza-Henry reaction of (nitromethyl)benzene catalyzed chiral ammonium betaine

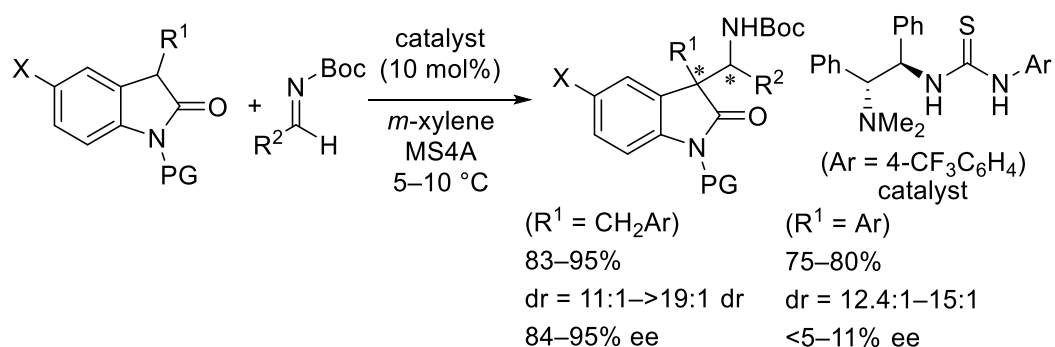
1.3.2 Chiral Ammonium Betaine-Catalyzed Asymmetric Mannich-Type Reaction of Oxindoles

Chiral indole alkaloids possessing a C-3 quaternary indoline frameworks are an important class of biologically relevant molecules (Figure 5).²¹

Figure 5 Examples of C-3 quaternary indoline compounds possessing biological activities.

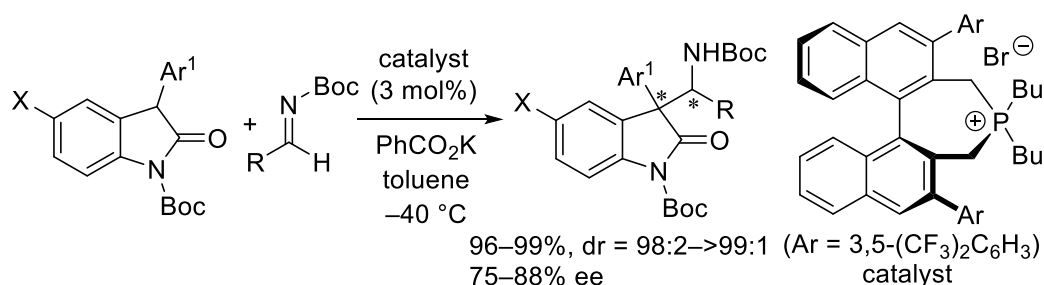


A numerous efforts have been made for the development of reliable synthetic methodologies to enable the installation of the C-3 stereogenic center. Among them, the direct stereoselective functionalization of 3-monosubstituted oxindoles is a straightforward method for accessing a wide array of chiral indoline skeletons. The most common strategy in this approach is to utilize an oxindole enolates as a nucleophile, because facile deprotonation from the C-3 carbon is ensured by the inductive effect of the α -carbonyl group and by the enolate stability arising from the aromatic character.²² However, successful examples of Mannich-type reactions with imines are surprisingly limited despite allowing efficient construction of vicinal quaternary and tertiary stereocenters. In particular, the application of 3-aryl substituted oxindoles seems problematic; hence, the full potential of this useful carbon-carbon bond formation is yet to be realized. For example, Chen et al. reported first asymmetric Mannich reaction of oxindoles catalyzed by thiourea derived chiral acid-base bifunctional catalyst.²³ But this catalyst couldn't be applied to 3-aryl substituted oxindoles (Scheme 15).



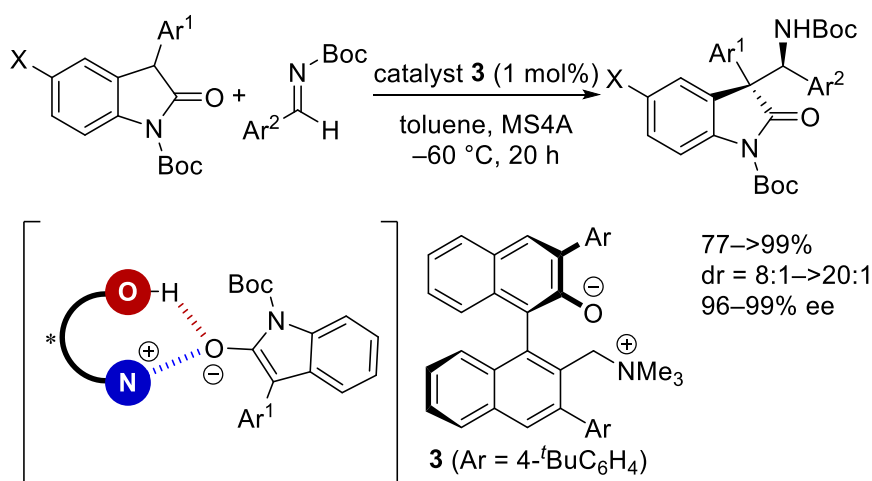
Scheme 15 Asymmetric Mannich reaction catalyzed bifunctional base catalyst

Maruoka et al. reported an asymmetric Mannich reaction of oxindoles catalyzed by a new chiral phosphonium molecule as a phase transfer catalyst.²⁴ However the enantioselectivity is moderate and substrate scope is limited (Scheme 16).



Scheme 16 Asymmetric Mannich reaction catalyzed chiral phase transfer catalyst

Author discovered a chiral ammonium betaine catalyzed Mannich-type reaction of 3-aryl oxindoles with imine in almost quantitative yields and excellent stereoselectivity. The conjugate acids of betaines can recognize a reactive anion by cooperative function of hydrogen bonding and ionic interaction (Chapter 2, Scheme 17).

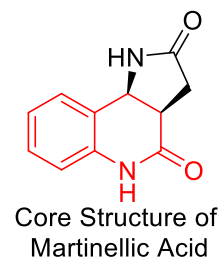
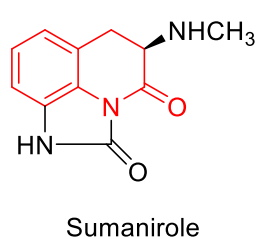
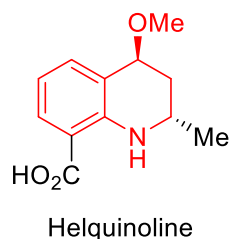


Scheme 17 Asymmetric Mannich reaction catalyzed chiral ammonium betaine

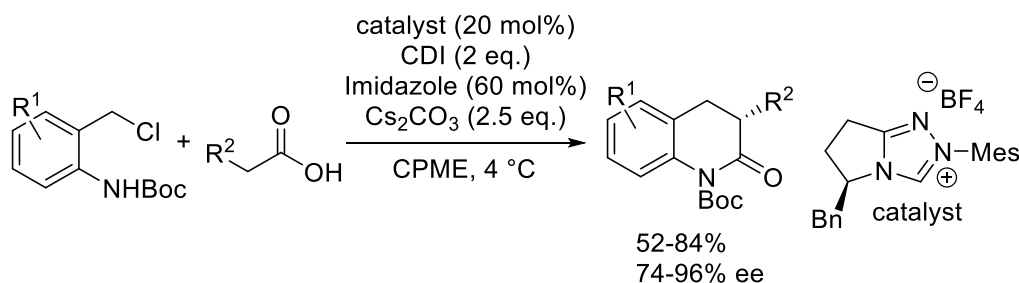
1.3.3 Stereoselective Aza-Henry Reaction of 3-Nitro Dihydro-2(3*H*)-Quinolones with *N*-Boc Aldimines under the Catalysis of Chiral Ammonium Betaines

Dihydro-quinolones have emerged as a valuable scaffold for the assembly of stereochemically defined, chiral tetrahydroquinoline frameworks possessing biologically relevant molecules (Figure 6).²⁵

Figure 6 Examples of chiral tetrahydroquinoline frameworks possessing biological activities.

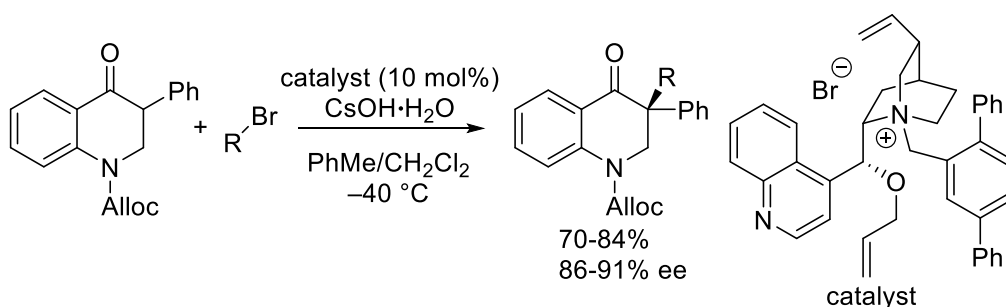


Therefore, notable efforts have been paid to develop a variety of stereoselective methodologies for constructing hydroquinolines possessing a stereogenic carbon center. However, most efforts toward this purpose was focused on asymmetric cyclization reactions and introduction of chirality to a hydroquinoline core has been scarcely developed. In a previously known catalytic approaches toward the synthesis of chiral hydroquinolones, Scheidt et al. reported an enantioselective cyclization of carboxylic acid and *o*-aminobenzyl chloride catalyzed by chiral NHC catalyst (Scheme 18).²⁶



Scheme 18 A synthesis of chiral hydroquinolones by asymmetric catalytic cyclization.

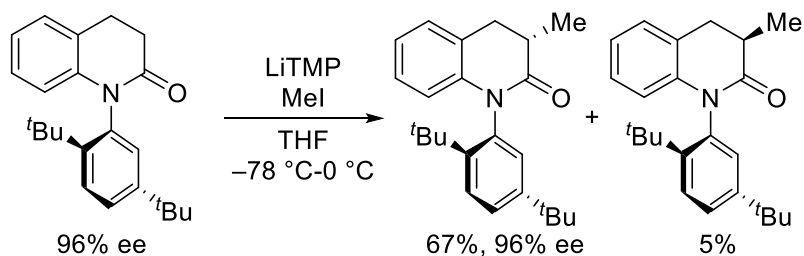
On the other hand, the enantioselective α -functionalization of the carbonyl moiety of hydroquinolones could provide a direct method for the synthesis of a tetrasubstituted stereogenic carbon center at the C3 position of this important class of heterocycles. For an example, Scheidt et al. developed the first asymmetric alkylation of 4-oxo-2,3-dihydroquinoline by using chiral phase transfer catalyst (Scheme 19).²⁷



Scheme 19 A synthesis of chiral 4-oxo-2,3-dihydroquinolines by asymmetric alkylation

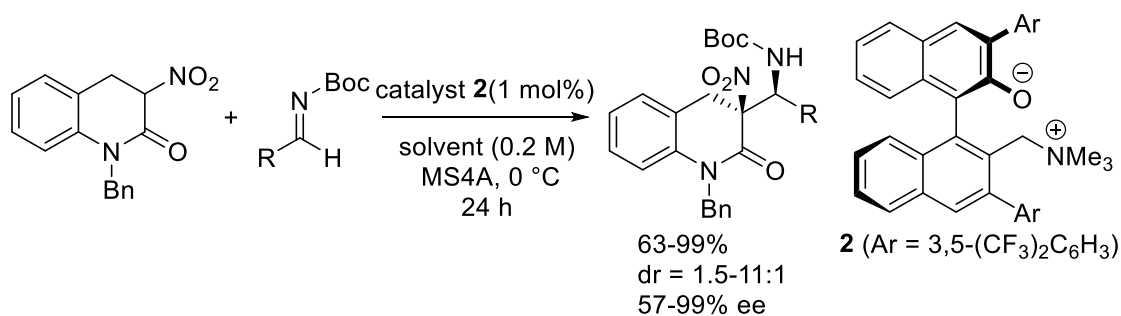
But surprisingly, catalytic asymmetric functionalization of 2-oxo-3,4-dihydroquinoline have not been reported. Only method for the synthesis of a chiral 2-oxo-3,4-dihydroquinoline was diastereometric alkylation of 2-oxo-3,4-

dihydroquinoline possessing chiral functional group reported by Taguchi group (Scheme 20).²⁸



Scheme 20 A synthesis of chiral 2-oxo-3,4-dihydroquinoline

Author developed an asymmetric aza-Henry reaction of 2-oxo-3-nitro-3,4-dihydroquinoline catalyzed by chiral ammonium betaine. In the result, the conjugate acids of betaines can recognize not only 3-aryloxindole but also dihydroquinoline by double function of hydrogen bonding and ionic interaction (Chapter 3, Scheme 21).

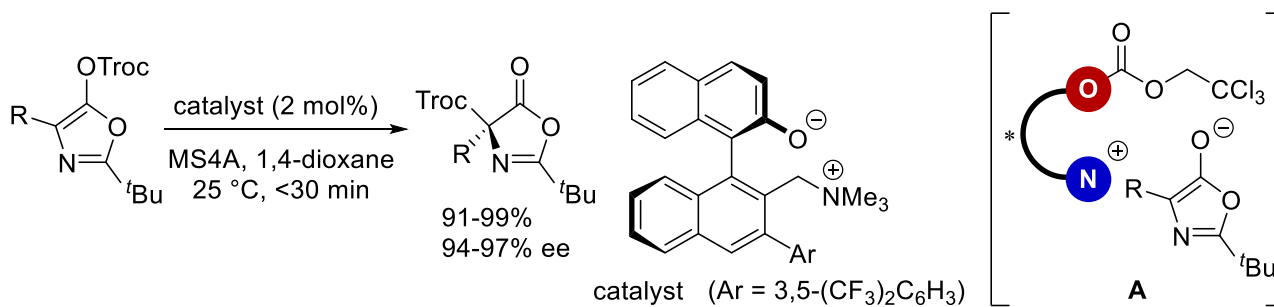


Scheme 21 Asymmetric aza-Henry reaction catalyzed chiral ammonium betaine

1.4 Other Function of Intramolecular Ion Pair Molecule

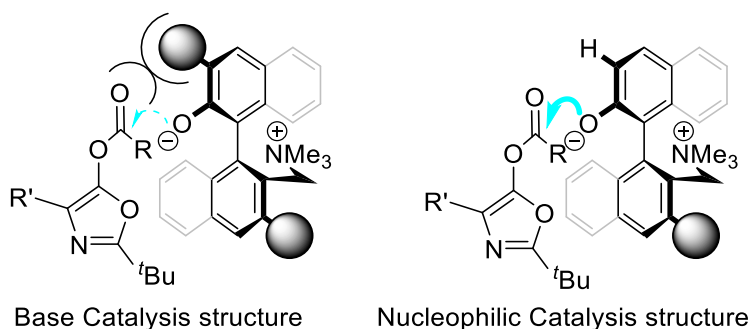
1.4.1 Nucleophile Catalyst

Our group also developed the utility of anionic moiety of ammonium betaine in asymmetric nucleophilic catalysis. The reaction proceeded through intermediate **A** which is important for obtaining high stereoselectivity (Scheme 22, Figure 7).²⁹

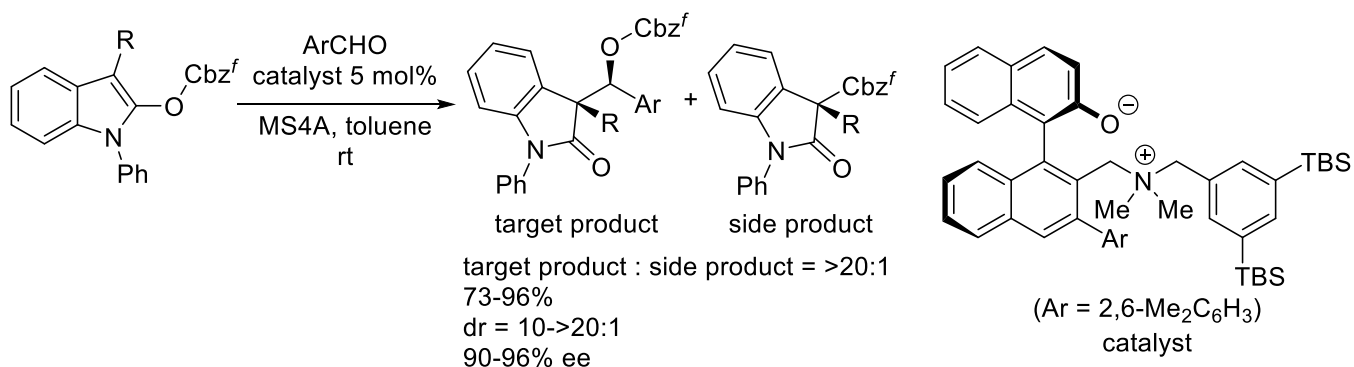


Scheme 22 Stereoselective Steglich reaction catalyzed chiral ammonium betaine

Figure 7 Different structure of base catalysis and nucleophilic catalysis



In 2012, our group demonstrated a stereoselective Steglich-aldol reaction catalyzed by a chiral intramolecular ion pair molecule.³⁰ This reaction works with an intramolecular ion pairs. Whereas if DMAP was applied as catalyst, a side product was obtained (Scheme 23).

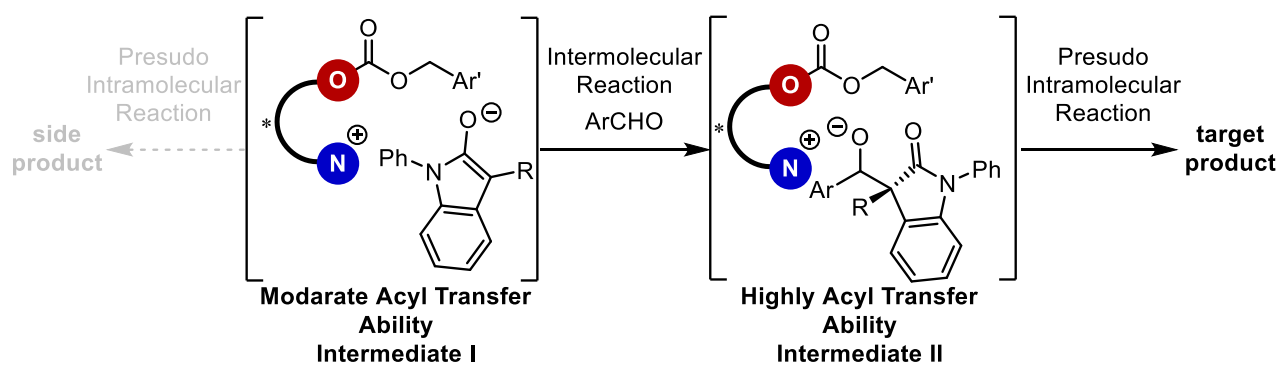


Scheme 23 Stereoselective Steglich-aldol reaction catalyzed chiral intramolecular ion pair molecules.

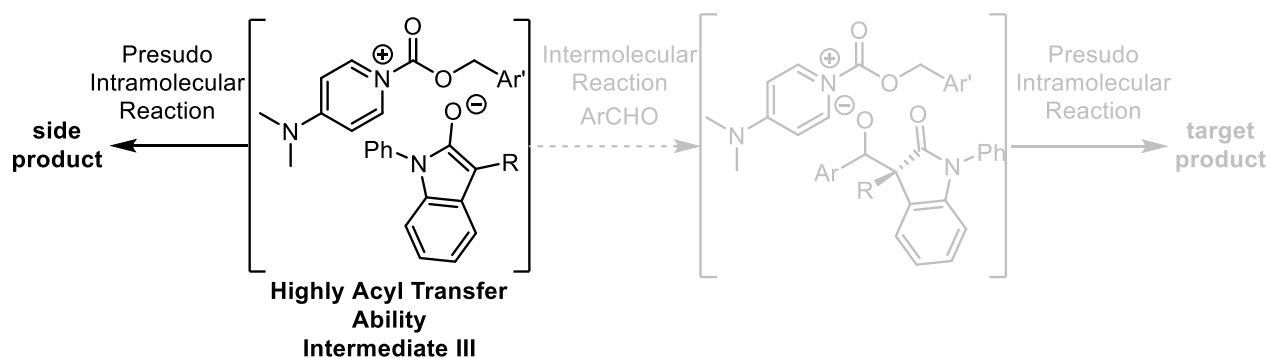
As shown in Scheme 18, the ion pair generated from betaine and oxindole carbonate (intermediate I) prefer to undergo an intermolecular reaction with aldehyde to generate the product. Whereas Intermediate III generated by the reaction of DMAP simply undergoes a pseudo-intramolecular reaction to generate the side product (Figure 8).

Figure 8 Intramolecular catalyst vs DMAP as a nucleophilic catalysis

Intramolecular Ion Pair Catalyst

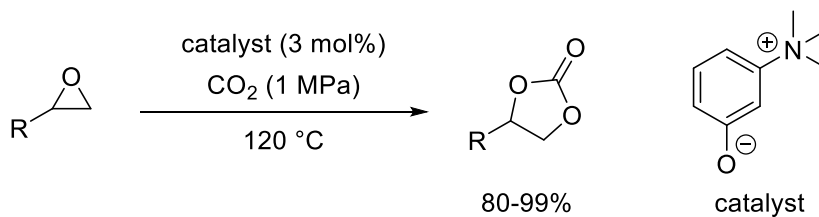


DMAP as a Nucleophilic Catalyst



1.4.2 Nucleophile Catalyst to a Carbon Dioxide as a Substrate

In 2010, groups of Sakai and Lu et al. reported the intramolecular ion pair catalyst as a Lewis base for carbon dioxide activation.³¹⁻³² Anionic moiety of the catalyst reacted with carbon dioxide under high pressure condition, to give ammonium carbonate as an intermediate which reacts further to yield desired products (Scheme 24-25).



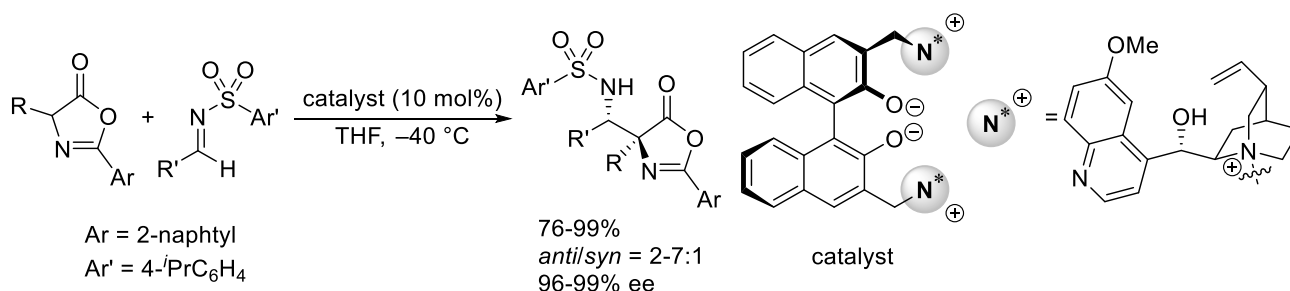
Scheme 24 Cyclization of epoxide using carbon dioxide catalyzed ammonium betaine



Scheme 25 Cyclization of alkynyl alcohol using carbon dioxide catalyzed imidazolium betaine

1.4.3 Bis(Intramolecular Ion Pair) Catalyst

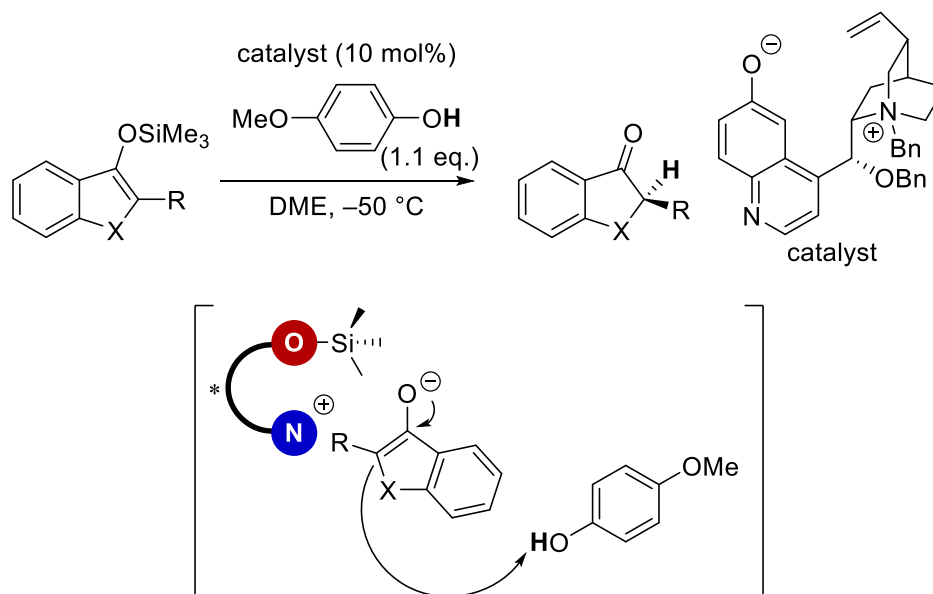
Gong et al. reported the bis(betaine) as new intramolecular ion pair catalyst for Mannich reaction of azlactone (Scheme 26).³³



Scheme 26 Mannich reaction of azlactone catalyzed chiral bis(betaine).

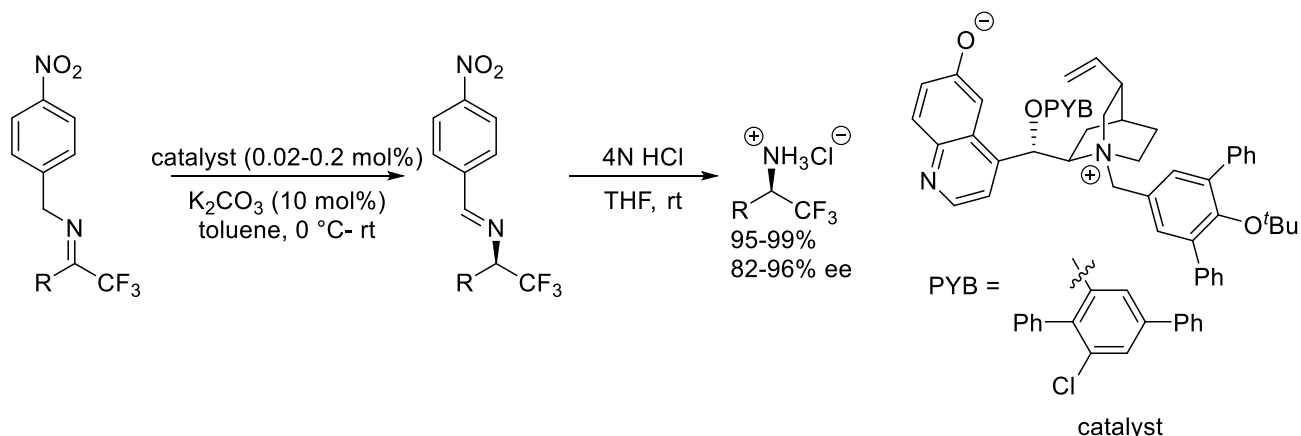
1.4.4 Asymmetric Protonation using Chiral Intramolecular Ion Pair Catalyst

In 2013, Levacher et al. reported an cinchona alkaloids derived chiral ammonium betaines catalyzed asymmetric protonation of silyl enolates.³⁴ Anionic moiety of the catalyst reacts with silyl enolate as a Lewis base. The generated chiral ammonium enolate was protonated by the aryl alcohol to afford the desired product (Scheme 27).



Scheme 27 Asymmetric protonation of silyl enolates catalyzed by chiral ammonium betaine.

Deng et al. also developed a chiral ammonium betaine catalyzed asymmetric isomerization reaction through a proton transfer reaction of trifluoromethyl imines to yield enantioselective trifluoromethylated amines with high enantioselectivity (Scheme 28).³⁵

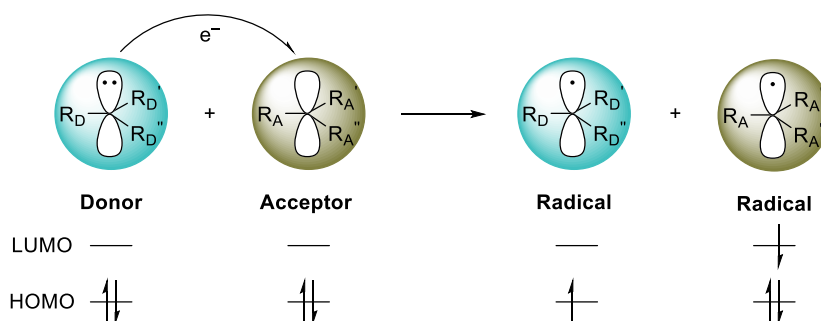


Scheme 28 Asymmetric isomerization reaction catalyzed by chiral ammonium betaine

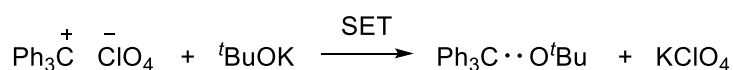
1.4.5 Design and Development of Betaine type Proton Coupled Electron Transfer Catalyst

Radical reaction is one of the most fundamental transformations in synthetic organic chemistry and radical species represent unique reactivity in specific reactions due to their unpaired electron.³⁶ However, controlling the radical intermediates is known to be problematic and methods for generating radicals are somewhat limited. Among the radical generating protocols, single electron transfer (SET) process is regarded as a relatively well utilized and straightforward approach. In the SET reaction, one electron from HOMO of a donor molecule is transferred to LUMO of an acceptor molecule to form two kinds of radical species (Scheme 35).³⁷

Figure 9 Model of single electron transfer reaction



For example, Bilevitch realized the formation of radical pair through a SET reaction by treating triphenylmethyl perchlorate with potassium *tert*-butoxide (Scheme 29).³⁸



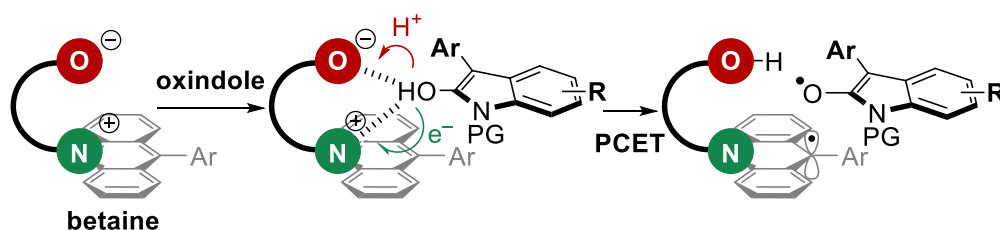
Scheme 29 A first report about single electron transfer reaction

Considering the synthetic importance and the reactivity of radical species, catalytic generation of them is a highly desirable protocol. However the development of a SET catalyst is still a challenging task. So we anticipated that a new tactic is required for overcoming this dilemma, which direct our attention to proton coupled electron transfer (PCET) process. PCET is one of the basic mechanism of chemical and biological redox transformations, where

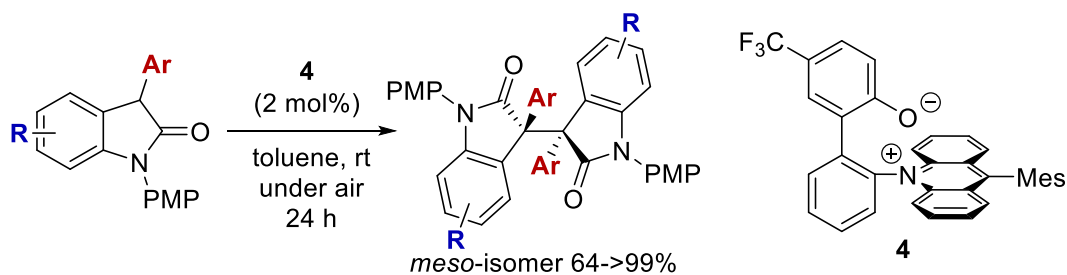
simultaneous transfer of one electron and proton between given substrates allows to generate high-energy intermediates.³⁹ Since PCET is known to proceed via more stable transition state than that expected in iterative electron-proton (or proton-electron) transfer processes, requisite reduction/oxidation potential of the catalyst is expected to be much lower than that of the two-step reaction, and the resulting reduced (or oxidized) catalyst could be restored under accessible conditions. However, this possibility has not been experimentally investigated yet.

So we initiated the study for developing a new PCET-catalyst. We envisaged a new betaine having an electron-transfer unit such as an acridinium structure as a cationic part and aryloxy as an anionic part. (Figure 10)

Figure 10 Model of betaine-type PCET catalyst



If this basic betaine could deprotonate from a pronucleophile such as carbonyl compounds at the same time as acting SET reaction, the resulting corresponding radical pair would be formed. To evaluate the performance of the betaine-type PCET catalyst, we selected homo-dimerization of oxindoles as a model reaction in consideration to importance of dimerized indole skeleton in biologically relevant molecules. In the result, we have developed a novel betaine-type PCET catalyst **4** comprising an acridinium moiety as electron transfer subunit and the betaine was found to be the prominent catalyst for the PCET mediated dimerization of 3-aryl oxindoles (Chapter 4, Scheme 30).



Scheme 30 Homo-coupling reaction of oxindole catalyzed acridinium betaine

Summary

In these studies, the author developed the intramolecular ion pair catalyst as a bifunctional base catalyst. He found the high catalytic activity of chiral ammonium betaines in asymmetric Mannich-type reaction of 3-aryloxindoles and asymmetric aza-Henry reaction of *N*-benzyl-3-nitro-3,4-dihydroquinolinone. Moreover as a part of our ongoing study on the catalysis of ammonium betaines, he also successfully developed a betaine-type proton coupled electron transfer catalyst that exhibits unique catalytic activity in a homo-coupling of radical enolates of oxindoles.

Reference

- (1) For review on organocatalyst, see: (a) Seayad, J.; List B. *Org. Biomol. Chem.*, **2005**, *3*, 719. (b) Brak K.; Jacobsen E. N. *Angew. Chem. Int. Ed.* **2013**, *52*, 534.
- (2) (a) Helder, H.; Arends, R.; Bolt, W.; Hiemstra, H.; Wynberg *Tetrahedron Lett.* **1977**, *18*, 2181. (b) Hiemtra, H.; Wynberg, H. *J. Am. Chem. Soc.* **1981**, *103*, 2181.
- (3) For review on chiral ammonium salts as phase-transfer catalysts, see: (a) Ooi, T.; Maruoka, K. *Angew. Chem. Int. Ed.* **2007**, *46*, 4222. (b) Hashimoto, T.; Maruoka, K. *Chem. Rev.* **2007**, *107*, 5656.
- (4) Dolling, U.-H.; Davis, P.; Grabowski, E. J. J. *J. Am. Chem. Soc.* **1984**, *106*, 446.
- (5) Corey, E. J.; Xu, F.; Noe, M. C. *J. Am. Chem. Soc.* **1997**, *119*, 12414.
- (6) Lygo, B.; Wainwright, P. G. *Tetrahedron Lett.* **1997**, *38*, 8595.
- (7) Ooi, T.; Kameda, M.; Maruoka, K. *J. Am. Chem. Soc.* **1999**, *121*, 6519.
- (8) Starks, C. M. *J. Am. Chem. Soc.* **1971**, *93*, 195.
- (9) *Phase-Transfer Catalysis: Fundamentals, Applications, and Industrial Perspectives*; Starks, C. M.; Liotta, C. Springer: 1994.
- (10) For review on biunctional catalyst, see: (a) Palomo, C.; Oiarbide, M.; López, R. *Chem. Soc. Rev.* **2009**, *38*, 632. (b) Alemán, J.; Parra, A.; Jiang, H.; Jørgensen, K. A. *Chem. Eur. J.* **2011**, *17*, 6890. (c) Connon, S. J. *Chem. Eur. J.* **2006**, *12*, 5418.
- (11) Okino, T.; Hoashi, Y.; Takemoto, Y. *J. Am. Chem. Soc.* **2003**, *125*, 12672.
- (12) Malerich, J. P.; Hagihara, K.; Rawal, V. *J. Am. Chem. Soc.* **2008**, *130*, 14416.
- (13) Mase, N.; Ohno, T.; Hoshikawa, N.; Ohishi, K.; Morimoto, H.; Yoda, H.; Tanabe, K. *Tetrahedron Lett.* **2003**, *44*, 4073.
- (14) Ooi, T.; Ohara, D.; Tamura, M.; Maruoka, K. *J. Am. Chem. Soc.* **2004**, *126*, 6844.
- (15) Uruguchi, D.; Koshimoto, K.; Ooi, T. *J. Am. Chem. Soc.* **2008**, *130*, 10878.
- (16) Uruguchi, D.; Koshimoto, K.; Sanada, C.; Ooi, T. *Tetrahedron Asymmetry* **2010**, *21*, 1189.
- (17) Uruguchi, D.; Koshimoto, K.; Ooi, T. *Chem. Comm.* **2010**, *46*, 300.
- (18) Uruguchi, D.; Oyaizu, K.; Ooi, T. *Chem. Eur. J.* **2012**, *18*, 8306.
- (19) Oyaizu, K.; Uruguchi, D.; Ooi, T. *Chem. Commun.* **2015**, *51*, 4437.
- (20) Uruguchi, D.; Oyaizu, K.; Noguchi, H.; Ooi, T. *Chem. Asian J.* **2014**, *10*, 334.
- (21) (a) Marti, C.; Carreira, E. M. *Eur. J. Org. Chem.* **2003**, 2209. (b) Galliford, C. V.; Scheidt, K. A. *Angew. Chem. Int. Ed.* **2007**, *46*, 8748. (c) Trost, B. M.; Brennan, M. K. *Synthesis* **2009**, 3003. (d) Singh, G. S.; Desta, Z. Y. *Chem. Rev.* **2012**, *112*, 6104.
- (22) (a) He, R.; Ding, C.; Maruoka, K. *Angew. Chem. Int. Ed.* **2009**, *48*, 4559. (b) Zhao, K.; Zhi, Y.; Wang, A.; Enders, D. *ACS Catal.* **2016**, *6*, 657.
- (23) Tian, X.; Jiang, K.; Peng, J.; Du, W.; Chen, Y.-C. *Org. Lett.* **2008**, *10*, 3583.
- (24) He, R.; Ding, C.; Maruoka, K. *Angew. Chem. Int. Ed.* **2009**, *48*, 4559.
- (25) Sridharan, V.; Suryavanshi, P. A.; Menéndez, J. C. *Chem. Rev.* **2011**, *111*, 7157
- (26) Lee, A.; Younai, A.; Price, C. K.; Izquierdo, J.; Mishra, R. K.; Scheidt, K. A. *J. Am. Chem. Soc.* **2014**, *136*, 10589.

- (27) Nibbs, A.; Baize, A. L.; Herter, R. M.; Scheidt, K. A. *Org. Lett.* **2009**, *11*, 4010.
- (28) Kitagawa, O.; Takahashi, M.; Yoshikawa, M.; Taguchi, T. *J. Am. Chem. Soc.* **2005**, *127*, 3676.
- (29) Uraguchi, D.; Koshimoto, K.; Miyake, S.; Ooi, T. *Angew. Chem. Int. Ed.* **2010**, *49*, 5567.
- (30) Uraguchi, D.; Koshimoto, K.; Ooi, T. *J. Am. Chem. Soc.* **2012**, *134*, 6972.
- (31) Tsutsumi, Y.; Yamakawa, K.; Yoshida, M.; Ema, T.; Sakai, T. *Org. Lett.* **2010**, *12*, 5728.
- (32) Wang, Y.-B.; Sun, D.-S.; Zhou, H.; Zhang, W.-Z.; Lu, X.-B. *Green Chem.* **2014**, *16*, 2266.
- (33) Zhang, W.-Q.; Cheng, L.-F.; Yu, J.; Gong, L.-Z. *Angew. Chem. Int. Ed.* **2012**, *51*, 4085.
- (34) Claraz, A.; Landelle, G.; Oudeyer, S.; Levacher, V. *Eur. J. Org. Chem.* **2013**, 7693.
- (35) Zhou, X.; Wu, Y.; Deng, L. *J. Am. Chem. Soc.* **2016**, *138*, 12297.
- (36) For review on radical reaction, see: (a) Crich, D. Quintero, L. *Chem. Rev.* **1989**, *89*, 1413. (b) Galli, C. *Chem. Rev.* **1988**, *88*, 765. (c) Jasperse, C. P.; Curran, D. P.; Fevig, T. L. *Chem. Rev.* **1991**, *91*, 1237.
- (37) *Electron Transfer Reactions in Organic Chemistry*; Ebersson, L. Springer-Verlag: 1987.
- (38) Bilevitch, K. A. *Tetrahedron Lett.* **1968**, *9*, 3465.
- (39) For reviews on PCET, see: (a) Huynh, M. H. V.; Meyer, T. J. *Chem. Rev.* **2007**, *107*, 5004. (b) Weinberg, D. R.; Gagliardi, C. J.; Hull, J. F.; Murphy, C. F.; Kent, C. A.; Westlake, B. C.; Paul, A.; Ess, D. H.; McCafferty, D. G.; Meyer, T. J. *Chem. Rev.* **2012**, *112*, 4016. (c) Yayla, H. G.; Knowles, R. R. *Synlett* **2014**, *20*, 2819. (d) Gentry, E. C.; Knowles, R. R. *Acc. Chem. Res.* **2016**, *49*, 1546.

Chapter 2

Chiral Ammonium Betaine-Catalyzed Asymmetric Mannich-Type Reaction of Oxindoles

Abstract

A highly diastereo- and enantioselective Mannich-type reaction of 3-aryl oxindoles with *N*-Boc aldimines was achieved under the catalysis of axially chiral ammonium betaines. This catalytic method provides a new tool for the construction of consecutive quaternary and tertiary stereogenic carbon centers on biologically intriguing molecular frameworks with high fidelity.

Introduction

Chiral indole alkaloids possessing C-3 quaternary indoline frameworks are an important class of biologically relevant molecules, and numerous efforts have been made for the development of reliable synthetic methodologies to enable the installation of the C-3 stereogenic center.¹⁻⁴ Among them, the direct stereoselective functionalization of 3-monosubstituted oxindoles is a straightforward method for accessing a wide array of chiral indoline skeletons.⁵⁻⁸ The most common strategy in this approach is to utilize an oxindole enolates as a nucleophile, because facile deprotonation from the C-3 carbon is ensured by the inductive effect of the α -carbonyl group and by the enolate stability arising from the aromatic character. Accordingly, a number of catalytic methods are available for the asymmetric functionalization of oxindole enolates with various different electrophiles. However, successful examples of Mannich-type reactions with imines are surprisingly limited despite allowing efficient construction of vicinal quaternary and tertiary stereocenters.⁹⁻²¹ In particular, the application of 3-*aryl* substituted oxindoles seems problematic; hence, the full potential of this useful carbon-carbon bond formation is yet to be realized.^{12,14}

Ammonium betaines are defined as intramolecular ion-pairing quaternary ammonium salts. In 2008, we employed this structurally distinct molecular scaffold for designing a novel bifunctional organic base catalyst,²² namely axially chiral ammonium betaines of type **1**,^{23,24} and uncovered their extraordinary catalytic performance.²⁵⁻³⁴ The salient feature of **1** is that, upon abstracting a proton from a pro-nucleophile, the resulting conjugate acid, **1**-H, has the ability to recognize the nucleophilic anion through cooperative electrostatic (ionic) and hydrogen-bonding interactions, thereby precisely controlling the stereochemical outcome of the subsequent bond-forming event. Taking advantage of this unique property, we have developed a series of highly stereoselective transformations, and disclose herein the effectiveness of **1** in solving a challenging problem regarding the rigorous control of relative and absolute stereochemistry in the asymmetric Mannich-type reaction of 3-*aryl* oxindoles.

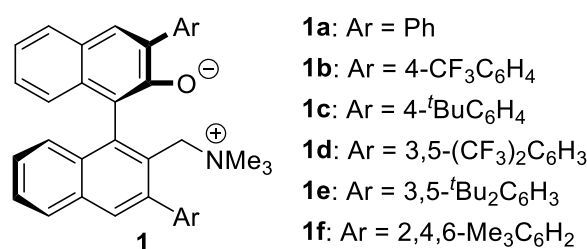


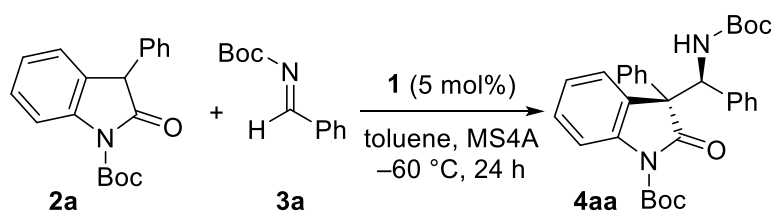
Figure 1. Chiral ammonium betaines

Results and Discussion

As an initial attempt, the reaction of *N*-Boc 3-phenyl oxindole (**2a**) with benzaldehyde-derived *N*-Boc imine **3a**³⁵ was conducted in the presence of a catalytic amount of chiral ammonium betaine **1a** (5 mol%) in toluene with 4 Å molecular sieves (MS4A) at -60 °C. Bond formation occurred smoothly and, after 24 h of stirring, the desired Mannich adduct **4aa** was isolated as a mixture of diastereomers in 90% yield. Although the diastereomeric ratio was moderate (dr = 7.3:1), the enantiomeric excess (ee) of the major isomer was determined to be 98% (Table 1, entry 1). The investigation then focused on the effects of catalyst structure, primarily on diastereocontrol, which revealed the importance of steric bulk at the periphery of aromatic substituents at the 3,3'-positions of both naphthyl units (Ar),

rather than their electronic attributes (entries 2-6). For instance, while 4-trifluoromethylphenyl-substituted betaine **1b** had no positive impact on the reaction profile (entry 2), the use of **1c**, bearing 4-*tert*-butylphenyl groups, delivered a critical improvement in diastereoselectivity, affording **4aa** quantitatively and establishing consecutive quaternary and tertiary stereocenters with almost complete fidelity (entry 3). Further examination of the reactions under the influence of **1d**, having 3,5-bis(trifluoromethyl)phenyl groups, and **1e**, bearing 3,5-bis(*tert*-butyl)phenyl groups, showed similar tendencies, but a considerable decrease in reactivity and selectivity was observed when using **1d** (entries 4 and 5). On the other hand, however, the introduction of 2,4,6-trimethylphenyl appendages (**1f**), which extended steric hindrance over the catalytically active sites, eroded catalytic activity and diastereocontrol (entry 6). These observations demonstrated the superior capability of **1c** in facilitating this stereoselective Mannich-type transformation, for which the loading was reduced to 1 mol% without sacrificing reaction efficiency (entry 7). It is noteworthy that the present system is scalable; the reaction with 1.0 g of **2a** reached completion within 20 h to afford **4aa** with a similar degree of stereoselectivity (entry 8), and subsequent recrystallization furnished 0.83 g of essentially stereochemically pure **4aa**.

Table 1. Optimazation of catalyst structure^a



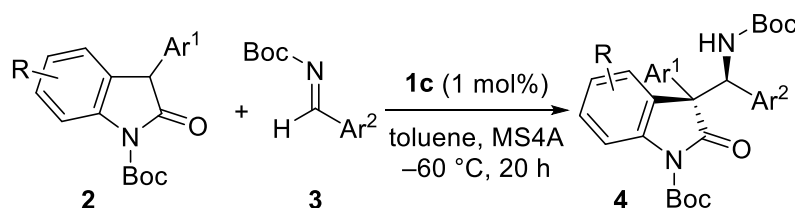
entry	Ar (1)	yield (%) ^b	dr ^c	ee (%) ^d
1	Ph (1a)	90	7.3:1	98/20
2	4-CF ₃ C ₆ H ₄ (1b)	>99	7.3:1	98/6
3	4- <i>t</i> -BuC ₆ H ₄ (1c)	>99	>20:1	99/-
4	3,5-(CF ₃) ₂ C ₆ H ₃ (1d)	54	1:1.3	98/-35
5	3,5- <i>t</i> -Bu ₂ C ₆ H ₃ (1e)	>99	10:1	98/-
6	2,4,6-Me ₃ C ₆ H ₂ (1f)	73	1.8:1	98/63
7	1c ^e	92	>20:1	97/-
8	1c ^{e,f}	>99	>20:1	98/-

^a Unless otherwise noted, reactions were conducted with 0.1 mmol of **2a**, 0.12 mmol of **3a**, and 5 mol% of **1** in toluene (0.5 mL) containing 50.0 mg of MS4A at -60 °C for 24 h. ^b Isolated yield was indicated. ^c The diastereomeric ratio was determined by ¹H NMR (400 MHz) analysis of crude aliquot. ^d Enantiomeric excess was analyzed by chiral stationary phase HPLC (DAICEL CHIRALPAK AD-3). Absolute configuration of **4aa** was assigned by analogy to **4ca** (see Fig. 2). ^e 1 mol% of **1c** was used. ^f The reaction was performed on a 1.0-gram scale regarding **2a**.

Having identified **1c** as an optimal catalyst, the substrate scope of this asymmetric Mannich protocol was explored. As seen in representative results summarized in Table 2, excellent enantioselectivities were generally attained irrespective of the steric and electronic properties of both oxindoles **2** and *N*-Boc aldimines **3**, but reactivity and diastereoselectivity sometimes fluctuated depending on the structure of these substrates. While significant

variation in the imine substituents was feasible, the introduction of electron-withdrawing groups at the *meta*-position slightly reduced diastereoselectivity (entries 1-4). Sterically demanding 2-tolualdehyde-derived imine **3f** served as a good electrophile and the corresponding Mannich adduct **4af** was isolated as virtually a single stereoisomer (entry 5). 3-Thiophenyl aldimine **3g** was also well tolerated, but a substantial decrease in diastereoselectivity was observed in the reaction with 2-furyl aldimine **3h**, owing to the requisite higher reaction temperature (entries 6 and 7). Catalysis with **1c** was also applicable to aliphatic imines, which required prolonged reactions and slightly higher catalyst loadings to achieve adequate conversions; the desired adducts, **4ai** and **4aj**, were obtained with high enantioselectivities and moderate diastereoselectivities (entries 8 and 9). With respect to oxindoles **2**, the electronic nature of the 3-aryl moiety affected the diastereoselection; the incorporation of electron-deficient aromatics proved beneficial and the presence of electron-rich aryl components seemed detrimental (entries 10-14). However, the diastereoselectivity was robust with regard to electronic differences in the oxindole core, and both 5-fluoro- and methoxy-substituted **2g** and **2h** were efficiently converted into **4ga** and **4ha** with rigorous relative and absolute stereocontrol (entries 15 and 16). The absolute configuration of **4ca** was unequivocally determined by X-ray crystallographic analysis (Fig. 2), and the stereochemistry of the remaining examples was assumed to be analogous.

Table 2. Substrate scope^a



entry	Ar ¹ , R (2)	Ar ² (3)	yield (%) ^b	dr ^c	ee (%) ^d	prod.
1	Ph, H (2a)	4-MeOC ₆ H ₄ (3b)	96	>20:1	99	4ab
2	Ph, H (2a)	4-ClC ₆ H ₄ (3c)	96	>20:1	99	4ac
3	Ph, H (2a)	3-MeOC ₆ H ₄ (3d)	92	>20:1	97	4ad
4	Ph, H (2a)	3-BrC ₆ H ₄ (3e)	>99	14:1	99	4ae
5	Ph, H (2a)	2-MeC ₆ H ₄ (3f)	95	>20:1	99	4af
6	Ph, H (2a)	3-thiophenyl (3g)	90	>20:1	99	4ag
7 ^e	Ph, H (2a)	2-furyl (3h)	86	9:1	97	4ah
8 ^f	Ph, H (2a)	Ph(CH ₂) ₂ (3i)	55	5:1	98/75	4ai
9 ^g	Ph, H (2a)	Me(CH ₂) ₇ (3j)	44	3.5:1	93/60	4aj
10	4-MeOC ₆ H ₄ , H (2b)	Ph (3a)	96	12:1	98	4ba
11	4-ClC ₆ H ₄ , H (2c)	Ph (3a)	92	>20:1	97	4ca
12	3-MeOC ₆ H ₄ , H (2d)	Ph (3a)	89	4:1	98	4da
13	3-MeC ₆ H ₄ (2e)	Ph (3a)	87	13:1	99	4ea
14	3-CF ₃ C ₆ H ₄ , H (2f)	Ph (3a)	80	>20:1	99	4fa
15	Ph, 5-F (2g)	Ph (3a)	85	>20:1	97	4ga
16	Ph, 5-MeO (2h)	Ph (3a)	89	>20:1	96	4ha

^a Unless otherwise noted, reactions were performed on 0.2 mmol scale with 1.2 equiv of **3a** in the presence of **1c** (1 mol%) and MS4A (100.0 mg) in toluene (1.0 mL) at $-60\text{ }^{\circ}\text{C}$ for 24 h. ^b Isolated yield was reported. ^c The diastereomeric ratio was determined by ^1H NMR (400 MHz) analysis of crude aliquot. ^d Enantiomeric excess of the major isomer was indicated, which was analyzed by chiral stationary phase HPLC. Absolute configuration of **4ca** was determined by single crystal X-ray diffraction analysis (Fig. 2) and that of the other **4** was assumed to be analogous. ^e The reaction was conducted at $-40\text{ }^{\circ}\text{C}$ for 110 h. ^f The reaction was stirred for 117 h. ^g The reaction time was 72 h.

Conclusion

In summary, we have clearly demonstrated that chiral ammonium betaine **1c** acts as a uniquely effective catalyst in promoting a Mannich-type reaction between 3-aryl oxindoles and *N*-Boc aldimines with high levels of diastereo- and enantioselectivity under mild conditions. This study greatly expands the scope of this mode of stereoselective Mannich-type reaction, which involve the generation of vicinal quaternary and tertiary stereocenters. Further investigations into the potential utility of ammonium betaine catalysis are underway in our laboratory.

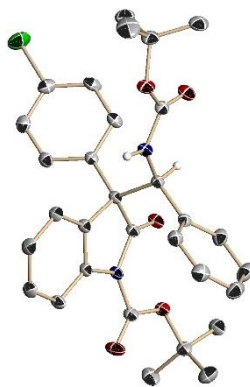


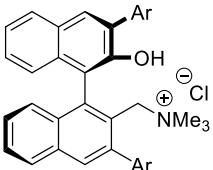
Figure 2. ORTEP diagram of **4ca** (Ellipsoids displayed at 50% probability. Calculated hydrogen atoms except it attaches to stereogenic carbon are omitted for clarity. Black: carbon, Red: oxygen, Blue: nitrogen, Green: chlorine).

General Information: Infrared spectra were recorded on a SHIMADZU IRAffinity-1 spectrometer. ¹H NMR spectra were recorded on a JEOL JNM-ECS400 (400 MHz) spectrometer or JEOL JNM-ECA600 (600 MHz) spectrometer. Chemical shifts are reported in ppm from the solvent resonance ((CD₃)₂SO: 2.50 ppm, CD₃CN: 1.94 ppm) or tetramethylsilane (0.00 ppm; CDCl₃, CD₃OD) resonance as the internal standard. Data are reported as follows: chemical shift, integration, multiplicity (s = singlet, d = doublet, t = triplet, m = multiplet, br = broad, brd = broad-doublet), and coupling constants (Hz). ¹³C NMR spectra were recorded on a JEOL JNM-ECS400 (100 MHz) spectrometer or JEOL JNM-ECA600 (151 MHz) spectrometer with complete proton decoupling. Chemical shifts are reported in ppm from the solvent resonance (CDCl₃: 77.16 ppm, CD₃OD: 49.00 ppm, (CD₃)₂SO: 39.52 ppm, CD₃CN: 1.32 ppm). ¹⁹F NMR spectra were recorded on a JEOL JNM-ECS400 (373 MHz) spectrometer with complete proton decoupling. Chemical shifts are reported in ppm. The high resolution mass spectra were conducted on Thermo Fisher Scientific Exactive (ESI). Analytical thin layer chromatography (TLC) was performed on Merck precoated TLC plates (silica gel 60 F₂₅₄, 0.25 mm). Flash column chromatography was performed on Silica gel 60N (spherical neutral, 40-50 μm; Kanto Chemical Co., Inc.) or Chromatorex NH-DM2035 silica gel (Fuji Silysia Chemical Ltd.). Enantiomeric excesses were determined by HPLC analysis using chiral columns [φ 4.6 mm x 250 mm, DAICEL CHIRALPAK AD-3 (AD-3), CHIRALPAK AZ-3 (AZ-3), CHIRALPAK IC-3 (IC-3), CHIRALPAK IE-3 (IE-3), CHIRALPAK IF-3 (IF-3), and CHIRALCEL OZ-3 (OZ-3)] with hexane (H), 2-propanol (IPA), and ethanol (EtOH) as eluent.

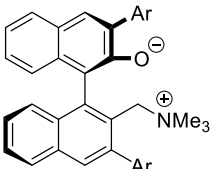
Toluene was supplied from Kanto Chemical Co., Inc. as “Dehydrated” and further purified by passing through neutral alumina under nitrogen atmosphere. Betaines²³, oxindoles³⁶, and *N*-Boc imines³⁷ were prepared by following literature procedure. Powdered 4Å molecular sieves (MS4A) was supplied by Sigma-Aldrich Co. Other simple chemicals were purchased and used as such.

Experimental Section:

Characterization of Betaine Precursor **1c**·HCl and Betaine **1c**:

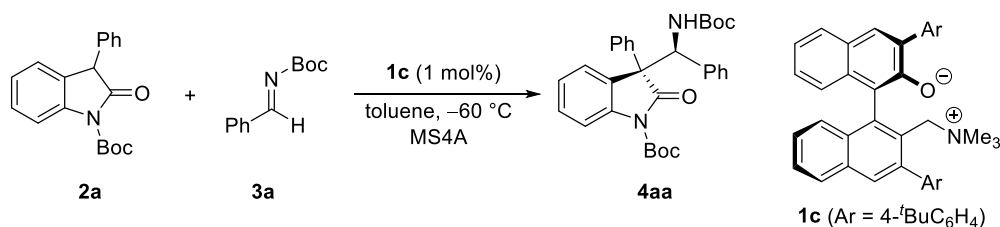

(Ar = 4-^tBuC₆H₄)

1c·HCl: ¹H NMR (600 MHz, (CD₃)₂SO, 80 °C) δ 8.73 (1H, s), 8.12 (2H, t, *J* = 3.9 Hz), 8.08 (1H, s), 8.02 (1H, d, *J* = 7.8 Hz), 7.66-7.63 (5H, m), 7.58 (2H, d, *J* = 7.8 Hz), 7.53 (2H, d, *J* = 7.8 Hz), 7.43 (1H, t, *J* = 7.8 Hz), 7.40 (1H, t, *J* = 7.8 Hz), 7.34 (1H, t, *J* = 7.8 Hz), 7.27 (1H, d, *J* = 7.8 Hz), 6.91 (1H, d, *J* = 7.8 Hz), 4.90 (1H, br), 4.85 (1H, br), 2.52 (9H, s), 1.40 (9H, s), 1.38 (9H, s); ¹³C NMR (151 MHz, (CD₃)₂SO, 80 °C) δ 150.4, 149.7, 140.8, 137.9, 134.7, 133.8, 132.3, 131.5, 130.9, 130.8, 129.3, 128.8, 128.3, 128.2, 127.9, 127.6, 126.9, 126.8, 126.5, 125.4, 124.6, 123.4, 117.7, 64.4, 53.6, 34.0, 33.9, 30.7₇, 30.7₃, five carbon atoms were not found probably due to broadening or overlapping; IR (film) 3439, 2961, 1717, 1622, 1474, 1364, 1267, 1148, 1067, 1026, 839, 752; HRMS (ESI) Calcd for C₄₄H₄₈NO⁺ ([M-Cl]⁺) 606.3730, Found 606.3718.


(Ar = 4-^tBuC₆H₄)

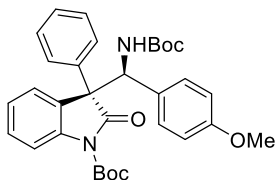
1c: ¹H NMR (600 MHz, CD₃OD) δ 7.97 (2H, br), 7.89 (1H, br), 7.83 (1H, br), 7.73 (1H, br), 7.62 (3H, br), 7.56 (3H, br), 7.47 (3H, d, *J* = 7.8 Hz), 7.38-7.20 (2H, br), 7.04 (1H, s), 6.79-6.69 (1H, br), 5.12 (1H, dd, *J* = 13.2, 29.4 Hz), 4.34 (1H, d, *J* = 13.2 Hz), 2.61 (5H, s), 2.23 (4H, s), 1.40 (9H, s), 1.36 (9H, s); ¹³C NMR analysis gave broad spectrum and it was not assignable; IR (film) 3402, 2961, 2361, 1609, 1485, 1423, 1393, 1269, 1152, 1024, 837, 752; HRMS (ESI) Calcd for C₄₄H₄₈NO⁺ [(M+H)⁺] 606.3730, Found 606.3725.

Representative Procedure for Asymmetric Mannich-type Reaction of Oxindole **2a** to Imine **3a** Catalyzed by Chiral Ammonium Betaine **1c**:

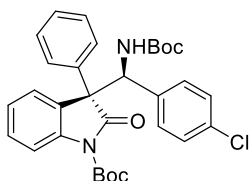


A magnetic stirrer bar and oven-dried 4Å molecular sieves (MS4A) (100.0 mg) were placed in an oven-dried test tube under argon (Ar) atmosphere. The test tube was heated with a heat gun under reduced pressure for 3 min and it was refilled with Ar. Then, chiral ammonium betaine **1c** (1.21 mg, 0.0020 mmol) and oxindole **2a** (61.9 mg, 0.2 mmol) were added to the test tube. After cooling to -60 °C, toluene (1.0 mL) and imine **3a** (49.3 mg, 0.24 mmol) were introduced and stirring was continued for 20 h. The reaction was quenched by the addition of a solution of trifluoroacetic acid in toluene (1.0 M, 2.0 μL) and hydrochloric acid (1.0 M, 2.0 mL). The aqueous phase was extracted with ethyl acetate (EA) twice. The combined organic phases were washed with brine, dried over Na₂SO₄, and filtered. All volatiles were removed by evaporation to afford the crude residue, which was analyzed by ¹H NMR (600 MHz) to determine the diastereomeric ratio (dr = >20:1). Purification of the residue by column chromatography on Silica gel 60N (H/EA = 10:1 to 5:1 as eluent) gave **4aa** as a mixture of isomers (113.8 mg, 92%). Enantiomeric ratio was determined by chiral stationary phase HPLC (98% ee). **4aa**: HPLC AD-3, H/IPA/EtOH = 48:1:1, flow rate = 0.3 mL/min, λ = 210 nm, 22.8 min (major isomer of major diastereomer), 25.7 min (minor diastereomer), 28.6 min (minor isomer of major diastereomer), 37.7 min (minor diastereomer); ¹H NMR

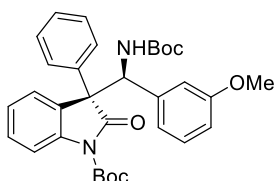
(600 MHz, CDCl₃) δ 7.65 (1H, d, J = 7.8 Hz), 7.53 (2H, d, J = 7.8 Hz), 7.48 (1H, brd, J = 7.8 Hz), 7.39-7.28 (5H, m), 7.11 (1H, t, J = 7.8 Hz), 7.04 (2H, t, J = 7.8 Hz), 6.80 (2H, d, J = 7.8 Hz), 5.92 (1H, br), 5.13 (1H, br), 1.47 (9H, s), 1.30 (9H, s); ¹³C NMR (151 MHz, CDCl₃) δ 174.3, 154.9, 148.6, 141.0, 137.1, 136.3, 129.5, 128.8, 128.7, 128.1, 127.9, 127.8, 127.7, 127.4, 125.4, 124.4, 115.5, 84.2, 80.4, 62.5, 59.5, 28.3, 28.1; IR (film) 2978, 1761, 1732, 1695, 1607, 1481, 1368, 1346, 1302, 1287, 1250, 1152, 1059 cm⁻¹; HRMS (ESI) Calcd for C₃₁H₃₄N₂NaO₅⁺ ([M+Na]⁺) 537.2360, Found 537.2359.



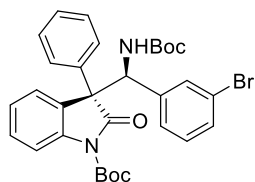
4ab: HPLC IE-3, H/EtOH = 19:1, flow rate = 0.5 mL/min, λ = 210 nm, 25.9 min (minor diastereomer), 30.3 min (minor diastereomer), 44.9 min (minor isomer of major diastereomer), 51.3 min (major isomer of major diastereomer); ¹H NMR (600 MHz, CDCl₃) δ 7.68 (1H, d, J = 7.8 Hz), 7.52 (2H, d, J = 7.8 Hz), 7.47 (1H, brd, J = 7.8 Hz), 7.38 (1H, t, J = 7.8 Hz), 7.34 (2H, t, J = 7.8 Hz), 7.32-7.27 (2H, m), 6.71 (2H, d, J = 8.7 Hz), 6.57 (2H, d, J = 8.7 Hz), 5.87 (1H, br), 5.10 (1H, brd, J = 6.0 Hz), 3.68 (3H, s), 1.48 (9H, s), 1.30 (9H, s); ¹³C NMR (151 MHz, CDCl₃) δ 174.4, 159.1, 154.8, 148.6, 141.0, 136.3, 129.4, 129.2, 128.9, 128.7, 128.6, 128.1, 127.5, 125.4, 124.4, 115.6, 113.0, 84.1, 80.2, 62.5, 58.9, 55.2, 28.3, 28.0; IR (film) 2980, 1761, 1732, 1697, 1611, 1514, 1368, 1346, 1304, 1288, 1252, 1153, 1034 cm⁻¹; HRMS (ESI) Calcd for C₃₂H₃₆N₂NaO₆⁺ ([M+Na]⁺) 567.2466, Found 567.2454.



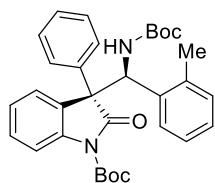
4ac: HPLC IF-3, H/EtOH = 97:3, flow rate = 0.3 mL/min, λ = 210 nm, 23.1 min (minor diastereomer), 26.3 min (minor diastereomer), 28.2 min (minor isomer of major diastereomer), 32.4 min (major isomer of major diastereomer); ¹H NMR (600 MHz, CDCl₃) δ 7.67 (1H, d, J = 7.8 Hz), 7.49 (2H, d, J = 7.8 Hz), 7.47 (1H, brd, J = 7.8 Hz), 7.39 (1H, t, J = 7.8 Hz), 7.35 (2H, t, J = 7.8 Hz), 7.32-7.29 (2H, m), 7.02 (2H, d, J = 7.8 Hz), 6.77 (2H, d, J = 7.8 Hz), 5.87 (1H, br), 5.17 (1H, br), 1.49 (9H, s), 1.30 (9H, s); ¹³C NMR (151 MHz, CDCl₃) δ 174.2, 154.8, 148.4, 140.9, 135.9, 135.8, 133.7, 129.6, 129.2, 128.7, 128.6, 128.3, 127.8, 126.9, 125.4, 124.5, 115.6, 84.4, 80.6, 62.2, 59.0, 28.3, 28.0; IR (film) 2980, 1759, 1732, 1695, 1607, 1491, 1368, 1346, 1304, 1287, 1250, 1150, 1098 cm⁻¹; HRMS (ESI) Calcd for C₃₁H₃₃³⁵ClN₂NaO₅⁺ [(M+Na)⁺] 571.1970, Found 571.1970.



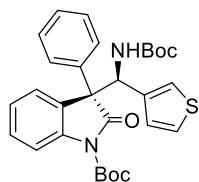
4ad: HPLC OZ-3, H/EtOH = 9:1, flow rate = 0.5 mL/min, λ = 210 nm, 8.3 min (minor diastereomer), 9.4 min (minor diastereomer), 10.2 min (minor isomer of major diastereomer), 12.2 min (major isomer of major diastereomer); ¹H NMR (600 MHz, CDCl₃) δ 7.69 (1H, d, J = 8.4 Hz), 7.53 (2H, d, J = 8.4 Hz), 7.47 (1H, brd, J = 8.4 Hz), 7.38 (1H, t, J = 8.4 Hz), 7.35 (2H, t, J = 8.4 Hz), 7.33-7.28 (2H, m), 6.95 (1H, t, J = 8.1 Hz), 6.66 (1H, dd, J = 2.1, 8.1 Hz), 6.40 (1H, d, J = 8.1 Hz), 6.33 (1H, s), 5.90 (1H, br), 5.11 (1H, br), 3.57 (3H, s), 1.48 (9H, s), 1.31 (9H, s); ¹³C NMR (151 MHz, CDCl₃) δ 174.2, 158.9, 154.8, 148.6, 141.1, 138.5, 136.2, 129.4, 128.7, 128.6, 128.1, 128.0, 127.3, 125.4, 124.3, 120.2, 115.6, 114.4, 112.5, 84.2, 80.3, 62.4, 59.5, 55.1, 28.3, 28.0; IR (film) 2978, 1761, 1732, 1695, 1603, 1491, 1368, 1346, 1304, 1288, 1252, 1152, 1053 cm⁻¹; HRMS (ESI) Calcd for C₃₂H₃₆N₂NaO₆⁺ ([M+Na]⁺) 567.2466, Found 567.2452.



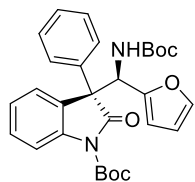
4ae: HPLC OZ-3, H/IPA = 99:1, flow rate = 0.5 mL/min, λ = 210 nm, 12.2 min (minor diastereomer), 16.1 min (minor diastereomer), 22.8 min (minor isomer of major diastereomer), 41.2 min (major isomer of major diastereomer); $^1\text{H NMR}$ (600 MHz, CDCl_3) δ 7.70 (1H, d, J = 7.8 Hz), 7.50 (2H, d, J = 7.8 Hz), 7.46 (1H, brd, J = 7.8 Hz), 7.40 (1H, t, J = 7.8 Hz), 7.36 (2H, t, J = 7.8 Hz), 7.34-7.30 (2H, m), 7.24 (1H, d, J = 7.8 Hz), 6.98 (1H, s), 6.91 (1H, t, J = 7.8 Hz), 6.75 (1H, d, J = 7.8 Hz), 5.85 (1H, br), 5.14 (1H, br), 1.51 (9H, s), 1.31 (9H, s); $^{13}\text{C NMR}$ (151 MHz, CDCl_3) δ 174.0, 154.8, 148.5, 140.8, 139.5, 135.8, 131.0, 130.9, 129.7, 129.1, 128.8, 128.6, 128.3, 126.8, 126.4, 125.3, 124.5, 121.7, 115.6, 84.5, 80.6, 62.2, 59.1, 28.3, 28.0; IR (film) 2978, 1761, 1734, 1697, 1607, 1570, 1479, 1368, 1346, 1302, 1288, 1252, 1151, 1059 cm^{-1} ; HRMS (ESI) Calcd for $\text{C}_{31}\text{H}_{33}^{79}\text{BrN}_2\text{NaO}_5^+$ ($[\text{M}+\text{Na}]^+$) 615.1465, Found 615.1451.



4af: HPLC IE-3, H/IPA = 23:2, flow rate = 0.5 mL/min, λ = 210 nm, 17.6 min (minor diastereomer), 20.7 min (minor isomer of major diastereomer), 22.6 min (major isomer of major diastereomer), 29.2 min (minor diastereomer); $^1\text{H NMR}$ (600 MHz, CDCl_3) δ 7.77 (1H, d, J = 7.8 Hz), 7.58 (2H, br), 7.50 (1H, br), 7.45 (1H, t, J = 7.8 Hz), 7.37-7.27 (4H, m), 7.07 (1H, d, J = 7.8 Hz), 7.02 (1H, t, J = 7.8 Hz), 6.72 (1H, t, J = 7.8 Hz), 6.35 (1H, br), 5.98 (1H, d, J = 7.8 Hz), 5.14 (1H, brd, J = 9.6 Hz), 2.57 (3H, s), 1.41 (9H, s), 1.32 (9H, s); $^{13}\text{C NMR}$ (151 MHz, CDCl_3) δ 173.9, 154.7, 148.6, 141.4, 136.9, 136.7, 136.2, 130.5, 129.6, 128.7, 128.5, 127.9, 127.8, 126.1, 125.7, 125.3, 124.5, 115.5, 83.8, 80.2, 61.8, 53.3, 28.3, 27.9, 20.2, one carbon atom was not found probably due to overlapping; IR (film) 2980, 1763, 1732, 1697, 1607, 1479, 1368, 1348, 1304, 1288, 1252, 1152, 1057 cm^{-1} ; HRMS (ESI) Calcd for $\text{C}_{32}\text{H}_{36}\text{N}_2\text{NaO}_5^+$ ($[\text{M}+\text{Na}]^+$) 551.2516, Found 551.2506.

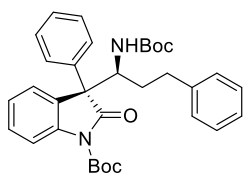


4ag: HPLC IC-3, H/EtOH = 49:1, flow rate = 0.3 mL/min, λ = 210 nm, 22.2 min (minor diastereomer), 24.2 min (minor diastereomer), 30.8 min (minor isomer of major diastereomer), 34.9 min (major isomer of major diastereomer); $^1\text{H NMR}$ (600 MHz, CDCl_3) δ 7.73 (1H, d, J = 7.8 Hz), 7.53 (2H, d, J = 7.8 Hz), 7.49 (1H, br), 7.39 (1H, t, J = 7.8 Hz), 7.34 (2H, t, J = 7.8 Hz), 7.29 (2H, t, J = 7.8 Hz), 6.96 (1H, dd, J = 2.6, 4.8 Hz), 6.81 (1H, d, J = 2.6 Hz), 6.36 (1H, d, J = 4.8 Hz), 6.06 (1H, br), 5.10 (1H, br), 1.51 (9H, s), 1.31 (9H, s); $^{13}\text{C NMR}$ (151 MHz, CDCl_3) δ 174.4, 154.8, 148.7, 141.0, 138.3, 136.0, 129.4, 128.6, 128.5, 128.1, 127.6, 126.4, 125.3, 124.8, 124.4, 123.3, 115.5, 84.3, 80.4, 62.2, 55.8, 28.3, 28.1; IR (film) 2978, 2916, 1761, 1732, 1695, 1607, 1481, 1368, 1348, 1302, 1288, 1252, 1152, 1057 cm^{-1} ; HRMS (ESI) Calcd for $\text{C}_{29}\text{H}_{32}\text{N}_2\text{NaO}_5\text{S}^+$ ($[\text{M}+\text{Na}]^+$) 543.1924, Found 543.1922.

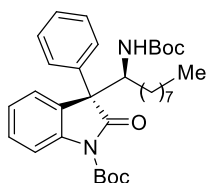


4ah: HPLC AD-3, H/IPA = 19:1, flow rate = 0.5 mL/min, λ = 210 nm, 16.1 min (major isomer of major diastereomer), 21.3 min (minor isomer of major diastereomer), 27.6 min (minor diastereomer), 49.2 min (minor diastereomer); $^1\text{H NMR}$ (600 MHz, CDCl_3) δ 7.80 (1H, d, J = 8.4 Hz), 7.51 (2H, brd, J = 7.2 Hz), 7.45 (1H, br), 7.37 (1H, dt, J = 1.5, 8.0 Hz), 7.31 (2H, t, J = 7.2 Hz), 7.30-7.24 (2H, m), 7.02 (1H, s), 6.10 (1H, dd, J = 1.8, 3.0 Hz), 6.10 (1H, br), 5.94 (1H, br), 5.16 (1H, brd, J = 10.2 Hz), 1.56 (9H, s), 1.32 (9H, s); $^{13}\text{C NMR}$ (151 MHz, CDCl_3) δ 174.2, 154.7, 150.8, 149.0, 142.0, 140.5, 135.8, 129.2, 128.5, 128.4, 128.0, 127.3, 125.4, 124.3, 115.4, 110.1, 107.6, 84.3, 80.3, 61.6, 54.2, 28.2, 28.1; IR (film) 2980, 1763, 1730, 1697, 1607, 1481, 1368, 1346, 1302, 1287, 1252, 1150, 1061 cm^{-1} ; HRMS (ESI) Calcd for

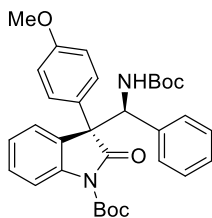
$C_{29}H_{32}N_2NaO_6^+$ ($[M+Na]^+$) 527.2153, Found 527.2144.



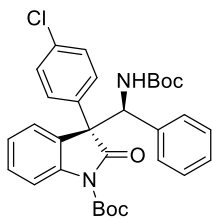
4ai: Purification by column chromatography was performed on Chromatorex NH-DM2035 silica gel (H/EA = 50:1 to 10:1 as eluent). HPLC AD-3, H/IPA = 19:1, flow rate = 0.5 mL/min, $\lambda = 210$ nm, 11.3 min (minor diastereomer), 14.1 min (minor isomer of major diastereomer), 16.2 min (major isomer of major diastereomer), 26.6 min (minor diastereomer); 1H NMR (600 MHz, CD_3CN) δ 7.84 (1H, d, $J = 7.8$ Hz), 7.41-7.38 (2H, m), 7.29-7.23 (8H, m), 7.16 (1H, t, $J = 7.8$ Hz), 7.11 (2H, d, $J = 7.8$ Hz), 5.34 (1H, d, $J = 10.8$ Hz), 4.81 (1H, t, $J = 10.8$ Hz), 2.66-2.62 (1H, m), 2.54-2.49 (1H, m), 1.57 (11H, s), 1.29 (9H, s); ^{13}C NMR (151 MHz, CD_3CN) δ 176.1, 156.9, 149.8, 142.5, 140.9, 139.1, 129.7, 129.5, 129.3₂, 129.2₈, 128.7, 128.6, 126.9, 126.7, 125.3, 115.8, 85.2, 79.6, 62.6, 56.3, 34.6, 33.1, 28.5, 28.3, one carbon atom was not found probably due to overlapping; IR (film) 2978, 1759, 1732, 1694, 1605, 1497, 1479, 1366, 1348, 1304, 1287, 1248, 1148, 1057, 908 cm^{-1} ; HRMS (ESI) Calcd for $C_{33}H_{38}N_2NaO_5^+$ ($[M+Na]^+$) 565.2673, Found 565.2668.



4aj: Purification by column chromatography was performed on Chromatorex NH-DM2035 silica gel (H/EA = 50:1 to 10:1 as eluent). HPLC AZ-3, H/IPA = 97:3, flow rate = 0.5 mL/min, $\lambda = 210$ nm, 11.3 min (minor diastereomer), 12.4 min (major isomer of major diastereomer), 14.5 min (minor isomer of major diastereomer), 27.2 min (minor diastereomer); 1H NMR (600 MHz, CD_3CN) δ 7.88 (1H, d, $J = 7.8$ Hz), 7.42 (2H, t, $J = 7.8$ Hz), 7.36 (2H, d, $J = 7.8$ Hz), 7.30-7.25 (4H, m), 5.15 (1H, d, $J = 10.8$ Hz), 4.78 (1H, t, $J = 10.8$ Hz), 1.58 (9H, s), 1.26 (13H, br), 1.22 (10H, br), 0.86 (3H, t, $J = 7.2$ Hz); ^{13}C NMR (151 MHz, CD_3CN) δ 176.2, 157.0, 149.9, 141.0, 139.2, 129.7₄, 129.6₈, 129.3, 128.8, 128.6, 126.7, 125.3, 115.9, 85.2, 79.5, 62.6, 56.6, 32.6, 32.3, 30.1, 29.8, 29.6, 28.5, 28.3, 26.9, 23.3, 14.4; IR (film) 2928, 1759, 1732, 1694, 1607, 1464, 1366, 1348, 1302, 1287, 1248, 1148, 1057, 910 cm^{-1} ; HRMS (ESI) Calcd for $C_{33}H_{46}N_2NaO_5^+$ ($[M+Na]^+$) 573.3299, Found 573.3305.

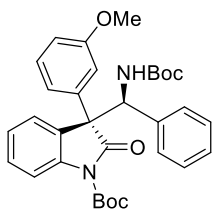


4ba: HPLC OZ-3, H/IPA/EtOH = 48:1:1, flow rate = 0.3 mL/min, $\lambda = 210$ nm, 17.7 min (minor diastereomer), 19.2 min (minor diastereomer), 23.7 min (major isomer of major diastereomer), 28.5 min (minor isomer of major diastereomer); 1H NMR (600 MHz, $CDCl_3$) δ 7.64 (1H, d, $J = 7.8$ Hz), 7.47 (1H, br), 7.44 (2H, d, $J = 7.8$ Hz), 7.35 (1H, t, $J = 7.8$ Hz), 7.29 (1H, t, $J = 7.8$ Hz), 7.09 (1H, t, $J = 7.8$ Hz), 7.03 (2H, t, $J = 7.8$ Hz), 6.88 (2H, d, $J = 7.8$ Hz), 6.80 (2H, d, $J = 7.8$ Hz), 5.86 (1H, br), 5.19 (1H, d, $J = 8.4$ Hz), 3.78 (3H, s), 1.47 (9H, s), 1.30 (9H, s); ^{13}C NMR (151 MHz, $CDCl_3$) δ 174.6, 159.4, 154.9, 148.6, 140.8, 137.1, 129.9, 129.3, 128.1, 127.7₁, 127.6₇, 127.6, 125.9, 125.3, 124.3, 115.4, 114.0, 84.0, 80.2, 61.8, 59.4, 55.3, 28.2, 28.0; IR (film) 2978, 1761, 1732, 1697, 1607, 1512, 1368, 1346, 1304, 1288, 1252, 1152, 1034 cm^{-1} ; HRMS (ESI) Calcd for $C_{32}H_{36}N_2NaO_6^+$ ($[M+Na]^+$) 567.2466, Found 567.2465.

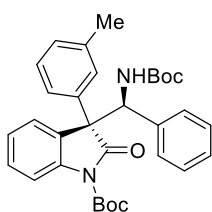


4ca: HPLC AD-3, H/IPA = 97:3, flow rate = 0.5 mL/min, $\lambda = 210$ nm, 19.4 min (major isomer of major diastereomer), 24.2 min (minor diastereomer), 26.0 min (minor isomer of major diastereomer), 31.1 min (minor diastereomer); 1H NMR (600 MHz, $CDCl_3$) δ 7.65 (1H, d, $J = 8.0$ Hz), 7.50 (2H, d, $J = 8.0$ Hz), 7.47 (1H, br), 7.38 (1H, t, $J = 8.0$ Hz), 7.34-7.28 (3H, m), 7.11 (1H, t, $J = 8.0$ Hz), 7.04 (2H, t, $J = 8.0$ Hz), 6.78 (2H, d, $J = 8.0$ Hz), 5.89 (1H, br), 5.22 (1H, br), 1.47 (9H, s), 1.31 (9H, s); ^{13}C NMR (151 MHz, $CDCl_3$) δ 174.0, 154.8, 148.4, 140.9, 136.7, 134.8, 134.2, 130.2, 129.6, 128.6, 128.0, 127.7, 127.6, 126.8, 125.2, 124.5, 115.6, 84.3, 80.5, 62.1, 59.4, 28.2, 28.0; IR (film) 2926, 1763,

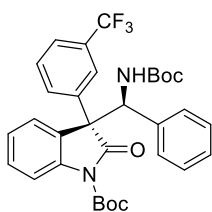
1734, 1697, 1607, 1493, 1368, 1346, 1304, 1287, 1252, 1152, 1098 cm^{-1} ; HRMS (ESI) Calcd for $\text{C}_{31}\text{H}_{33}^{35}\text{ClN}_2\text{NaO}_5^+$ ($[\text{M}+\text{Na}]^+$) 571.1970, Found 571.1961.



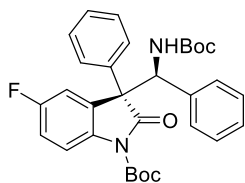
4da: HPLC OZ-3, H/EtOH = 97:3, flow rate = 0.5 mL/min, $\lambda = 210$ nm, 10.6 min (minor isomer of major diastereomer), 12.6 min (minor diastereomer), 16.5 min (minor diastereomer), 24.5 min (major isomer of major diastereomer); ^1H NMR (600 MHz, CDCl_3) δ 7.64 (1H, d, $J = 8.4$ Hz), 7.46 (1H, br), 7.36 (1H, t, $J = 8.1$ Hz), 7.29 (1H, t, $J = 7.8$ Hz), 7.26-7.23 (1H, m), 7.14 (1H, s), 7.10 (1H, t, $J = 7.2$ Hz), 7.03 (3H, t, $J = 7.5$ Hz), 6.85 (1H, d, $J = 7.8$ Hz), 6.80 (2H, d, $J = 7.8$ Hz), 5.92 (1H, br), 5.17 (1H, br), 3.80 (3H, s), 1.47 (9H, s), 1.31 (9H, s); ^{13}C NMR (151 MHz, CDCl_3) δ 174.1, 159.8, 154.9, 148.5, 140.9, 139.9, 138.9, 137.8, 137.0, 129.4, 127.8, 127.7, 127.6, 125.3, 124.4, 121.0, 115.4, 113.9, 113.2, 84.1, 80.3, 62.4, 58.8, 55.4, 28.3, 28.0; IR (film) 2978, 1759, 1732, 1695, 1603, 1493, 1368, 1344, 1302, 1288, 1252, 1150, 1059 cm^{-1} ; HRMS (ESI) Calcd for $\text{C}_{32}\text{H}_{36}\text{N}_2\text{NaO}_6^+$ ($[\text{M}+\text{Na}]^+$) 567.2466, Found 567.2456.



4ea: HPLC AD-3, H/IPA = 97:3, flow rate = 0.5 mL/min, $\lambda = 210$ nm, 13.7 min (major isomer of major diastereomer), 15.6 min (minor diastereomer), 18.2 min (minor isomer of major diastereomer), 28.7 min (minor diastereomer); ^1H NMR (600 MHz, CDCl_3) δ 7.65 (1H, d, $J = 7.8$ Hz), 7.44 (1H, br), 7.37-7.34 (2H, m), 7.29 (1H, t, $J = 7.2$ Hz), 7.23-7.20 (2H, m), 7.11 (1H, d, $J = 6.6$ Hz), 7.09 (1H, d, $J = 7.8$ Hz), 7.03 (2H, t, $J = 7.5$ Hz), 6.80 (2H, d, $J = 7.2$ Hz), 5.92 (1H, br), 5.18 (1H, brd, $J = 9.0$ Hz), 2.33 (3H, s), 1.47 (9H, s), 1.31 (9H, s); ^{13}C NMR (151 MHz, CDCl_3) δ 174.3, 154.9, 148.6, 140.9, 138.2, 137.1, 136.3, 129.34, 129.30, 128.9, 128.4, 127.7, 127.6, 126.3, 126.2, 125.7, 125.3, 124.4, 115.4, 84.0, 80.2, 62.4, 59.0, 28.2, 28.0, 21.7; IR (film) 2978, 1761, 1732, 1699, 1605, 1481, 1368, 1344, 1032, 1287, 1250, 1150, 1096, 1061, 910 cm^{-1} ; HRMS (ESI) Calcd for $\text{C}_{32}\text{H}_{36}\text{N}_2\text{NaO}_5^+$ ($[\text{M}+\text{Na}]^+$) 551.2516, Found 551.2507.

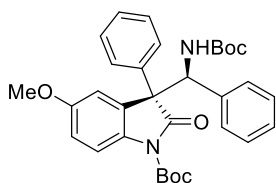


4fa: HPLC IE-3, H/IPA = 19:1, flow rate = 0.5 mL/min, $\lambda = 210$ nm, 15.2 min (minor diastereomer), 16.8 min (minor isomer of major diastereomer), 19.1 min (minor diastereomer), 22.7 min (major isomer of major diastereomer); ^1H NMR (600 MHz, CDCl_3) δ 7.80 (2H, br), 7.68 (1H, d, $J = 7.8$ Hz), 7.58 (1H, d, $J = 7.8$ Hz), 7.49 (2H, t, $J = 7.8$ Hz), 7.41 (1H, dt, $J = 1.8, 7.8$ Hz), 7.35 (1H, t, $J = 7.8$ Hz), 7.13 (1H, t, $J = 7.8$ Hz), 7.05 (2H, t, $J = 7.8$ Hz), 6.77 (2H, d, $J = 7.8$ Hz), 5.99 (1H, br), 5.19 (1H, brd, $J = 10.2$ Hz), 1.47 (9H, s), 1.30 (9H, s); ^{13}C NMR (151 MHz, CDCl_3) δ 173.8, 154.7, 148.4, 141.1, 137.5, 136.5, 132.5, 130.8 (q, $J_{\text{F-C}} = 32.8$ Hz), 129.9, 129.0, 128.1, 127.8, 127.7, 126.6, 125.5, 125.4, 125.0, 124.7, 124.2 (q, $J_{\text{F-C}} = 272.8$ Hz), 115.7, 84.4, 80.6, 62.5, 59.4, 28.2, 28.0; ^{19}F NMR (373 MHz, CDCl_3) δ -62.3; IR (film) 2980, 1761, 1734, 1697, 1607, 1481, 1369, 1346, 1329, 1287, 1252, 1152, 1128, 1080 cm^{-1} ; HRMS (ESI) Calcd for $\text{C}_{32}\text{H}_{33}\text{F}_3\text{N}_2\text{NaO}_5^+$ ($[\text{M}+\text{Na}]^+$) 605.2234, Found 605.2220.



4ga: HPLC IE-3, H/IPA = 19:1, flow rate = 0.5 mL/min, $\lambda = 210$ nm, 18.5 min (minor diastereomer), 21.5 min (minor diastereomer), 28.1 min (minor isomer of major diastereomer), 29.8 min (major isomer of major diastereomer); ^1H NMR (400 MHz, CDCl_3) δ 7.65 (1H, dd, $J_{\text{H-H}} = 4.4$ Hz, $J_{\text{F-H}} = 9.2$ Hz), 7.52 (2H, d, $J = 8.8$ Hz), 7.40-7.28 (3H, m), 7.27 (1H, br), 7.15-7.00 (4H, m), 6.86 (2H, d, $J = 7.2$ Hz), 5.91 (1H, br), 5.24 (1H, br), 1.47 (9H, s), 1.29 (9H, s); ^{13}C NMR (100 MHz, CDCl_3) δ 173.9, 159.7 (d, $J_{\text{F-C}} = 245.3$ Hz), 154.9, 148.5, 136.9 (d, $J_{\text{F-C}} = 6.8$ Hz), 135.6, 129.0, 128.7, 128.6, 128.3, 127.9, 127.73, 127.66, 116.7 (d, $J_{\text{F-C}} = 7.7$ Hz), 115.9 (d, $J_{\text{F-C}} = 22.1$ Hz), 113.1 (d, $J_{\text{F-C}} = 22.1$

Hz), 84.3, 80.5, 62.7, 59.8, 28.2, 28.0, one carbon atom was not found probably due to overlapping; ^{19}F NMR (373 MHz, CDCl_3) δ -117.0; IR (film) 2980, 1765, 1732, 1695, 1607, 1483, 1368, 1346, 1298, 1269, 1244, 1150, 1059 cm^{-1} ; HRMS (ESI) Calcd for $\text{C}_{31}\text{H}_{33}\text{FN}_2\text{NaO}_5^+$ ($[\text{M}+\text{Na}]^+$) 555.2266, Found 555.2255.



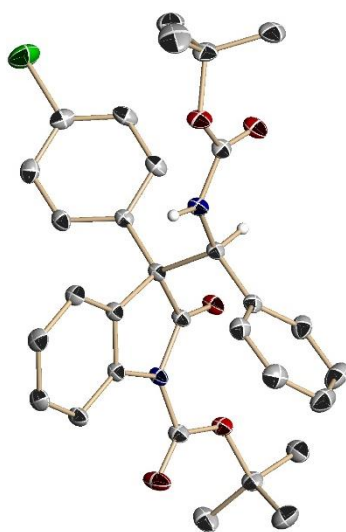
4ha: HPLC OZ-3, H/EtOH = 97:3, flow rate = 0.5 mL/min, λ = 210 nm, 11.2 min (minor diastereomer), 13.5 min (minor diastereomer), 20.2 min (minor isomer of major diastereomer), 28.2 min (major isomer of major diastereomer); ^1H NMR (600 MHz, CDCl_3) δ 7.59 (1H, d, J = 7.8 Hz), 7.53 (2H, d, J = 7.8 Hz), 7.35 (2H, t, J = 7.8 Hz), 7.30 (1H, t, J = 7.8 Hz), 7.12 (1H, t, J = 7.8 Hz), 7.06 (2H, t, J = 7.8 Hz), 7.03 (1H, s), 6.89 (1H, d, J = 7.8 Hz), 6.84 (2H, d, J = 7.8 Hz), 5.92 (1H, br), 5.17 (1H, brd, J = 7.8 Hz), 3.88 (3H, s), 1.46 (9H, s), 1.30 (9H, s); ^{13}C NMR (151 MHz, CDCl_3) δ 174.2, 156.7, 154.8, 148.6, 137.1, 136.2, 134.5, 128.7, 128.6, 128.1, 127.8₃, 127.7₈, 127.6, 125.9, 116.3, 113.2, 112.4, 83.9, 80.3, 62.7, 59.1, 55.9, 28.3, 28.0; IR (film) 2978, 1759, 1728, 1694, 1599, 1487, 1368, 1300, 1279, 1246, 1152, 1036 cm^{-1} ; HRMS (ESI) Calcd for $\text{C}_{32}\text{H}_{36}\text{N}_2\text{NaO}_6^+$ ($[\text{M}+\text{Na}]^+$) 567.2466, Found 567.2451.

Crystallographic Structure Determination: The single crystal, obtained by the procedure described below, was mounted on MicroMesh. Data of X-ray diffraction were collected at 123 K on a Rigaku FR-X with Pilatus 200K with fine-focus sealed tube Mo/ $K\alpha$ radiation (λ = 0.71075 Å). An absorption correction was made using Crystal Structure. The structure was solved by direct methods and Fourier syntheses, and refined by full-matrix least squares on F^2 by using SHELXL-2014.³⁸ All non-hydrogen atoms were refined with anisotropic displacement parameters. A hydrogen atom bonded to a nitrogen atom was located from a difference synthesis and their coordinates and isotropic thermal parameters refined. The other hydrogen atoms were placed in calculated positions and isotropic thermal parameters refined.

Recrystallization of 4ac: Recrystallization of **4ac** was performed by using a $\text{CHCl}_3/\text{Et}_2\text{O}$ solvent system at room temperature.

Table S1. Crystal data and structure refinement for cat **4ac**.

Empirical formula	C ₃₁ H ₃₃ Cl N ₂ O ₅	
Formula weight	549.04	
Temperature	123(2) K	
Wavelength	0.71075 Å	
Crystal system	Monoclinic	
Space group	P21	
Unit cell dimensions	a = 8.9878(10) Å	$\alpha = 90^\circ$
	b = 14.6983(18) Å	$\beta = 90.983(3)^\circ$
	c = 10.8669(13) Å	$\gamma = 90^\circ$
Volume	1435.4(3) Å ³	
Z	2	
Density (calculated)	1.270 Mg/m ³	
Absorption coefficient	0.175 mm ⁻¹	
F(000)	580	
Crystal size	0.30 x 0.20 x 0.10 mm ³	
Theta range for data collection	3.2 to 27.5°	
Index ranges	-10 ≤ h ≤ 10, -17 ≤ k ≤ 17, -23 ≤ l ≤ 11	
Reflections collected	9914	
Independent reflections	4860 [R _{int} = 0.0128]	
Completeness to theta = 27.48°	98.4 %	
Absorption correction	Semi-empirical from equivalents	
Max. and min. transmission	0.886 and 1.000	
Refinement method	Full-matrix least-squares on F ²	
Data / restraints / parameters	4860 / 1 / 363	
Goodness-of-fit on F ²	1.080	
Final R indices [I > 2σ(I)]	R ₁ = 0.0241, wR ₂ = 0.0626	
R indices (all data)	R ₁ = 0.0244, wR ₂ = 0.0628	
Absolute structure parameter	0.003(11)	
Largest diff. peak and hole	0.237 and -0.295 e.Å ⁻³	

**Fig. S1.** Molecular structure of **4ac**. The thermal ellipsoids of non-hydrogen atoms are shown at the 50% probability level. Blue = nitrogen, green = chlorine, red = oxygen, black = carbon.

References

- (1) Marti, C.; Carreira, E. M. *Eur. J. Org. Chem.* **2003**, 2209.
- (2) Galliford, C. V.; Scheidt, K. A. *Angew. Chem. Int. Ed.* **2007**, *46*, 8748.
- (3) Trost, B. M.; Brennan, M. K. *Synthesis* **2009**, 3003.
- (4) Singh, G. S.; Desta, Z. Y. *Chem. Rev.* **2012**, *112*, 6104.
- (5) Zhou, F.; Liu, Y.-L.; Zhou, J. *Adv. Synth. Catal.* **2010**, *352*, 1381.
- (6) Dalpozzo, R.; Bartoli, G.; Bencivenni, G. *Chem. Soc. Rev.* **2012**, *41*, 7247.
- (7) Cao, Z.-Y.; Wang, Y.-H.; Zeng, X.-P.; Zhou, J. *Tetrahedron Lett.* **2014**, *55*, 2571.
- (8) Ziarani, G. M.; Gholamzadeh, P.; Lashgari, N.; Hajiabbasi, P. *ARKIVOC* **2013**, (i), 470.
- (9) Ting, A.; Schaus, S. E. *Eur. J. Org. Chem.* **2007**, 5797.
- (10) Verkade, J. M. M.; van Hemert, L. J. C.; Quaedflieg, P. J. L. M.; Rutjes, F. P. J. T. *Chem. Soc. Rev.* **2008**, *37*, 29.
- (11) Xiao-Hua, C.; Bing, X. *ARKIVOC* **2013**, (i), 264.
- (12) Tian, X.; Jiang, K.; Peng, J.; Du, W.; Chen, Y.-C. *Org. Lett.* **2008**, *10*, 3583.
- (13) Cheng, L.; Liu, L.; Jia, H.; Wang, D.; Chen, Y.-J. *J. Org. Chem.* **2009**, *74*, 4650.
- (14) He, R.; Ding, C.; Maruoka, K. *Angew. Chem. Int. Ed.* **2009**, *48*, 4559.
- (15) Jin, Y.; Chen, D.; Zhang, X. R. *Chirality* **2014**, *26*, 801.
- (16) Shimizu, S.; Tsubogo, T.; Xu, P.; Kobayashi, S. *Org. Lett.* **2015**, *17*, 2006.
- (17) Trost, B. M. *Synthesis* **2006**, 369.
- (18) Cozzil, P. G.; Hilgraf, R.; Zimmermann, N. *Eur. J. Org. Chem.* **2007**, 5969.
- (19) Bella, M.; Gasperi, T. *Synthesis* **2009**, 1583.
- (20) Minko, Y.; Marek, I. *Chem. Commun.* **2014**, *50*, 12597.
- (21) Vetica, F.; de Figueiredo, R. M.; Orsini, M.; Tofani, D.; Gasperi, T. *Synthesis* **2015**, *47*, 2139.
- (22) Uraguchi, D.; Koshimoto, K.; Ooi, T. *J. Am. Chem. Soc.* **2008**, *130*, 10878.
- (23) Uraguchi, D.; Koshimoto, K.; Ooi, T. *Chem. Commun.* **2010**, *46*, 300.
- (24) Uraguchi, D.; Koshimoto, K.; C. Sanada, Ooi, T. *Tetrahedron: Asymmetry* **2010**, *21*, 1189.
- (25) Uraguchi, D.; Oyaizu, K.; Ooi, T. *Chem. Eur. J.* **2012**, *18*, 8306.
- (26) Uraguchi, D.; Oyaizu, K.; Noguchi, H.; Ooi, T. *Chem. Asian J.* **2015**, *10*, 334.
- (27) Oyaizu, K.; Uraguchi, D.; Ooi, T. *Chem. Commun.* **2015**, *51*, 4437.
- (28) Zhang, W.-Q.; Cheng, L.-F.; Yu, J.; Gong, L.-Z. *Angew. Chem. Int. Ed.* **2012**, *51*, 4085.
- (29) Claraz, A.; Landelle, G.; Oudeyer, S.; Levacher, V. *Eur. J. Org. Chem.* **2013**, 7693.
- (30) Wang, Y.-B.; Sun, D.-S.; Zhou, H.; Zhang, W.-Z.; Lu, X.-B. *Green Chem.* **2014**, *16*, 2266.
- (31) Tsutsumi, Y.; Yamakawa, K.; Yoshida, M.; Ema, T.; Sakai, T. *Org. Lett.* **2010**, *12*, 5728.
- (32) Guillermin, B.; Lemaire, V.; Cornil, J.; Lazzaroni, R.; Dubois, P.; Coulembier, O. *Chem. Commun.* **2014**, *50*, 10098.
- (33) Uraguchi, D.; Koshimoto, K.; Miyake, S.; Ooi, T. *Angew. Chem. Int. Ed.* **2010**, *49*, 5567.
- (34) Uraguchi, D.; Koshimoto, K.; Ooi, T. *J. Am. Chem. Soc.* **2012**, *134*, 6972.
- (35) Vesely, J.; Rios, R. *Chem. Soc. Rev.* **2014**, *43*, 611.
- (36)(a) Hamashima, Y.; Suzuki, T.; Takano, H.; Shimura, Y.; Sodeoka, M. *J. Am. Chem. Soc.* **2005**, *127*, 10164. (b) Duan, S.-W.; An, J.; Chen, J.-R.; Xiao, W.-J. *Org. Lett.* **2011**, *13*, 2290.
- (37)(a) Wenzel, A. G.; Jacobsen, E. N. *J. Am. Chem. Soc.* **2002**, *124*, 12964. (b) Song, J.; Wang, Y.; Deng, L. *J. Am.*

Chem. Soc. **2006**, *128*, 604

(38) Sheldrick, G. M. *Acta Cryst.* 2015, **C71**, 3.

Chapter 3

Stereoselective Aza-Henry Reaction of 3-Nitro Dihydro-2(3*H*)-Quinolones with *N*-Boc Aldimines under the Catalysis of Chiral Ammonium Betaines

Abstract – First asymmetric aza-Henry reaction of 3-nitro dihydro-2(3*H*)-quinolones with *N*-Boc aldimines was developed in highly enantioselective manner by using a chiral ammonium betaine as a catalyst. The protocol provides a direct synthetic method and casts light on reliability of α -functionalization of dihydroquinolones for accessing hydroquinoline derivatives having tetrasubstituted stereogenic carbon center at C3 position.

Introduction

Optically pure *N*-heterocyclic compounds constitute a common structural core of putative chemotherapeutics and natural products. Among them, hydroquinoline derivatives have attracted much attention owing to their prominent pharmaceutical activities.¹ In particular, dihydro-2(3*H*)-quinolones have emerged as a valuable scaffold for the assembly of stereochemically defined, chiral tetrahydroquinoline frameworks. The previously known catalytic approaches toward the synthesis of chiral hydroquinolones mostly rely on the construction of the heterocyclic ring, possessing an enantiomerically enriched C4-carbon, by means of asymmetric cyclizations.²⁻⁵ Although the enantioselective α -functionalization of the carbonyl moiety of hydroquinolones could provide a direct method for the installation of a tetrasubstituted stereogenic carbon center at the C3 position of this important class of heterocycles, this possibility remains unexplored and no catalytic systems are available for enabling this mode of bond formation with rigorous absolute stereocontrol.⁶ With this methodological deficiency in mind, we envisaged that *C*₁-symmetric chiral ammonium betaines of type **1** (Fig. 1) would function as an effective organic base catalyst for facilitating the enolization of hydroquinolones, bearing a suitable electron-withdrawing functionality at the carbonyl α -carbon, and subsequent stereoselective bond connections. This hypothesis was based on the consideration of the ability of the conjugate acids of **1** to precisely recognize and control reactive enolates through cooperative hydrogen-bonding and ionic interactions.⁷⁻¹¹ Herein, we report the development of the first highly stereoselective aza-Henry reaction of 3-nitro dihydro-2(3*H*)-quinolones **2** with *N*-Boc aldimines **3** under the catalysis of **1**.¹²⁻¹⁴

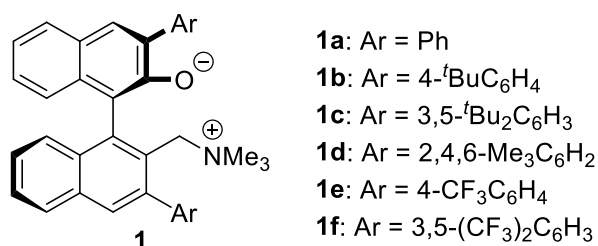


Figure 1 Chiral Ammonium Betaines

Results and Discussion

Initial investigation was made by treating *N*-benzyl 3-nitro dihydro-2(3*H*)-quinolone (**2a**) with *N*-Boc benzaldimine (**3a**) in toluene at 0 °C in the presence of chiral ammonium betaine **1a** (2 mol%) and molecular sieves 4 Å (MS4A)¹⁵ (Table 1, entry 1). The reaction proceeded smoothly to give the desired aza-Henry adduct **4a** as a mixture of diastereomers in a ratio of 1.8:1, which was determined by 600 MHz ¹H NMR analysis of the crude aliquot. After the standard silica gel column chromatography, **4a** was isolated in 91% yield and enantiomeric excesses of both diastereomers were revealed to be 92% ee and 90% ee, respectively, by chiral HPLC analysis. Encouraged by these promising results, we next evaluated the effect of the catalyst structure on the reactivity and selectivity. While increase in the steric demand of the 3,3'-substituents of **1** led to the considerable decrease in the catalytic activity and stereocontrolling ability (entries 2-4), introduction of electron-deficient aromatic appendages, particularly 3,5-bis(trifluoromethyl)phenyl group (**1f**), delivered marked improvement in diastereo- and enantioselectivity (entries 5

and 6). It should be noted that catalyst loading can be reduced into 1 mol% without sacrificing reaction efficiency and stereoselectivity by conducting the reaction at higher substrate concentration (0.2 M with respect to **2**) (entry 7).

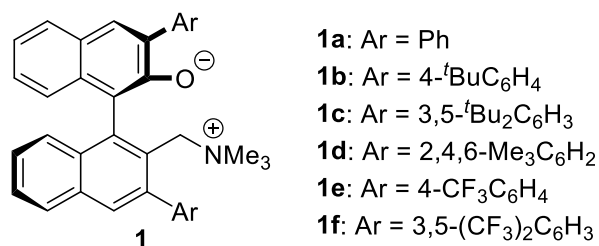
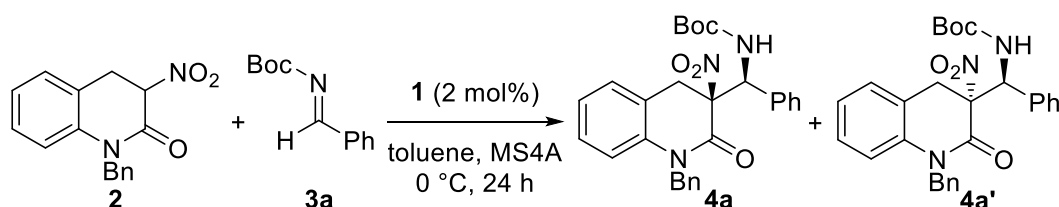


Figure 1 Chiral Ammonium Betaines

Table 1 Catalyst Optimization^a

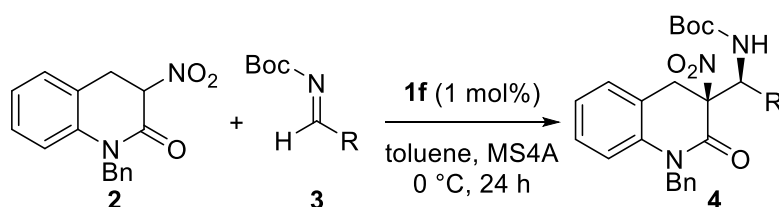


entry	1	yield (%) ^b	dr ^c	ee (%) ^d
1	1a (Ar = Ph)	91	1.8:1	92/90
2	1b (Ar = 4- <i>t</i> BuC ₆ H ₄)	94	1.4:1	90/86
3	1c (Ar = 3,5- <i>t</i> Bu ₂ C ₆ H ₃)	63	1:1.4	38/2.3
4	1d (Ar = 2,4,6-Me ₃ C ₆ H ₂)	68	1:1.6	29/39
5	1e (Ar = 4-CF ₃ C ₆ H ₄)	96	2.3:1	98/96
6	1f (Ar = 3,5-(CF ₃) ₂ C ₆ H ₃)	88	6.5:1	99/93
7 ^e	1f	99	6.6:1	99/92

^a Unless otherwise noted, the reaction was performed with 0.1 mmol of **2a**, 0.11 mmol of **3a**, and 2 mol% of **1** in toluene (1.0 mL) with MS4A (100 mg) at 0 °C. ^b Isolated yield. ^c Diastereomeric ratios were determined by 600 MHz ¹H NMR analysis of crude aliquots. ^d Enantiomeric excesses were analyzed by chiral stationary phase HPLC. Relative and absolute configurations of **4a** was assigned as analogy to **4g** (vide infra). ^e 1 mol% of **1f** was used in 1.0 mL of toluene on 0.2 mmol scale.

The optimal catalyst **1f** and the reaction conditions were then used for probing the scope of *N*-Boc aldimine **3** (Table 2). With substituted benzaldehyde-derived *N*-Boc imines **3b-3h**, excellent enantioselectivity was consistently observed irrespective of their steric and electronic properties, while diastereoselectivity was generally moderate (entries 1-7). Although nearly complete enantiocontrol was feasible, higher catalyst loading was required for ensuring the sufficient conversion of *N*-Boc 2-naphthaldimine **3i** (entry 8). A relatively high level of diastereoselectivity was attained in the reaction with imine **3j** derived from 3-thiophenecarboxaldehyde and the corresponding aza-Henry adduct **4j** was obtained in an almost enantiomerically pure form (entry 9). When aliphatic *N*-Boc aldimines were employed as an electrophile, substantial erosion of reactivity and stereoselectivity was inevitable (entries 10 and 11).

Table 2 Substrate Generality^a



entry	R (3)	yield (%) ^b	dr ^c	ee (%) ^d	prod.
1	4-MeOC ₆ H ₄ (3b)	99	7.8:1	98/88	4b
2	4-MeC ₆ H ₄ (3c)	90	5.5:1	98/89	4c
3	4-ClC ₆ H ₄ (3d)	96	6.7:1	99/94	4d
4 ^e	3-MeOC ₆ H ₄ (3e)	95	5.1:1	99/93	4e
5	3-BrC ₆ H ₄ (3f)	99	4.0:1	95/87	4f
6	2-MeC ₆ H ₄ (3g)	73	2.4:1	96/93	4g
7	2-FC ₆ H ₄ (3h)	99	4.3:1	99/98	4h
8	2-naphthyl (3i)	99	6.5:1	98/93	4i
9	3-thiophenyl (3j)	99	11:1	99/93	4j

10	Me ₂ CHCH ₂ (3k)	84	1.5:1	57/41	4k
11	Me(CH ₂) ₆ (3l)	76	1.9:1	59/41	4l

^a The reaction was performed with 0.2 mmol of **2**, 0.22 mmol of **3**, and 1 mol% of **1f** in toluene (1.0 mL) with MS4A (100 mg) at 0 °C. ^b Isolated yield. ^c Diastereomeric ratios were determined by 600 MHz ¹H NMR analysis of crude aliquots. ^d Enantiomeric excesses were analyzed by chiral stationary phase HPLC. Relative and absolute configurations of **4f** were determined by X-ray crystallographic analysis and those of other **4** were assigned by analogy (see Fig. 2). ^e 2 mol% of catalyst was used.

The absolute and relative configurations of both diastereomers of the aza-Henry adduct **4f** were unambiguously determined by single-crystal X-ray diffraction analysis, respectively (Fig. 2). The ORTEP diagrams thus obtained revealed that absolute stereochemistries of the stereogenic carbon atom connected to the *N*-Boc amide group are identical in both diastereomers, which implies that chiral ammonium betaine **1f** rigorously discriminates the prochiral faces of **3** rather than those of the enolate generated from **2** in the carbon-carbon bond-forming event. The absolute configuration of major diastereomer of **4f** was unequivocally determined by X-ray crystallographic analysis (Fig. 2), and the stereochemistry of the remaining examples was assumed to be analogous.

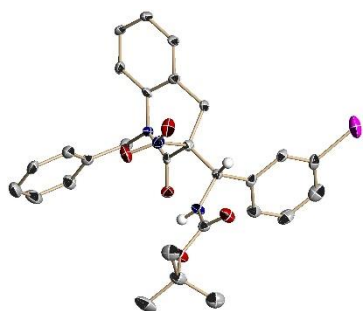


Figure 2 ORTEP diagrams of major diastereomers of **4f** (Ellipsoids displayed at 50% probability. Calculated hydrogen atoms except for them attached to stereogenic carbon are omitted for clarity. Gray: carbon, red: oxygen, blue: nitrogen, pink: bromine.)

Summery

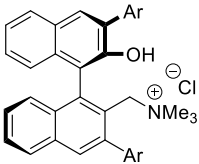
In summary, we have developed a highly enantioselective aza-Henry reaction of 3-nitro dihydro-2(3*H*)-quinolones with *N*-Boc aldimines under the catalysis of chiral ammonium betaines. This unprecedented protocol offers a convenient access to useful precursors of optically active tetrahydroquinolines, the privileged structural motif found in biologically relevant molecules, and would stimulate further development of novel asymmetric transformations from tetrahydro-2(3*H*)-quinolones.

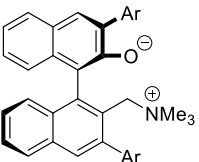
General Information: Infrared spectra were recorded on a SHIMADZU IRAffinity-1 spectrometer. ¹H NMR spectra were recorded on a JEOL ECA500II (500 MHz) spectrometer or JEOL JNM-ECA600 (600 MHz) spectrometer. Chemical shifts are reported in ppm from the solvent resonance ((CD₃)₂SO: 2.50 ppm, CD₃CN: 1.94 ppm) or tetramethylsilane (0.00 ppm; CDCl₃, CD₃OD) resonance as the internal standard. Data are reported as follows: chemical shift, integration, multiplicity (s = singlet, d = doublet, t = triplet, m = multiplet, br = broad), and coupling constants (Hz). ¹³C NMR spectra were recorded on a JEOL ECA500II (126 MHz) spectrometer or JEOL JNM-ECA600 (151 MHz) spectrometer with complete proton decoupling. Chemical shifts are reported in ppm from the solvent resonance (CDCl₃: 77.16 ppm, CD₃OD: 49.00 ppm, (CD₃)₂SO: 39.52 ppm, CD₃CN: 1.32 ppm). ¹⁹F NMR spectra were recorded on a JEOL ECA500II (471 MHz) spectrometer with complete proton decoupling. Chemical shifts are reported in ppm from benzotrifluoride (−64.0 ppm) resonance as the external standard. The high resolution mass spectra were conducted on Thermo Fisher Scientific Exactive (ESI). Analytical thin layer chromatography (TLC) was performed on Merck precoated TLC plates (silica gel 60 F₂₅₄, 0.25 mm). Flash column chromatography was performed on Silica gel 60N (spherical neutral, 40-50 μm; Kanto Chemical Co., Inc.) or Chromatorex NH-DM2035 silica gel (Fuji Silysia Chemical Ltd.). Enantiomeric excesses were determined by HPLC analysis using chiral columns [ϕ 4.6 mm x 250 mm, DAICEL CHIRALPAK AD-3 (AD-3), CHIRALPAK AZ-3 (AZ-3), CHIRALPAK IA-3 (IA-3), CHIRALPAK IC-3 (IC-3), CHIRALPAK ID-3 (ID-3), CHIRALPAK IG-3 (IG-3), and CHIRALCEL OD-3 (OD-3)] with hexane (H), 2-propanol (IPA), and ethanol (EtOH) as eluent.

Toluene was supplied from Kanto Chemical Co., Inc. as “Dehydrated” and further purified by passing through neutral alumina under nitrogen atmosphere. Betaines^{8b} and *N*-Boc imines¹⁶ were prepared by following literature procedure. Powdered 4 Å molecular sieves (MS4A) was supplied by Sigma-Aldrich Co. Other simple chemicals were purchased and used as such.

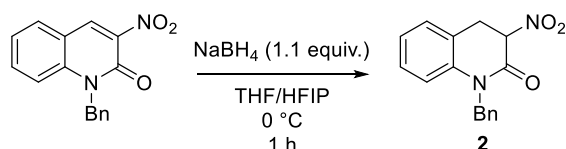
Experimental Section:

Characterization of Betaine Precursor 1f·HCl and Betaine 1f:

**1f·HCl:** ^1H NMR (500 MHz, $(\text{CD}_3)_2\text{SO}$, 80 °C) δ 9.20 (1H, br), 8.42-8.30 (5H, m), 8.25-8.14 (3H, m), 8.12 (1H, d, $J = 8.0$ Hz), 8.09 (1H, s), 7.71 (1H, t, $J = 8.0$ Hz), 7.48 (1H, t, $J = 8.0$ Hz), 7.45 (1H, t, $J = 8.0$ Hz), 7.40 (1H, t, $J = 8.0$ Hz), 7.28 (1H, d, $J = 8.0$ Hz), 7.03 (1H, d, $J = 8.0$ Hz), 4.65 (1H, brd, $J = 13.5$ Hz), 4.55 (1H, br), 2.58 (9H, s); ^{13}C NMR (126 MHz, $(\text{CD}_3)_2\text{SO}$, 80 °C) δ 149.4, 143.6, 140.4, 138.7, 138.2, 133.6, 133.2, 132.5, 132.1, 131.9, 130.8 (q, $J_{\text{C-F}} = 32.6$ Hz), 130.3, 129.9₃, 129.9₁ (q, $J_{\text{C-F}} = 33.9$ Hz), 128.7, 128.1, 128.0, 127.6, 127.5, 126.7, 123.9, 123.7, 123.1 (q, $J_{\text{C-F}} = 273.7$ Hz), 122.9 (d, $J_{\text{C-F}} = 273.8$ Hz), 121.3, 120.4, 117.6, 64.1, 53.3, three carbon atoms were not found probably due to overlapping; ^{19}F NMR (471 MHz, $(\text{CD}_3)_2\text{SO}$, 80 °C) δ -61.2, -61.1; IR (film) 3017, 1618, 1472, 1375, 1275, 1171, 1125, 1107, 1024, 895, 845; HRMS (ESI) Calcd for $\text{C}_{40}\text{H}_{28}\text{ONF}_{12}^+$ ($[\text{M}-\text{Cl}]^+$) 766.1974. Found 766.1971.

**1f:** ^1H NMR (500 MHz, CD_3OD) δ 8.49 (2H, br), 8.43 (2H, br), 8.11 (1H, br), 8.05-7.91 (3H, m), 7.84 (1H, br), 7.81 (1H, brd, $J = 7.5$ Hz), 7.58 (1H, br), 7.46 (1H, br), 7.33 (1H, br), 7.04 (2H, br), 6.73 (1H, br), 5.00-4.70 (2H, br), 2.46 (9H, s); ^{13}C NMR analysis gave broad spectrum and it was not assignable; ^{19}F NMR (471 MHz, CD_3OD) δ -64.0, -63.9; IR (film) 3051, 3030, 1614, 1489, 1472, 1423, 1373, 1277, 1177, 1130, 889, 845 cm^{-1} ; HRMS (ESI) Calcd for $\text{C}_{40}\text{H}_{28}\text{ONF}_{12}^+$ ($[\text{M}+\text{H}]^+$) 766.1974. Found 766.1963.

Synthesis of 1-Benzyl-3-Nitro-3,4-Dihydroquinolin-2(1H)-one:

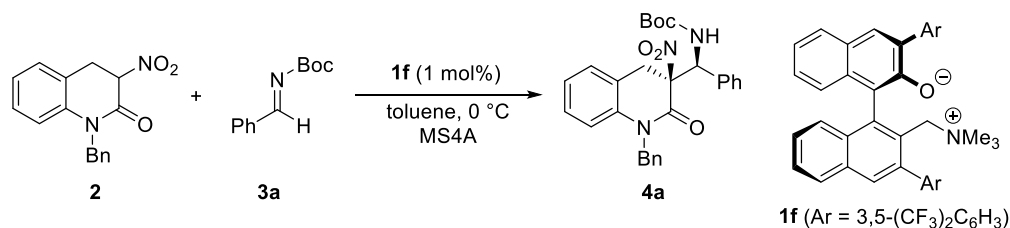


1-Benzyl-3-nitroquinolin-2(1H)-one was prepared by following the literature procedure¹⁷. To a solution of 1-Benzyl-3-nitroquinolin-2(1H)-one (840.8 mg, 3.0 mmol) in THF (30.0 mL) and HFIP (3.0 mL) was added NaBH₄ (124.8 mg, 3.3 mmol) portionwise at 0 °C and the reaction mixture was stirred at 0 °C. The resulting mixture was poured into brine. After being stirred for 1 h at room temperature, this mixture was filtered through a pad of Celite and the filtrate was extracted with ethyl acetate (EA) twice and the combined extracts were dried over Na₂SO₄. Removal of volatiles under reduced pressure and purification of the residue by column chromatography on silica gel (H/EA = 5:1-1:1 as eluent) furnished **2** (282.0 mg, 1.0 mmol, 33%) as a white solid.

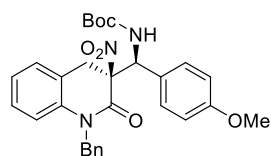
2: ^1H NMR (600 MHz, CDCl_3) δ 7.34₂ (1H, t, $J = 8.0$ Hz), 7.33₆ (1H, d, $J = 8.0$ Hz), 7.29 (1H, d, $J = 8.0$ Hz), 7.28 (2H, t, $J = 8.0$ Hz), 7.22 (1H, d, $J = 8.0$ Hz), 7.20 (1H, t, $J = 8.0$ Hz), 7.06 (1H, t, $J = 8.0$ Hz), 6.97 (1H, d, $J = 8.0$ Hz), 5.45 (1H, dd, $J = 8.4, 5.4$ Hz), 5.33 (1H, d, $J = 16.2$ Hz), 5.12 (1H, d, $J = 16.2$ Hz), 3.82 (1H, dd, $J = 15.6, 8.4$ Hz), 3.47 (1H, dd, $J = 15.6, 5.4$ Hz); ^{13}C NMR (151 MHz, CDCl_3) δ 161.1, 138.4, 135.9, 129.1, 129.0, 128.9, 127.7, 126.6, 124.5, 120.6, 116.4, 83.7, 47.5, 31.2; IR (neat) 3032, 2957, 1684, 1605, 1558, 1497, 1466, 1369, 1267 cm^{-1} ;

HRMS (ESI) Calcd for $C_{16}H_{14}O_3N_2Na$ ($[M+Na]^+$) 305.0897. Found 305.0894.

Representative Procedure for Asymmetric Aza-Henry Reaction of Dihydroquinolinone 2 to Imine 3a Catalyzed by Chiral Ammonium Betaine 1f:

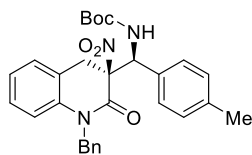


A magnetic stirrer bar and oven-dried 4 Å molecular sieves (MS4A) (100.0 mg) were placed in an oven-dried test tube under argon (Ar) atmosphere. The test tube was heated with a heat gun under reduced pressure for 3 min and it was refilled with Ar. Then, chiral ammonium betaine **1f** (1.53 mg, 2.00 μmol) and Dihydroquinolinone **2** (56.5 mg, 0.20 mmol) were added to the test tube. After cooling to 0 °C, toluene (1.0 mL) and imine **3a** (45.2 mg, 0.22 mmol) were introduced and stirring was continued for 24 h. The reaction was quenched by the addition of a solution of trifluoroacetic acid in toluene (1.0 M, 2.0 μL) and hydrochloric acid (1.0 M, 2.0 mL). The aqueous phase was extracted with EA twice. The combined organic phases were washed with brine, dried over Na₂SO₄, and filtered. All volatiles were removed by evaporation to afford the crude residue, which was analyzed by ¹H NMR (600 MHz) to determine the diastereomeric ratio (dr = 6.6:1). Purification of the residue by column chromatography on Silica gel 60N (H/EA = 10:1 to 5:1 as eluent) gave **4a** as a mixture of diastereomers (97.7 mg, 0.20 mmol). Enantiomeric ratio was determined by chiral stationary phase HPLC (99% ee). **4a**: HPLC IC-3, H/IPA = 10:1, flow rate = 0.5 mL/min, λ = 210 nm, 23.6 min (minor isomer of major diastereomer), 32.1 min (minor isomer of minor diastereomer), 41.6 min (major isomer of major diastereomer), 56.6 min (major isomer of minor diastereomer); ¹H NMR (600 MHz, CDCl₃) major diastereomer δ 7.59 (2H, d, *J* = 7.8 Hz), 7.38-7.26 (7H, m), 7.21 (1H, d, *J* = 10.2 Hz), 7.14 (1H, d, *J* = 7.8 Hz), 7.11 (1H, t, *J* = 7.8 Hz), 6.99 (1H, t, *J* = 7.8 Hz), 6.86 (1H, d, *J* = 7.8 Hz), 5.62 (1H, d, *J* = 10.2 Hz), 5.55 (1H, d, *J* = 16.2 Hz), 4.77 (1H, d, *J* = 16.2 Hz), 3.59 (1H, d, *J* = 16.2 Hz), 3.11 (1H, d, *J* = 16.2 Hz), 1.35 (9H, s); ¹³C NMR (151 MHz, CDCl₃) major diastereomer δ 162.5, 155.0, 137.6, 136.4, 135.8, 129.3, 129.1, 128.9, 128.8, 128.6₃, 128.6₀, 127.6, 126.2, 124.6, 120.5, 116.1, 93.3, 80.1, 61.0, 48.1, 36.6, 28.4; IR (film) 3429, 2978, 1713, 1670, 1607, 1557, 1485, 1464, 1393, 1366, 1233, 1161, 1018 cm⁻¹; HRMS (ESI) Calcd for C₂₈H₂₉O₅N₃Na⁺ ($[M+Na]^+$) 510.1999. Found 510.2002.



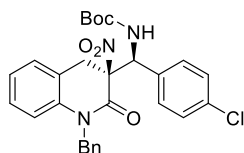
4b: HPLC AZ-3, H/IPA = 10:1, flow rate = 1.0 mL/min, λ = 210 nm, 37.0 min (major isomer of major diastereomer), 46.4 min (minor isomer of minor diastereomer), 52.6 min (minor isomer of major diastereomer), 61.6 min (major isomer of minor diastereomer); ¹H NMR (600 MHz, CDCl₃) major diastereomer δ 7.51 (2H, d, *J* = 8.4 Hz), 7.35 (2H, t, *J* = 7.8 Hz), 7.31 (2H, d, *J* = 7.8 Hz), 7.28 (1H, t, *J* = 7.8 Hz), 7.16-7.13 (2H, m), 7.11 (1H, t, *J* = 7.8 Hz), 6.99 (1H, t, *J* = 7.8 Hz), 6.90-6.84 (3H, m), 5.57 (1H, d, *J* = 9.6 Hz), 5.55 (1H, d, *J* = 16.2 Hz), 4.77 (1H, d, *J* = 16.2 Hz), 3.79 (3H, s), 3.57 (1H, d, *J* = 16.8 Hz), 3.12 (1H, d, *J* = 16.8 Hz), 1.35 (9H, s); ¹³C NMR (151 MHz, CDCl₃) major diastereomer δ 162.6, 160.0, 155.0, 137.7, 135.8, 130.5, 129.1, 128.9, 128.6, 128.4, 127.6, 126.2, 124.5, 120.6, 116.0, 114.1, 93.4, 80.0, 60.5, 55.4, 48.1, 36.6, 28.4; IR (film) 3428, 2978, 1713, 1670, 1607, 1557, 1512, 1485, 1464, 1393, 1366, 1252,

1233, 1161, 1022 cm^{-1} ; HRMS (ESI) Calcd for $\text{C}_{29}\text{H}_{31}\text{O}_6\text{N}_3\text{Na}^+$ $[(\text{M}+\text{Na})^+]$ 540.2105. Found 540.2106.



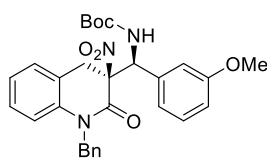
4c: HPLC ID-3, H/IPA = 10:1, flow rate = 1.0 mL/min, $\lambda = 210$ nm, 19.1 min (major isomer of major diastereomer), 22.9 min (minor isomer of major diastereomer), 25.5 min (minor isomer of minor diastereomer), 36.2 min (major isomer of minor diastereomer); ^1H NMR (600 MHz, CDCl_3) major diastereomer δ 7.47 (2H, d, $J = 7.8$ Hz), 7.35 (2H, t, $J = 7.8$ Hz),

7.31 (2H, d, $J = 7.8$ Hz), 7.30 (1H, d, $J = 7.8$ Hz), 7.28 (1H, t, $J = 7.8$ Hz), 7.20-7.09 (5H, m), 6.98 (1H, t, $J = 7.8$ Hz), 6.85 (1H, d, $J = 7.8$ Hz), 5.58 (1H, d, $J = 15.9$ Hz), 5.55 (1H, d, $J = 15.9$ Hz), 4.75 (1H, d, $J = 15.9$ Hz), 3.57 (1H, d, $J = 17.1$ Hz), 3.12 (1H, d, $J = 17.1$ Hz), 2.33 (3H, s), 1.35 (9H, s); ^{13}C NMR (151 MHz, CDCl_3) major diastereomer δ 162.6, 155.0, 138.8, 137.7, 135.9, 133.5, 129.5, 129.2, 129.1, 128.9, 128.6, 127.6, 126.2, 124.5, 120.6, 116.0, 93.3, 80.0, 60.8, 48.1, 36.6, 28.4, 21.2; IR (film) 3428, 2978, 1713, 1672, 1607, 1557, 1485, 1464, 1391, 1366, 1350, 1233, 1163, 1020 cm^{-1} ; HRMS (ESI) Calcd for $\text{C}_{29}\text{H}_{31}\text{O}_5\text{N}_3\text{Na}^+$ $[(\text{M}+\text{Na})^+]$ 524.2156. Found 524.2155.



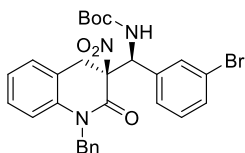
4d: HPLC IA-3, H/IPA = 10:1, flow rate = 1.0 mL/min, $\lambda = 210$ nm, 15.3 min (major isomer of minor diastereomer), 17.5 min (major isomer of major diastereomer), 23.8 min (minor isomer of minor diastereomer), 31.4 min (minor isomer of major diastereomer); ^1H NMR (600 MHz, CDCl_3) major diastereomer δ 7.54 (1H, d, $J = 7.8$ Hz), 7.40-7.25 (4H, m), 7.18-

7.10 (3H, m), 7.01 (1H, t, $J = 7.8$ Hz), 6.88 (1H, d, $J = 7.8$ Hz), 5.59 (1H, d, $J = 10.2$ Hz), 5.55 (1H, d, $J = 15.6$ Hz), 4.77 (1H, d, $J = 15.6$ Hz), 3.59 (1H, d, $J = 16.5$ Hz), 3.09 (1H, d, $J = 16.5$ Hz), 1.36 (9H, s); ^{13}C NMR (151 MHz, CDCl_3) major diastereomer δ 162.4, 154.9, 137.6, 135.7, 135.0, 134.9, 130.7, 129.1₁, 129.0₅, 129.0, 128.6, 127.6, 126.2, 124.7, 120.3, 116.1, 93.1, 80.4, 60.4, 48.2, 36.5, 28.3; IR (film) 3426, 2978, 1713, 1670, 1607, 1557, 1487, 1464, 1393, 1337, 1233, 1161, 1092, 1015 cm^{-1} ; HRMS (ESI) Calcd for $\text{C}_{28}\text{H}_{28}\text{O}_5\text{N}_3^{35}\text{Cl Na}^+$ $[(\text{M}+\text{Na})^+]$ 544.1610. Found 544.1606.

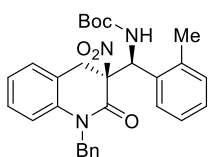


4e: HPLC ID-3, H/IPA = 97:3, flow rate = 0.5 mL/min, $\lambda = 210$ nm, 44.1 min (major isomer of major diastereomer), 57.7 min (minor isomer of major diastereomer), 78.2 min (minor isomer of minor diastereomer), 102.6 min (major isomer of minor diastereomer); ^1H NMR (600 MHz, CDCl_3) major diastereomer δ 7.35 (2H, t, $J = 7.8$ Hz), 7.30 (2H, d, $J = 7.2$ Hz),

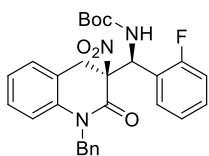
7.28-7.12 (5H, m), 7.10 (1H, d, $J = 7.8$ Hz), 7.01-6.95 (2H, m), 6.89-6.85 (2H, m), 5.60 (1H, d, $J = 10.2$ Hz), 5.55 (1H, d, $J = 15.9$ Hz), 4.78 (1H, d, $J = 15.9$ Hz), 3.79 (3H, s), 3.57 (1H, d, $J = 16.5$ Hz), 3.12 (1H, d, $J = 16.5$ Hz), 1.36 (9H, s); ^{13}C NMR (151 MHz, CDCl_3) major diastereomer δ 162.6, 159.9, 155.0, 137.9, 137.6, 135.8, 129.8, 129.1, 128.9, 128.6, 127.6, 126.2, 124.5, 121.8, 120.5, 116.0, 114.7, 114.4, 93.2, 80.1, 61.0, 55.4, 48.1, 36.6, 28.3; IR (film) 3431, 2976, 1715, 1670, 1605, 1557, 1485, 1464, 1393, 1350, 1261, 1161, 1043 cm^{-1} ; HRMS (ESI) Calcd for $\text{C}_{29}\text{H}_{31}\text{O}_6\text{N}_3\text{Na}^+$ $[(\text{M}+\text{Na})^+]$ 540.2105. Found 540.2102.



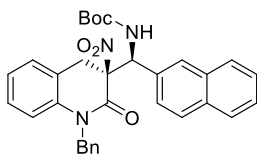
4f: HPLC AD-3, H/IPA = 10:1, flow rate = 0.5 mL/min, λ = 210 nm, 28.4 min (major isomer of minor diastereomer), 34.3 min (major isomer of major diastereomer), 37.4 min (minor isomer of major diastereomer), 61.3 min (minor isomer of minor diastereomer); ^1H NMR (600 MHz, CDCl_3) major diastereomer δ 7.77 (1H, s), 7.53 (1H, d, J = 7.8 Hz), 7.48 (1H, d, J = 7.8 Hz), 7.37 (2H, t, J = 7.8 Hz), 7.31 (2H, d, J = 7.8 Hz), 7.29 (1H, t, J = 7.8 Hz), 7.24 (1H, t, J = 7.8 Hz), 7.20-7.12 (3H, m), 7.02 (1H, t, J = 7.8 Hz), 6.90 (1H, d, J = 7.8 Hz), 5.57 (1H, d, J = 9.6 Hz), 5.53 (1H, d, J = 15.9 Hz), 4.82 (1H, d, J = 15.9 Hz), 3.58 (1H, d, J = 16.8 Hz), 3.08 (1H, d, J = 16.8 Hz), 1.36 (9H, s); ^{13}C NMR (151 MHz, CDCl_3) major diastereomer δ 162.4, 154.9, 138.8, 137.6, 135.8, 132.2₁, 132.1₃, 130.4, 129.1₃, 129.0₉, 128.7, 128.1, 127.6, 126.3, 124.7, 123.0, 120.3, 116.1, 93.0, 80.4, 60.5, 48.1, 36.5, 28.4; IR (film) 3424, 2978, 1713, 1670, 1607, 1557, 1485, 1464, 1393, 1368, 1346, 1233, 1157, 1020 cm^{-1} ; HRMS (ESI) Calcd for $\text{C}_{28}\text{H}_{28}\text{O}_5\text{N}_3^{79}\text{Br Na}^+$ ($[\text{M}+\text{Na}]^+$) 588.1105. Found 588.1103.



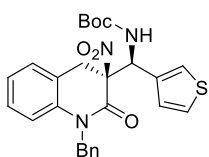
4g: HPLC IA-3, H/IPA = 10:1, flow rate = 1.0 mL/min, λ = 210 nm, 6.4 min (minor isomer of major diastereomer), 8.7 min (major isomer of minor diastereomer), 9.9 min (minor isomer of minor diastereomer), 12.1 min (major isomer of major diastereomer); ^1H NMR (600 MHz, CDCl_3) major diastereomer δ 7.73 (1H, d, J = 7.8 Hz), 7.36 (2H, t, J = 7.8 Hz), 7.32 (3H, m), 7.28 (1H, t, J = 7.8 Hz), 7.24-7.17 (3H, m), 7.12 (1H, t, J = 7.8 Hz), 7.11 (1H, d, J = 7.8 Hz), 6.98 (1H, t, J = 7.8 Hz), 6.88 (1H, d, J = 7.8 Hz), 6.10 (1H, d, J = 10.2 Hz), 5.57 (1H, d, J = 16.2 Hz), 4.87 (1H, d, J = 16.2 Hz), 3.61 (1H, d, J = 16.8 Hz), 3.01 (1H, d, J = 16.8 Hz), 2.72 (3H, s), 1.35 (9H, s); ^{13}C NMR (151 MHz, CDCl_3) major diastereomer δ 163.0, 155.1, 137.6, 137.4, 135.8, 131.2, 129.1, 129.0, 128.7, 127.6, 127.1, 126.3, 124.5, 120.3, 116.1, 94.1, 80.0, 55.9, 48.1, 35.1, 28.4, 20.9, three carbon atoms were not found probably due to overlapping; IR (film) 3428, 2978, 1713, 1670, 1607, 1557, 1485, 1464, 1393, 1366, 1233, 1159, 1020 cm^{-1} ; HRMS (ESI) Calcd for $\text{C}_{29}\text{H}_{31}\text{O}_5\text{N}_3\text{Na}^+$ ($[\text{M}+\text{Na}]^+$) 524.2156. Found 524.2153.



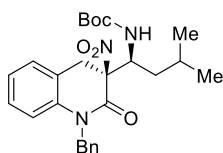
4h: HPLC IG-3, H/IPA = 10:1, flow rate = 1.0 mL/min, λ = 210 nm, 22.9 min (minor isomer of major diastereomer), 24.7 min (major isomer of major diastereomer), 42.7 min (minor isomer of minor diastereomer), 51.3 min (major isomer of minor diastereomer); ^1H NMR (600 MHz, CDCl_3 , 50 $^\circ\text{C}$) major diastereomer δ 7.76 (1H, br), 7.35-7.29 (2H, m), 7.27 (2H, d, J = 7.8 Hz), 7.25 (1H, t, J = 7.8 Hz), 7.18-7.12 (3H, m), 7.11 (1H, d, J = 7.8 Hz), 7.09 (1H, t, J = 7.8 Hz), 6.99 (1H, t, J = 7.8 Hz), 6.88 (1H, d, J = 7.8 Hz), 6.15 (1H, brd, J = 7.8 Hz), 5.50 (1H, d, J = 16.2 Hz), 4.80 (1H, d, J = 16.2 Hz), 3.79 (1H, brd, J = 15.9 Hz), 3.08 (1H, brd, J = 15.9 Hz), 1.35 (9H, s); ^{13}C NMR (151 MHz, CDCl_3 , 50 $^\circ\text{C}$) major diastereomer δ 162.5, 160.8 (d, $J_{\text{C-F}}$ = 207.5 Hz), 154.9, 137.8, 135.9, 130.6 (d, $J_{\text{C-F}}$ = 35.3 Hz), 130.1, 129.1, 129.0, 128.8, 127.6, 126.4, 124.9, 124.6, 124.2 (d, $J_{\text{C-F}}$ = 10.8 Hz), 120.6, 116.1, 115.5 (d, $J_{\text{C-F}}$ = 19.3 Hz), 93.6, 80.3, 52.7, 48.1, 35.2, 28.4; ^{19}F NMR (471 MHz, CDCl_3) δ -113.6; IR (film) 3428, 2978, 1717, 1670, 1607, 1557, 1487, 1464, 1393, 1366, 1233, 1159, 1020 cm^{-1} ; HRMS (ESI) Calcd for $\text{C}_{28}\text{H}_{28}\text{O}_5\text{N}_3\text{FNa}^+$ ($[\text{M}+\text{Na}]^+$) 528.1905. Found 528.1905.



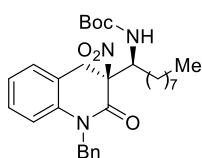
4i: HPLC IC-3, H/EtOH = 10:1, flow rate = 0.5 mL/min, λ = 210 nm, 14.8 min (minor isomer of major diastereomer), 16.9 min (major isomer of major diastereomer), 18.5 min (major isomer of minor diastereomer), 20.0 min (minor isomer of minor diastereomer); ^1H NMR (600 MHz, CDCl_3) major diastereomer δ 8.06 (1H, s), 7.90-7.76 (4H, m), 7.71 (1H, d, J = 7.8 Hz), 7.53-7.45 (2H, m), 7.35 (1H, d, J = 7.8 Hz), 7.34-7.27 (4H, m), 7.25 (1H, t, J = 7.8 Hz), 7.12 (1H, d, J = 7.8 Hz), 7.08 (1H, t, J = 7.8 Hz), 6.96 (1H, t, J = 7.8 Hz), 6.84 (1H, d, J = 7.8 Hz), 5.81 (1H, d, J = 10.2 Hz), 5.52 (1H, d, J = 15.6 Hz), 4.75 (1H, d, J = 15.6 Hz), 3.65 (1H, d, J = 16.8 Hz), 3.11 (1H, d, J = 16.8 Hz), 1.35 (9H, s); ^{13}C NMR (151 MHz, CDCl_3) major diastereomer δ 162.6, 155.0, 137.5, 135.8, 133.8, 133.4, 133.1, 129.1, 128.9, 128.6, 128.5, 128.4, 127.7, 127.5, 126.8, 126.6, 126.4, 126.3, 126.2, 124.5, 120.5, 116.0, 93.3, 80.2, 61.2, 48.1, 36.7, 28.3; IR (film) 3428, 2978, 1713, 1670, 1607, 1557, 1485, 1464, 1391, 1327, 1233, 1159, 1020 cm^{-1} ; HRMS (ESI) Calcd for $\text{C}_{32}\text{H}_{31}\text{O}_5\text{N}_3\text{Na}^+$ ($[\text{M}+\text{Na}]^+$) 560.2156. Found 560.2155.



4j: HPLC IA-3, H/IPA = 97:3, flow rate = 1.0 mL/min, λ = 210 nm, 44.2 min (major isomer of minor diastereomer), 76.6 min (major isomer of major diastereomer), 84.6 min (minor isomer of major diastereomer), 112.0 min (minor isomer of minor diastereomer); ^1H NMR (600 MHz, CDCl_3) major diastereomer δ 7.47 (1H, brs), 7.36 (2H, t, J = 7.8 Hz), 7.31 (2H, d, J = 7.8 Hz), 7.30-7.26 (2H, m), 7.24 (1H, d, J = 4.8 Hz), 7.13 (1H, t, J = 7.8 Hz), 7.12 (1H, t, J = 7.8 Hz), 7.01-6.96 (2H, m), 6.88 (1H, d, J = 12.3 Hz), 5.76 (1H, d, J = 12.3 Hz), 5.56 (1H, d, J = 16.2 Hz), 4.82 (1H, d, J = 16.2 Hz), 3.57 (1H, d, J = 16.8 Hz), 3.16 (1H, d, J = 16.8 Hz), 1.36 (9H, s); ^{13}C NMR (151 MHz, CDCl_3) major diastereomer δ 162.7, 154.9, 137.7, 137.1, 135.8, 129.1, 128.9, 128.6, 128.0, 127.6, 126.4, 126.2, 125.6, 124.6, 120.5, 116.1, 92.9, 80.1, 56.3, 48.1, 36.3, 28.3; IR (film) 3429, 2978, 2363, 1713, 1670, 1607, 1557, 1485, 1464, 1391, 1329, 1233, 1161, 1020 cm^{-1} ; HRMS (ESI) Calcd for $\text{C}_{26}\text{H}_{27}\text{O}_5\text{N}_3\text{NaS}^+$ ($[\text{M}+\text{Na}]^+$) 516.1564. Found 516.1567.



4k: Purification by column chromatography was performed on Chromatorex NH-DM2035 silica gel (H/EA = 50:1 to 10:1 as eluent). HPLC OD-3, H/IPA = 10:1, flow rate = 0.5 mL/min, λ = 210 nm, 10.1 min (minor isomer of minor diastereomer), 12.2 min (major isomer of major diastereomer), 20.1 min (minor isomer of major diastereomer), 30.1 min (major isomer of minor diastereomer); ^1H NMR (600 MHz, CD_3CN , 60 $^\circ\text{C}$) major diastereomer δ 7.39-7.32 (4H, m), 7.29 (1H, t, J = 7.8 Hz), 7.25 (1H, d, J = 7.8 Hz), 7.21 (1H, t, J = 7.8 Hz), 7.07 (1H, t, J = 7.8 Hz), 7.02 (1H, d, J = 7.8 Hz), 5.73 (1H, br), 5.40 (1H, d, J = 16.2 Hz), 5.04 (1H, d, J = 16.2 Hz), 4.51 (1H, br), 3.69 (1H, d, J = 16.8 Hz), 3.57 (1H, d, J = 16.8 Hz), 1.83-1.72 (1H, m), 1.66-1.61 (2H, m), 1.41 (9H, s), 1.01 (1H, d, J = 6.6 Hz), 0.97 (1H, d, J = 6.6 Hz); ^{13}C NMR (151 MHz, CDCl_3) major diastereomer δ 162.7, 155.6, 138.3, 136.1, 129.1, 129.0, 128.8, 127.6, 126.3, 124.5, 120.9, 116.3, 93.8, 80.0, 53.6, 48.0, 41.1, 35.2, 28.4, 25.5, 23.8; IR (film) 3437, 2959, 1713, 1676, 1607, 1553, 1497, 1466, 1391, 1368, 1254, 1161, 1047, 1020 cm^{-1} ; HRMS (ESI) Calcd for $\text{C}_{26}\text{H}_{33}\text{O}_5\text{N}_3\text{Na}^+$ ($[\text{M}+\text{Na}]^+$) 490.2312. Found 490.2313.



4l: Purification by column chromatography was performed on Chromatorex NH-DM2035 silica gel (H/EA = 50:1 to 10:1 as eluent). HPLC OD-3, H/IPA = 10:1, flow rate = 0.5 mL/min, λ = 210 nm, 9.9 min (minor isomer of minor diastereomer), 12.2 min (major isomer of major diastereomer), 41.1 min (minor isomer of major diastereomer), 52.5 min (major isomer of minor

diastereomer); ^1H NMR (600 MHz, CD_3CN , 60 $^\circ\text{C}$) major diastereomer δ 7.39-7.33 (4H, m), 7.29 (1H, t, $J = 7.8$ Hz), 7.25 (1H, d, $J = 7.8$ Hz), 7.22 (1H, t, $J = 7.8$ Hz), 7.07 (1H, t, $J = 7.8$ Hz), 7.02 (1H, d, $J = 7.8$ Hz), 5.74 (1H, br), 5.39 (1H, d, $J = 16.5$ Hz), 5.06 (1H, d, $J = 16.5$ Hz), 4.43 (1H, brt, $J = 9.6$ Hz), 3.68 (1H, d, $J = 16.8$ Hz), 3.58 (1H, d, $J = 16.8$ Hz), 1.93-1.84 (1H, m), 1.66-1.56 (1H, m), 1.54-1.45 (1H, m), 1.41-1.39 (11H, br), 1.32 (9H, br), 0.91 (3H, t, $J = 6.6$ Hz); ^{13}C NMR (151 MHz, CDCl_3) major diastereomer δ 162.7, 155.8, 138.3, 136.1, 129.1, 129.0, 128.8, 127.6, 126.3, 124.5, 120.9, 116.2, 93.7, 80.0, 55.3, 48.0, 35.3, 32.1, 32.0, 29.6, 29.4, 29.3, 28.4, 26.5, 22.8, 14.2; IR (film) 3435, 2926, 2855, 1717, 1678, 1607, 1553, 1495, 1466, 1391, 1366, 1238, 1161, 1049, 1024 cm^{-1} ; HRMS (ESI) Calcd for $\text{C}_{30}\text{H}_{41}\text{O}_5\text{N}_3\text{Na}^+$ ($[\text{M}+\text{Na}]^+$) 546.2938. Found 546.2936.

Crystallographic Structure Determination: The single crystal, obtained by the procedure described below, was mounted on MicroMesh. Data of X-ray diffraction were collected at 123 K on a Rigaku FR-X with Pilatus 200K with fine-focus sealed tube Mo/ $\text{K}\alpha$ radiation ($\lambda = 0.71075$ Å). An absorption correction was made using Crystal Structure. The structure was solved by direct methods and Fourier syntheses, and refined by full-matrix least squares on F^2 by using SHELXL-2014.¹⁸ All non-hydrogen atoms were refined with anisotropic displacement parameters. A hydrogen atom bonded to a nitrogen atom was located from a difference synthesis and their coordinates and isotropic thermal parameters refined. The other hydrogen atoms were placed in calculated positions and isotropic thermal parameters refined.

Recrystallization of 4f: Recrystallization of **4f** was performed by using a CHCl_3 solvent system at room temperature.

Table S1. Crystal data and structure refinement for **4f**.

Empirical formula	C ₅₇ H ₅₇ Br ₂ Cl ₃ N ₆ O ₁₀	
Formula weight	1252.25	
Temperature	123(2) K	
Wavelength	0.71075 Å	
Crystal system	Monoclinic	
Space group	P 21	
Unit cell dimensions	a = 11.735(3) Å	$\alpha = 90^\circ$
	b = 10.150(2) Å	$\beta = 90.001(5)^\circ$
	c = 24.007(4) Å	$\gamma = 90^\circ$
Volume	2859.5(10) Å ³	
Z	2	
Density (calculated)	1.454 Mg/m ³	
Absorption coefficient	1.620 mm ⁻¹	
F(000)	1284	
Crystal size	0.330 x 0.240 x 0.200 mm ³	
Theta range for data collection	3.081 to 27.495°.	
Index ranges	-15 ≤ h ≤ 15, -10 ≤ k ≤ 13, -23 ≤ l ≤ 30	
Reflections collected	22322	
Independent reflections	10333 [R _{int} = 0.0929]	
Completeness to theta = 25.242°	99.6 %	
Absorption correction	Semi-empirical from equivalents	
Max. and min. transmission	1.000 and 0.740	
Refinement method	Full-matrix least-squares on F ²	
Data / restraints / parameters	10333 / 1 / 719	
Goodness-of-fit on F ²	0.807	
Final R indices [I > 2σ(I)]	R ₁ = 0.0468, wR ₂ = 0.1001	
R indices (all data)	R ₁ = 0.0679, wR ₂ = 0.1038	
Absolute structure parameter	0.003(9)	
Extinction coefficient	0	
Largest diff. peak and hole	0.647 and -0.624 e.Å ⁻³	

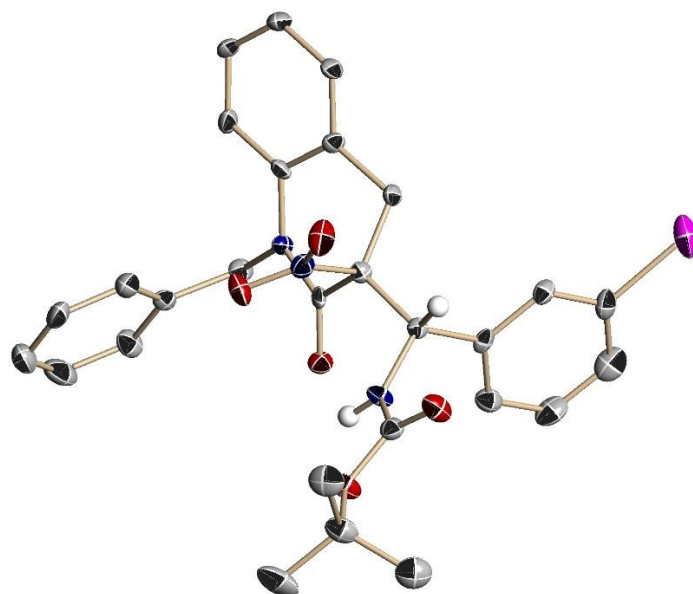


Fig. S1. Molecular structure of **4f**. The thermal ellipsoids of non-hydrogen atoms are shown at the 50% probability level. Gray: carbon, red: oxygen, blue: nitrogen, pink: bromine.

Reference and Note

- (1) Sridharan, V.; Suryavanshi, P. A.; Menéndez, J. C. *Chem. Rev.* **2011**, *111*, 7157.
- (2) (a) Kitagawa, O.; M. Takahashi, M. Yoshikawa, Taguchi, T. *J. Am. Chem. Soc.* **2005**, *127*, 3676. (b) Kitagawa, O.; Yoshikawa, M.; Tanabe, H.; Morita, T.; Takahashi, M.; Dobashi, Y.; Taguchi, T. *J. Am. Chem. Soc.* **2006**, *128*, 12923. (c) Takahashi, M.; Tanabe, H.; Nakamura, T.; Kuribara, D.; Yamazaki, T.; Kitagawa, O. *Tetrahedron* **2010**, *66*, 288. (d) Taylor J. G.; Correia, C. R. D. *J. Org. Chem.* **2011**, *76*, 857. (e) Yin, L.; Kanai, M.; Shibasaki, M. *Angew. Chem. Int. Ed.* **2011**, *50*, 7620. (f) Szöllösi, G.; Makra, Z.; Kovács, L.; Fülöp, F.; Bartók, M. *Adv. Synth. Catal.* **2013**, *355*, 1623. (g) He, N.; Huo, Y.; Liu, J.; Huang, Y.; Zhang, S.; Cai, Q. *Org. Lett.* **2015**, *17*, 374.
- (3) (a) Okuro, K.; Kai, H.; Alper, H. *Tetrahedron: Asymmetry* **1997**, *8*, 2307. (b) Dong, C.; Alper, H. *Tetrahedron: Asymmetry* **2004**, *15*, 35. (c) Lee, A.; Younai, A.; Price, C. K.; Izquierdo, J.; Mishra, R. K.; Scheidt, K. A. *J. Am. Chem. Soc.* **2014**, *136*, 10589.
- (4) Li, W.; Liu, X.; Hao, X.; Cai, Y.; Lin, L.; Feng, X. *Angew. Chem. Int. Ed.* **2012**, *51*, 8644.
- (5) (a) Harada, S.; Kumagai, N.; Kinoshita, T.; Matsunaga, S.; Shibasaki, M. *J. Am. Chem. Soc.* **2003**, *125*, 2582. (b) Hulin B.; Lopaze, M. G. *Tetrahedron: Asymmetry* **2004**, *15*, 1957. (c) Londregan, A. T.; Bernhardson, D.; Bradow, J.; Makowski, T. M.; Storer, G.; Warmus, J.; Wooten, C.; Yang, X. *Tetrahedron: Asymmetry* **2010**, *21*, 2072. (d) Ko, Y. K.; Im, C.; Do, J.; Park, Y. S. *Eur. J. Org. Chem.* **2014**, 3460. (e) Zhang, L.; Qureshi, Z.; Sonaglia, L.; Lautens, M. *Angew. Chem. Int. Ed.* **2014**, *53*, 13850.
- (6) Catalytic Enantioselective Construction of All-Carbon Quaternary Stereocenters: (a) Trost B. M.; Jiang, C. *Synthesis* **2006**, 369. (b) Cozzi, P. G.; Hilgraf, R.; Zimmermann, N. *Eur. J. Org. Chem.* **2007**, 5969. (c) Bella and T. Gasperi, *Synthesis* **2009**, 1583. Y. Minko and I. Marek, *Chem. Commun.* 2014, **50**, 12597; F. Vetica, M.; de Figueiredo, R. M.; Orsini, M.; Tofani, D.; Gasperi, T. *Synthesis* **2015**, 2139.
- (7) Godemert, J.; Oudeyer, S.; Levacher, V. *ChemCatChem* **2016**, *8*, 74.
- (8) (a) Uraguchi, D.; Koshimoto, K.; Ooi, T. *J. Am. Chem. Soc.* **2008**, *130*, 10878. (b) Uraguchi, D.; Koshimoto, K.; Ooi, T. *Chem. Commun.* **2010**, *46*, 300. (c) Uraguchi, D.; Koshimoto, K.; Sanada, C.; Ooi, T. *Tetrahedron: Asymmetry* **2010**, *21*, 1189. (d) Uraguchi, D.; Oyaizu, K.; Ooi, T. *Chem. Eur. J.* **2012**, *18*, 8306. (e) Uraguchi, D.; Oyaizu, K.; Noguchi, H.; Ooi, T. *Chem. Asian J.* **2015**, *10*, 334. (f) Oyaizu, K.; Uraguchi, D.; Ooi, T. *Chem. Commun.* **2015**, *51*, 4437. (g) Torii, M.; Kato, K.; Uraguchi, D.; Ooi, T. *Beilstein J. Org. Chem.* **2016**, *12*, 2099.
- (9) (a) Zhang, W.-Q.; Cheng, L.-F.; Yu, J.; Gong, L.-Z. *Angew. Chem. Int. Ed.* **2012**, *51*, 4085. (b) Claraz, A.; Landelle, G.; Oudeyer, S.; Levacher, V. *Eur. J. Org. Chem.* **2013**, 7693. (c) Zhou, X.; Wu, Y.; Deng, L. *J. Am. Chem. Soc.* **2016**, *138*, 12297.
- (10) (a) Wang, Y.-B.; Sun, D.-S.; Zhou, H.; Zhang, W.-Z.; Lu, X.-B. *Green Chem.* **2014**, *16*, 2266. (b) Tsutsumi, Y.; Yamakawa, K.; Yoshida, M.; Ema, T.; Sakai, T. *Org. Lett.* **2010**, *12*, 5728. (c) Guillerm, B.; Lemaure, V.; Cornil, J.; Lazzaroni, R.; Dubois, P.; Coulembier, O. *Chem. Commun.* **2014**, *50*, 10098.
- (11) (a) Uraguchi, D.; Koshimoto, K.; Miyake, S.; Ooi, T. *Angew. Chem. Int. Ed.* **2010**, *49*, 5567. (b) Uraguchi, D.; Koshimoto, K.; Ooi, T. *J. Am. Chem. Soc.* **2012**, *134*, 6972.
- (12) For reviews on Mannich-type reactions, see: (a) Ting A.; Schaus, S. E. *Eur. J. Org. Chem.* **2007**, 5797.

- (b) Verkade, J. M. M.; van Hemert, L. J. C.; Quaedflieg, P. J. L. M.; Rutjes, F. P. J. T. *Chem. Soc. Rev.* **2008**, *37*, 29. (c) Arrayás R. G.; Carretero, J. C. *Chem. Soc. Rev.* **2009**, *38*, 1940. (d) Bhadury P. S.; Song, B.-A. *Curr. Org. Chem.* **2010**, *14*, 1989. (e) Hatano M.; Ishihara, K. *Synthesis* **2010**, 3785. (f) Bernardi, L.; Ricci, A.; Franchini, M. C. *Curr. Org. Chem.* **2011**, *15*, 2210. (g) Matsunaga S.; Yoshino, T. *Chem. Rec.* **2011**, *11*, 260. (h) Han, B.; Li, J.-L.; Xiao, Y.-C.; Zhou, S.-L.; Chen, Y.-C. *Curr. Org. Chem.* **2011**, *15*, 4128. (i) Xiao-Hua, C.; Hui, G.; Bing, X. *Eur. J. Chem.* **2012**, *3*, 258. (j) Xiao-Hua, C.; Bing, X. *ARKIVOC* **2013**, (i), 264.
- (13) For a review on nitro-Mannich reaction, see: Noble A.; Anderson, J. C. *Chem. Rev.* **2013**, *113*, 2887; see also: (a) Anderson, J. C.; Barham, J. P.; Rundell, C. D. *Org. Lett.* **2015**, *17*, 4090. (b) Wang, H.-Y.; Zhang, K.; Zheng, C.-W.; Chai, Z.; Cao, D.-D.; Zhang, J.-X.; Zhao, G. *Angew. Chem. Int. Ed.* **2015**, *54*, 1775. (c) Hahn, R.; Jafari, E.; Raabe, G.; Enders, D. *Synthesis* **2015**, 472. (d) Maity R.; Pan, S. C. *Org. Biomol. Chem.* **2015**, *13*, 6825. (e) Isobe, T.; Kato, A.; Oriyama, T. *Chem. Lett.* **2015**, *44*, 483.
- (14) Vesely, J.; Rios, R. *Chem. Soc. Rev.* **2014**, *43*, 611.
- (15) The addition of MS4A is crucial for attaining reproducibility and high enantioselectivity probably because a small amount (<5%) of water from slightly hygroscopic **1** would be incorporated into a hydrogenbonding network in the transition state, causing a substantial decrease in enantioselectivity. The reaction between **2a** and **3a** with **1a** as a catalyst in the absence of MS4A afforded the adduct **4a** in 98% yield with diastereomeric ratio of 1.2:1 and the enantiomeric excesses were determined to be 79/55%, respectively.
- (16) (a)Wenzel, A. G.; Jacobsen, E. N. *J. Am. Chem. Soc.* **2002**, *124*, 12964. (b) Song, J.; Wang, Y.; Deng, L. *J. Am. Chem. Soc.* **2006**, *128*, 6048.
- (17) (a)Anderson, W. K.; Dalvie, D. K. *J. Heterocyclic Chem.* **1993**, *30*, 1533. (b) Fujita, R.; Wakayanagi, S.; Wakamatsu, H. *Journal of Tohoku Pharmaceutical University.* **2004**, *51*, 55.
- (18) Sheldrick, G. M. *Acta Cryst* **2015**, *C71*, 3.

Chapter 4

Acridinium Betaines as a Single-Electron-Transfer Catalyst: Molecular Design and Application to the Dimerization of Oxindoles

Abstract : An intramolecular ion-pairing acridinium phenoxide possessing a redox-active component and a basic site within a single molecular framework is developed. The potential of the acridinium betaine as a proton-coupled electron-transfer catalyst is demonstrated by its application to the homo-dimerization of 3-aryl oxindoles. Analysis of the kinetic profile has provided important clues to understand the reaction mechanism.

Introduction

Single-electron redox reactions are a powerful means to generate radical species and garner increasing attention owing to the significant potential of radical reactions for rapidly assembling organic frameworks in a manner otherwise difficult to execute.¹ Single-electron transfer (SET) events have previously been facilitated using over-stoichiometric amounts of chemical redox reagents such as low-valent metal salts, producing unrecyclable wastes after the reaction. Although this aspect seems incompatible with sustainable chemical synthesis,² chemical redox reaction does not require an external energy input and is highly reliable as it is still frequently employed in the synthesis of complex molecules. Therefore, novel catalysts or catalytic systems for chemical redox reaction with a clean terminal oxidant such as oxygen are much sought after in view of not only environmental consideration but also fully appreciating its advantages as a dependable synthetic tool. However, exploration of catalytically relevant chemical redox reagents has been limited so far, presumably because of the inherent difficulty in establishing a catalytic cycle with a satisfactory level of turnover efficiency. The generation of reactive radical intermediates from stable organic compounds requires high-energy redox-active reagents and this hampers the regeneration of the catalytically active species by commonly utilized terminal oxidants/reductants. Accordingly, a new strategy is awaited for overcoming this dilemma, which directs our attention to proton-coupled electron-transfer (PCET) process.³ PCET is one of the basic mechanisms of chemical and biological transformations, where simultaneous transfer of one electron and proton between given substrates allows the generation of high-energy intermediates. Since PCET is known to proceed via a more stable transition state than those involved in iterative electron-proton (or proton-electron) transfer processes, we envisioned that judicious incorporation of this mechanistic setup into chemical redox reactions would make the reduction/oxidation potential requisite for the redox reagent considerably lower than that required in the two-step manifold. The resulting reduced (or oxidized) reagent could thus be restored under accessible conditions, enabling the operation of chemical redox catalysis. However, this possibility remains experimentally unexplored. In conjunction with our continuing program of chiral ammonium betaine catalysis,⁴⁻⁸ we sought to design an intramolecular ion-pairing electron-transfer catalyst, namely, an acridinium phenoxide. We hypothesized that PCET would take place within a hydrogen-bonding complex of the basic catalyst possessing a redox-active site and an acidic substrate and that the resulting radical species could engage in a downstream bond formation. Herein, we describe the development of acridinium betaine **1** as a PCET catalyst and its application to a model reaction, homo-dimerization of *N*-(4-methoxyphenyl)-3-aryl oxindoles **2**, revealing extremely high catalytic activity. The reaction mechanism is discussed based on the kinetic analysis in order to gain insights into the origin of the prominent catalytic performance of **1**.

Results and Discussion

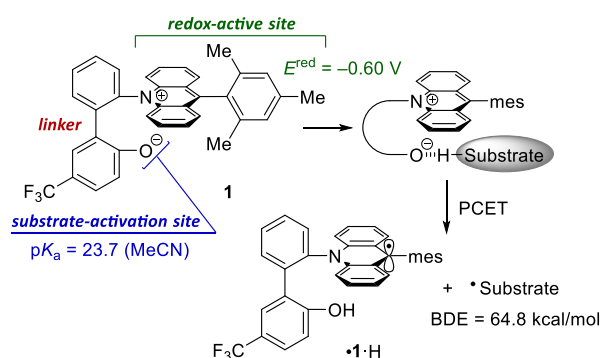


Figure 1. Structure and Properties of Acridinium Betaine **1**

The 9-mesityl acridinium subunit was chosen as a redox-active component suitable for our purpose because it fulfilled the following criteria: a relatively high reduction potential ($E^{\text{red}} = -0.50 \text{ V}$ vs SCE), robustness in the single-electron redox process, and susceptibility of its reduced radical form to oxidation with oxygen.^{9,10} A basic unit that would have hydrogen-bonding interaction with the acidic substrate was planned to be installed as a form of a phenoxide counterion through the formation of biaryl linkage, building up the molecular architecture of the PCET catalyst **1** (Fig. 1). Actual synthesis of **1** was implemented in a straightforward manner and its three-dimensional structure was unambiguously determined by single-crystal X-ray diffraction analysis (Fig. 2a and SI). The reduction potential of **1** was detected to be -0.60 V (vs SCE) through cyclic voltammetry (CV) measurements in MeCN and its $\text{p}K_{\text{a}}$ value was determined from the change in UV-Vis absorbance during acid-base titration with DBU or acetic acid ($\text{p}K_{\text{a}} = 23.7$ in MeCN).¹¹ These physical data suggested that **1** could oxidize organic compounds having an active proton (bond-dissociation energy (BDE) = 64.8 kcal/mol) through the PCET process.¹² In order to evaluate this possibility, *N*-PMP-3-aryl-oxindole **2** (BDE = 69.2 kcal/mol, calculated at B3LYP/6-31G* level)¹³ was selected as a precursor of the corresponding radical enolate that would undergo subsequent homo-dimerization.¹⁴

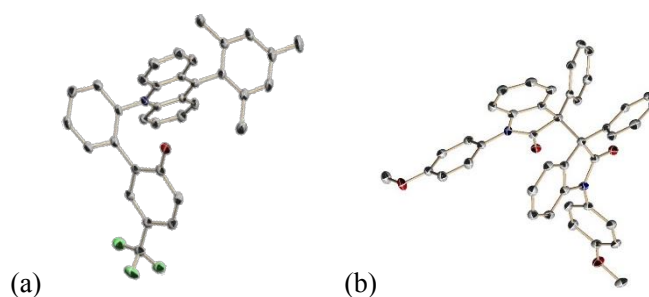


Figure 2. ORTEP Diagram of (a) **1** and (b) **3a** (Ellipsoids displayed at 50% probability. Calculated hydrogen atoms are omitted for clarity. Gray: carbon, red: oxygen, blue: nitrogen, green: fluorine.)

A catalytic mechanism proposed for this model system is depicted in Fig. 3. The reaction would be initiated by PCET between the acridinium betaine **1** and oxindole **2** to form the transient, intermediary radical pair **A**. The lifetime of **A** is estimated to be very short due to the frequent back-electron-transfer (BET) reaction to afford the parent substrate **2** and catalyst **1**. Assuming the proximity of oxygen molecule (O₂) to the radical pair, SET then

takes place to release the reactive radical enolate of **2** with concomitant regeneration of **1**. Subsequently, the radical enolate dimerizes to give the homo-coupling product **3** under diffusion control.

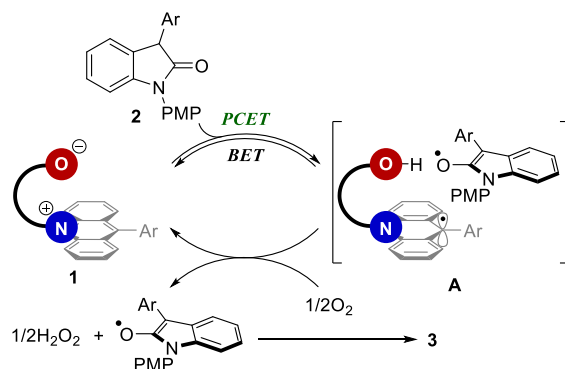
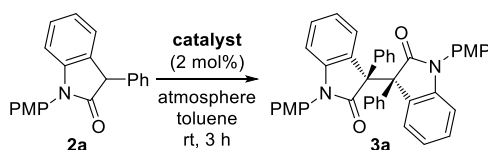


Figure 3. Proposed Catalytic Cycle (PMP = 4-MeOC₆H₄)

The validity of this hypothesis was assessed by treatment of **2a** with 2 mol% of **1** in toluene at room temperature in an oxygen atmosphere (Table 1, entry 1). The reaction proceeded smoothly and, after 3 h of stirring, the expected dimer **3a** was isolated in good yield. The structure of **3a** was confirmed by X-ray diffraction analysis, uncovering that it was a *meso*-isomer (Fig. 2b). While the replacement of oxygen with air did not affect the reaction outcome, the formation of **3a** was almost completely suppressed in the absence of oxygen even after a prolonged time of stirring (entries 2 and 3), clearly indicating that oxygen is essential for promoting the dimerization. When the reaction was performed with pyridinium betaine (**betaine**), which lacks a redox-active site, as a base catalyst, only α -hydroxylation product **4** was obtained in a very low yield as a consequence of α -oxidation of the enolate ion generated from the deprotonation of **2a** by **betaine** (entry 4). On the other hand, the simple acridinium salt (**acr**) without a basic site showed an activity for the homo-coupling to produce **3a** and a certain acceleration was observed under the binary catalysis of **acr** and **betaine**; however, the rate was markedly slower than that of the **1**-catalyzed reaction (entries 5 and 6). These results revealed the critical importance of the unique structural feature of **1**, which has redox-active and basic units embedded in the same molecular framework, to attain an optimal catalytic efficiency.

Table 1. Evaluation of Catalytic Performance of **1**^a



entry	catalyst	atmosphere	yield (%) ^b	yield of 4 (%) ^b
1	1	O ₂	80	trace
2	1	air	82	trace
3 ^c	1	Ar	<5	–
4 ^c	betaine	air	trace	9
5 ^c	acr	air	6	–

6^d

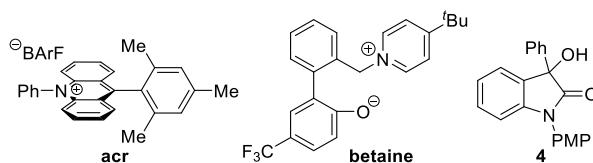
betaine + acr

air

29

<5

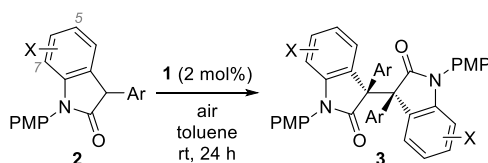
^a The reactions were performed with 0.1 mmol of **2a** with 2 mol% of catalysts in 1.0 mL of toluene at rt for 3 h. ^b Isolated yields are indicated. ^c Reaction time was 24 h. ^d **2a** was not completely consumed even after 24 h (56% yield).
BArF = [3,5-(CF₃)₂C₆H₃]₄B, PMP = 4-MeOC₆H₄



With the high-performance PCET catalyst **1** in hand, substrate generality was surveyed (Table 2). This system tolerated the incorporation of electron-rich and electron-deficient aromatic groups as a substituent at the 3-position consistently with a satisfactory level of efficiency (entries 1-10). However, the coupling reaction was found to be sensitive to steric hindrance around the C3 carbon and 2-tolyl-substituted oxindole could not be converted into the corresponding dimer (datum not shown). Oxindoles **2** with a substituent at the 5- or 7-position also appeared to be good candidates for the present dimerization (entries 11-14).

To gain mechanistic insight into the **1**-catalyzed dimerization of **2**, we analyzed its kinetic profile by monitoring the reaction progress through in-situ IR spectroscopy and compared it to the dimerization under the binary catalysis of **acr** and **betaine**. First, this analysis revealed that the initial rate of the reaction catalyzed by **1** was approximately 37-fold faster than that of the coupling with **acr** and **betaine** as catalysts (see Fig. S7).¹⁵ Secondly, the **1**-catalyzed dimerization showed a 1.1th order dependence on catalyst **1**, -0.85th order dependence on oxindole **2**, and 0.57th order dependence on O₂. While the observed non-integer orders suggested the involvement of equilibrium prior to the rate-limiting step, the negative dependence on the concentration of **2** could not

Table 2. Substrate Generality^a



entry	Ar	X	yield (%) ^b	prod.
1	Ph	H	88	3a
2	4-MeOC ₆ H ₄	H	99	3b
3	4-MeC ₆ H ₄	H	88	3c
4	4- ⁿ BuC ₆ H ₄	H	85	3d
5	4- ^t BuC ₆ H ₄	H	83	3e
6	4-ClC ₆ H ₄	H	81	3f
7	3-MeOC ₆ H ₄	H	95	3g

8	3-MeC ₆ H ₄	H	80	3h
9	3-FC ₆ H ₄	H	86	3i
10	2-naphthyl	H	85	3j
11	Ph	5-MeO	64	3k
12	Ph	5-Me	98	3l
13	Ph	5-F	83	3m
14	Ph	7-F	68	3n

^a The reactions were performed with 0.1 mmol of **2** with 2 mol% of **1** in 1.0 mL of toluene at rt for 24 h under air.

^b Isolated yields are indicated.

be rationalized by the initially proposed catalytic cycle (Fig. 3), and strongly implied the intervention of another pathway in this catalytic system. This notion led us to postulate a revised cycle as illustrated in Figure 4, which was based on the assumption that once the acridinium enolate of **2** was generated, SET from the enolate ion to the acridinium unit would be much more sluggish than with PCET.¹⁶ The acridinium enolate could be generated not only through the acid-base equilibrium between **1** and **2** but also from the ionic radical pair **1**·H·O₂• via deprotonation of **2** by the radical anion of O₂. The latter process competes with the regeneration of **1**, which is apparently the rate-limiting step, and thus effective concentration of **1** would decrease with increasing concentration of **2**. Meanwhile, considering the significant influence of O₂ on the rate-limiting step, we attempted the reaction of **2a** with a stoichiometric quantity of **1** in an argon atmosphere (Scheme 1). The homo-coupling product **3a** was obtained in a very low yield, corroborating that O₂ plays a crucial role in facilitating the carbon-carbon bond-forming step, presumably as a single-electron oxidant for liberating the radical enolate of **2** from the radical pair **A**. The overall turnover of this catalytic system should generate hydrogen peroxide (H₂O₂), which was indeed detected by the method developed by Takamura as the formation of peroxo[5,10,15,20-tetra(4-pyridyl)porphyrinato]titanium(IV) (see SI).¹⁷ Although clarification of the detailed mechanism requires additional studies, these observations support the operation of the PCET catalysis of **1** in the present dimerization reaction.

The synthetic potential of **1** as the PCET catalyst was further demonstrated by its application to different transformations. For instance, treatment of an equimolar mixture of *N*-Boc 1,2,3,4-tetrahydroisoquinoline and α -(4-bromophenyl)nitromethane with **1** (5 mol%) in toluene at 60 °C in an oxygen atmosphere resulted in the formation of a hetero-coupling product in high yield (Scheme 2).^{18,19}

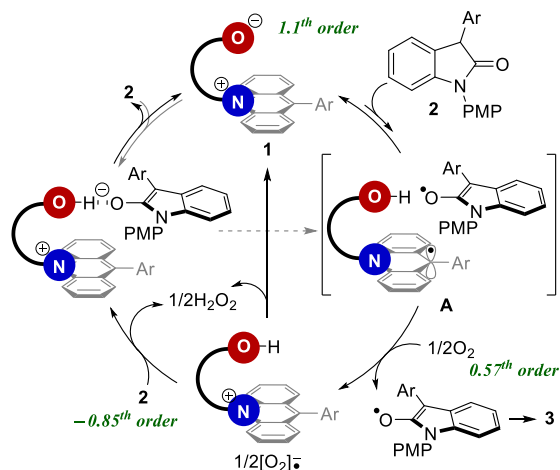
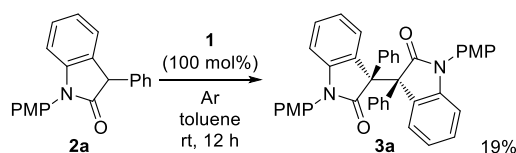
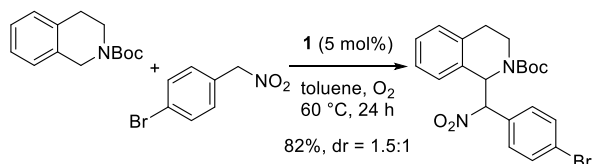


Figure 4. Revised Plausible Reaction Mechanism of Dimerization of **2** under the Catalysis of **1**

Scheme 1. Stoichiometric Usage of **1** in the Dimerization of **2a**



Scheme 2. Coupling Reaction of *N*-Boc 1,2,3,4-Tetrahydro-isoquinoline with α -Aryl Nitromethane under the Catalysis of **1**

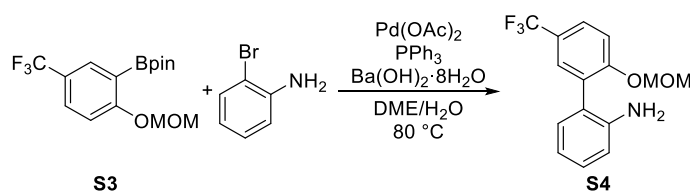


Summery

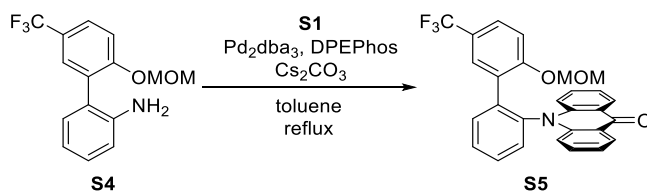
In conclusion, we have developed an acridinium betaine featuring an intramolecular ion-pairing between the redox-active acridinium cation and basic phenoxide anion. Its remarkably high performance as a PCET catalyst was unveiled in the homo-dimerization of 3-aryl oxindoles and the coupling of tetrahydroisoquinoline with a nitroalkane. Kinetic analysis revealed the crucial importance of the structural features of the acridinium betaine in attaining a high level of efficiency in the dimerization and allowed to understand the catalytic mechanism operative with PCET process. We believe that this study will stimulate further research efforts for the development of chemical redox catalysis.

General Information: Infrared spectra were recorded on a SHIMADZU IRAffinity-1 spectrometer. ¹H NMR spectra were recorded on a JEOL JNM-ECS400 (400 MHz) spectrometer, a JEOL ECA500II (500 MHz) spectrometer, or a JEOL JNM-ECA600 (600 MHz) spectrometer. Chemical shifts are reported in ppm from the solvent resonance (CD₃CN: 1.94 ppm) or tetramethylsilane (0.00 ppm) resonance as the internal standard. Data are reported as follows: chemical shift, integration, multiplicity (s = singlet, d = doublet, t = triplet, q = quartet, m = multiplet, br = broad), and coupling constants (Hz). ¹³C NMR spectra were recorded on a JEOL JNM-ECS400 (100 MHz), a JEOL ECA500II (126 MHz) spectrometer, or a JEOL JNM-ECA600 (151 MHz) spectrometer with complete proton decoupling. Chemical shifts are reported in ppm from the solvent resonance (CDCl₃: 77.16 ppm, CD₃OD: 49.00 ppm, CD₃CN: 1.32 ppm). ¹⁹F NMR spectra were recorded on a JEOL ECA500II (471 MHz) or a JEOL JNM-ECS400 (373 MHz) spectrometer with complete proton decoupling. Chemical shifts are reported in ppm from benzotrifluoride (−64.0 ppm) resonance as the external standard. The high resolution mass spectra were conducted on Thermo Fisher Scientific Exactive (ESI). Kinetic experiments were performed by using Mettla-Torred AutoChem IC15. Analytical thin layer chromatography (TLC) was performed on Merck precoated TLC plates (silica gel 60 GF254, 0.25 mm). Flash column chromatography was performed on silica gel 60 (spherical, 40-50 μm; Kanto Chemical Co., Inc.). Simple chemicals were purchased and used as such. Toluene was supplied from Kanto Chemical Co., Inc. as “Dehydrated” and further purified by passing through neutral alumina under nitrogen atmosphere. Trifluoromethanesulfonic anhydride (Tf₂O) was kindly supplied from Central Glass Co., Ltd.

temperature. After 8 h of stirring, the reaction mixture was filtered and concentrated. The residual solid was purified by column chromatography on silica gel (H/EA = 20:1-3:1 as eluent) to give **S3** (4.62 g, 13.9 mmol, 58% in two steps) as a colorless oil. **S3**: ^1H NMR (400 MHz, CDCl_3) δ 7.94 (1H, d, $J = 2.2$ Hz), 7.61 (1H, dd, $J = 8.8, 2.2$ Hz), 7.11 (1H, d, $J = 8.8$ Hz), 5.24 (2H, s), 3.50 (3H, s), 1.36 (12H, s); ^{13}C NMR (100 MHz, CDCl_3) δ 164.1, 133.9 (q, $J_{\text{C-F}} = 3.8$ Hz), 129.5 (q, $J_{\text{C-F}} = 3.9$ Hz), 124.5 (q, $J_{\text{C-F}} = 272.7$ Hz), 123.8 (q, $J_{\text{C-F}} = 32.6$ Hz), 114.6, 94.8, 84.0, 56.4, 24.9, one carbon atom was not found probably due to overlapping; ^{19}F NMR (373 MHz, CDCl_3) δ -61.6; IR (film): 2980, 2359, 1612, 1497, 1354, 1312, 1267, 1140, 1117, 1080, 1167, 988, 962, 851 cm^{-1} ; HRMS (ESI) Calcd for $\text{C}_{15}\text{H}_{20}\text{O}_4\text{BF}_3\text{Na}^+$ ($[\text{M}+\text{Na}]^+$) 355.1299. Found 355.1297.

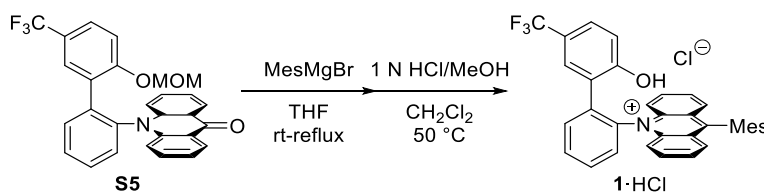


A reaction mixture of **S3** (1.99 g, 6.0 mmol), 2-bromoaniline (544.0 μL , 5.0 mmol), $\text{Pd}(\text{OAc})_2$ (112.3 mg, 0.50 mmol), PPh_3 (524.6 mg, 2.0 mmol), and $\text{Ba}(\text{OH})_2 \cdot 8\text{H}_2\text{O}$ (4.73 g, 15.0 mmol) in DME/ H_2O (v/v = 5:1; 25.0 mL) was subjected to a process of evacuation and refill with argon three times and was stirred at 80 $^\circ\text{C}$ for 12 h. The reaction mixture was filtered through a pad of Celite at rt. The concentrated filtrate was diluted with H_2O and extracted with EA twice. The combined organic extracts were washed with H_2O twice and brine, and dried over Na_2SO_4 . Evaporation of volatiles and subsequent purification of the residue by column chromatography on silica gel (H/EA = 20:1-3:1 as eluent) afforded **S4** (1.06 g, 3.55 mmol, 71%) as a brown viscous liquid. **S4**: ^1H NMR (500 MHz, CDCl_3) δ 7.58 (1H, d, $J = 8.5$ Hz), 7.55 (1H, s), 7.30 (1H, d, $J = 8.5$ Hz), 7.17 (1H, t, $J = 7.5$ Hz), 7.07 (1H, d, $J = 7.5$ Hz), 6.81 (1H, t, $J = 7.5$ Hz), 6.74 (1H, d, $J = 7.5$ Hz), 5.14 (2H, s), 3.61 (2H, br), 3.36 (3H, s); ^{13}C NMR (126 MHz, CDCl_3) δ 157.1, 144.4, 130.9, 129.14, 129.09, 126.3 (q, $J_{\text{C-F}} = 3.7$ Hz), 124.3 (q, $J_{\text{C-F}} = 272.1$ Hz), 124.5 (q, $J_{\text{C-F}} = 32.7$ Hz), 123.4, 118.5, 115.8, 115.3, 94.8, 56.4, one carbon atom was not found provably due to overlapping; ^{19}F NMR (373 MHz, CDCl_3) δ -61.6; IR (film): 3377, 2937, 2359, 1614, 1493, 1333, 1273, 1227, 1200, 1155, 1115, 1080, 980, 922 cm^{-1} ; HRMS (ESI) Calcd for $\text{C}_{15}\text{H}_{14}\text{O}_2\text{NF}_3\text{Na}^+$ ($[\text{M}+\text{Na}]^+$) 320.0869. Found 320.0866.

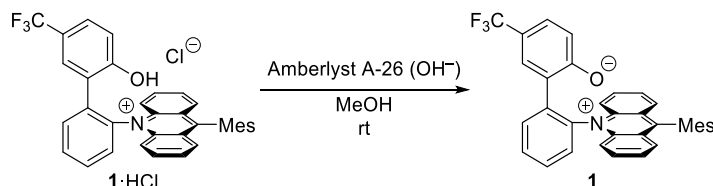


To a two-necked flask equipped with a condenser was placed **S4** (891.8 mg, 3.0 mmol), **S1** (2.15 g, 4.5 mmol), Pd_2dba_3 (54.9 mg, 0.060 mmol), DPEphos (64.6 mg, 0.12 mmol), and Cs_2CO_3 (2.93 g, 9.0 mmol). After the addition of toluene (15 mL), evacuation and refill with argon were repeated three times and the reaction mixture was stirred for 12 h under reflux. After being cooled to rt, the reaction mixture was filtered through a pad of Celite

at rt. The concentrated filtrate was purified by column chromatography on silica gel (cyclohexane/EA = 20:1-1:1 as eluent) to afford **S5** (1.14 g, 2.4 mmol, 84%) as a white solid. **S5**: ^1H NMR (600 MHz, CDCl_3) δ 8.44 (2H, dd, $J = 8.4, 1.8$ Hz), 7.75-7.67 (2H, m), 7.63 (1H, m), 7.52 (1H, m), 7.47 (2H, dt, $J = 8.4, 1.8$ Hz), 7.25-7.15 (3H, m), 7.04 (1H, d, $J = 1.8$ Hz), 7.00-6.86 (3H, m), 4.60 (2H, s), 3.19 (3H, s); ^{13}C NMR (151 MHz, CDCl_3) δ 178.0, 156.9, 142.9, 138.2, 137.3, 133.5, 132.9, 131.1, 130.4, 129.7, 127.7 (q, $J_{\text{C-F}} = 2.9$ Hz), 127.3, 127.0, 126.8, 126.7 (q, $J_{\text{C-F}} = 2.9$ Hz), 123.7 (q, $J_{\text{C-F}} = 271.8$ Hz), 123.1 (q, $J_{\text{C-F}} = 33.2$ Hz), 121.5, 121.6, 117.3, 94.5, 56.0; ^{19}F NMR (471 MHz, CDCl_3) δ -62.2; IR (film): 3408, 2359, 1607, 1584, 1539, 1437, 1385, 1331, 1283, 1161, 1115, 1074, 837 cm^{-1} ; HRMS (ESI) Calcd for $\text{C}_{28}\text{H}_{21}\text{O}_3\text{NF}_3^+$ ($[\text{M}+\text{H}]^+$) 476.1468. Found 476.1468.



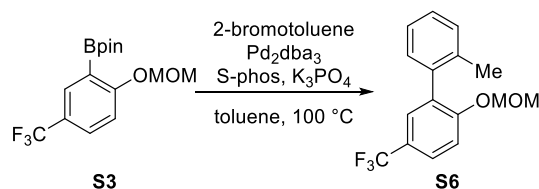
A solution of **S5** (950.9 mg, 2.0 mmol) in THF (10.0 mL) was introduced to a THF solution of 2-mesitylmagnesium bromide (ca. 1 M, 20 mL, 20.0 mmol) at rt and the reaction mixture was stirred for 6 h under reflux. The resulting mixture was cooled to ambient temperature and diluted with a saturated aqueous solution of NaHCO_3 . The aqueous phase was extracted with EA twice and the combined organic extracts were washed with brine. After drying over Na_2SO_4 and filtration, the organic phase was concentrated under reduced pressure. The crude residue was dissolved into CH_2Cl_2 (20.0 mL) and 1 N HCl/MeOH (20.0 mL) was added slowly to the mixture. After being stirred at 50 °C for 6 h and concentration, the residual solid was purified by column chromatography on silica gel (H/EA = 1:1 then $\text{CH}_2\text{Cl}_2/\text{MeOH} = 1:0-5:1$ as eluent) to give **1**·HCl (798.1 mg, 1.4 mmol, 70%). **1**·HCl: ^1H NMR (500 MHz, CD_3OD) δ 8.25 (2H, t, $J = 7.5$ Hz), 8.13-7.99 (3H, m), 7.94 (2H, d, $J = 9.0$ Hz), 7.89-7.72 (6H, m), 7.26 (1H, s), 7.20 (1H, s), 7.06 (1H, d, $J = 7.5$ Hz), 6.94 (1H, s), 6.49 (1H, d, $J = 8.5$ Hz), 2.47 (3H, s), 1.87 (3H, s), 1.37 (3H, s); ^{13}C NMR (126 MHz, CD_3OD) δ 165.4, 158.9, 143.3, 141.9, 139.9, 137.9, 137.2, 137.0, 136.7, 135.0, 133.2, 131.8, 130.6, 130.0, 129.9, 129.7, 129.4, 128.2 (q, $J_{\text{C-F}} = 3.5$ Hz), 127.9 (q, $J_{\text{C-F}} = 3.5$ Hz), 126.9, 125.2 (q, $J_{\text{C-F}} = 270.9$ Hz), 124.4, 122.1, 121.5 (q, $J_{\text{C-F}} = 32.6$ Hz), 116.3, 21.4, 20.0, 19.7, one carbon atom was not found provably due to overlapping; ^{19}F NMR (373 MHz, CD_3OD) δ -63.2; IR (film): 3390, 3061, 2531, 1607, 1539, 1437, 1331, 1283, 1161, 1113 cm^{-1} ; HRMS (ESI) Calcd for $\text{C}_{35}\text{H}_{27}\text{ONF}_3^+$ ($[\text{M}-\text{Cl}]^+$) 534.2039. Found 534.2039.



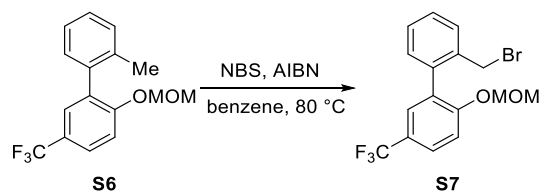
Acridinium betaine **1** was prepared by following the literature procedure.⁸ A methanolic solution of **1**·HCl was passed through a column of ion exchange resin (Amberlyst A-26, OH form). The solution was concentrated by rotary evaporation and the residual solid was washed with Et_2O on a funnel. The solid thus obtained

was dried under reduced pressure to afford **1** as a deep brown solid and **1** was used for the homo-dimerization of oxindoles without further purification. **1**: $^1\text{H NMR}$ (400 MHz, CD_3OD) δ 8.22-8.12 (2H, m), 7.97 (2H, d, $J = 8.8$ Hz), 7.96-7.91 (2H, m), 7.88-7.81 (2H, m), 7.75 (4H, d, $J = 4.0$ Hz), 7.23 (1H, s), 7.18 (1H, s), 6.71 (1H, dd, $J = 8.8, 2.2$ Hz), 6.48 (1H, d, $J = 2.2$ Hz), 6.18 (1H, d, $J = 8.8$ Hz), 2.46 (3H, s), 1.83 (3H, s), 1.47 (3H, s); $^{13}\text{C NMR}$ (100 MHz, CD_3OD) δ 170.5, 164.6, 143.6, 141.6, 141.4, 139.6, 137.2₄, 137.1₅, 136.9, 135.9, 132.6, 130.8, 130.1, 130.0, 129.8, 129.6, 129.2, 127.2 (q, $J_{\text{C-F}} = 2.9$ Hz), 126.9, 126.6 (q, $J_{\text{C-F}} = 2.8$ Hz), 126.5 (q, $J_{\text{C-F}} = 270.2$ Hz), 125.2, 122.4, 121.0, 112.9 (q, $J_{\text{C-F}} = 32.3$ Hz), 21.4, 20.0, 19.9; $^{19}\text{F NMR}$ (373 MHz, CD_3OD) δ -61.2; IR (film) 2918, 2860, 1607, 1584, 1485, 1435, 1381, 1359, 1321, 1117, 1078, 1065 cm^{-1} ; HRMS (ESI) Calcd for $\text{C}_{35}\text{H}_{27}\text{ONF}_3^+$ ($[\text{M}+\text{H}]^+$) 534.2039. Found 534.2035.

Preparation and Characterization of Pyridinium Betaine:

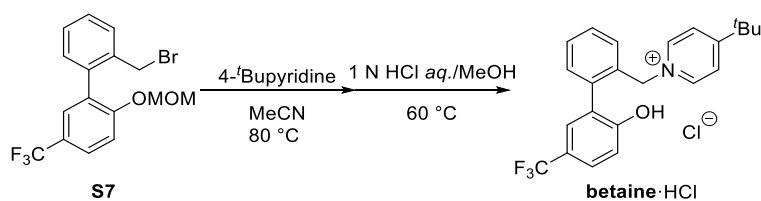


To a mixture of **S3** (3.87 g, 12.0 mmol), 2-bromotoluene (1.20 mL, 10.0 mmol), Pd_2dba_3 (183.1 mg, 0.20 mmol), S-phos (164.2 mg, 0.40 mmol), and K_3PO_4 (10.6 g, 50.0 mmol) in a two-necked flask equipped with a condenser was added toluene (20.0 mL) and evacuation of the flask and refill with argon were repeated three times. The reaction mixture was stirred for 12 h at 100 °C and then, it was filtered through a pad of Celite at rt. The filtrate was concentrated and the residue was purified by column chromatography on silica gel (H/EA = 20:1-3:1 as eluent) to afford **S6** (2.70 g, 9.1 mmol, 91%) as a brown viscous liquid. **S6**: $^1\text{H NMR}$ (600 MHz, CDCl_3) δ 7.58 (1H, dd, $J = 8.4, 1.8$ Hz), 7.43 (1H, d, $J = 1.8$ Hz), 7.33-7.21 (4H, m), 7.16 (1H, d, $J = 7.2$ Hz), 5.12 (2H, s), 3.36 (3H, s), 2.15 (3H, s); $^{13}\text{C NMR}$ (151 MHz, CDCl_3) δ 157.1, 137.4, 136.8, 132.4, 130.0, 129.9, 128.4 (q, $J_{\text{C-F}} = 4.4$ Hz), 128.0, 126.1 (q, $J_{\text{C-F}} = 4.4$ Hz), 125.7, 124.5 (q, $J_{\text{C-F}} = 272.0$ Hz), 124.1 (q, $J_{\text{C-F}} = 32.8$ Hz), 114.8, 94.8, 56.4, 20.1; $^{19}\text{F NMR}$ (471 MHz, CDCl_3) δ -61.5; IR (film): 2957, 1614, 1487, 1420, 1333, 1267, 1229, 1200, 1157, 1138, 1084, 827 cm^{-1} ; HRMS (ESI) Calcd for $\text{C}_{16}\text{H}_{15}\text{O}_2\text{F}_3\text{Na}^+$ ($[\text{M}+\text{Na}]^+$) 319.0916. Found 319.0917.

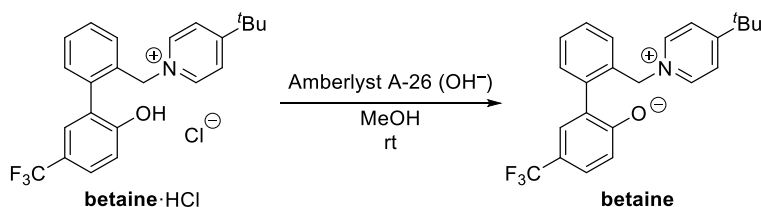


S6 (592.6 mg, 2.0 mmol), NBS (427.2 mg, 2.4 mmol), and AIBN (32.8 mg, 0.20 mmol) were suspended to benzene (20.0 mL) and the mixture was heated to 80 °C. After 1 h of stirring, the reaction mixture was allowed to cool to ambient temperature and poured into H_2O . The aqueous phase was extracted with EA twice and the combined organic extracts were washed with brine. After drying over Na_2SO_4 and filtration, the organic phase was concentrated under vacuum. The crude mixture was purified by column chromatography on silica gel (H/EA =

20:1-10:1 as eluent) to afford **S7** (337.7 mg, 0.9 mmol, 42%) as a colorless liquid. **S7**: $^1\text{H NMR}$ (600 MHz, CDCl_3) δ 7.62 (1H, dd, $J = 8.7, 2.1$ Hz), 7.55 (1H, d, $J = 7.2$ Hz), 7.53 (1H, d, $J = 2.1$ Hz), 7.40 (1H, dt, $J = 7.2, 1.2$ Hz), 7.36 (1H, dt, $J = 7.2, 1.2$ Hz), 7.32 (1H, d, $J = 8.7$ Hz), 7.19 (1H, d, $J = 7.2$ Hz), 5.16 (1H, d, $J = 6.9$ Hz), 5.11 (1H, d, $J = 6.9$ Hz), 4.39 (1H, d, $J = 10.5$ Hz), 4.29 (1H, d, $J = 10.5$ Hz), 3.35 (3H, s); $^{13}\text{C NMR}$ (151 MHz, CDCl_3) δ 156.9, 137.2, 136.3, 130.8, 130.6, 130.2, 128.7, 128.5₈ (q, $J_{\text{C-F}} = 4.4$ Hz), 128.5₂, 126.8 (q, $J_{\text{C-F}} = 4.2$ Hz), 124.4 (q, $J_{\text{C-F}} = 271.3$ Hz), 124.1 (q, $J_{\text{C-F}} = 32.8$ Hz), 114.8, 94.8, 56.5, 31.7; $^{19}\text{F NMR}$ (471 MHz, CDCl_3) δ -61.6; IR (film): 2957, 1614, 1335, 1269, 1231, 1200, 1157, 1121, 1184, 984, 826, 768 cm^{-1} ; HRMS (ESI) Calcd for $\text{C}_{16}\text{H}_{14}\text{O}_2\text{F}_3^{79}\text{BrNa}^+$ ($[\text{M}+\text{Na}]^+$) 397.0027. Found 397.0023.



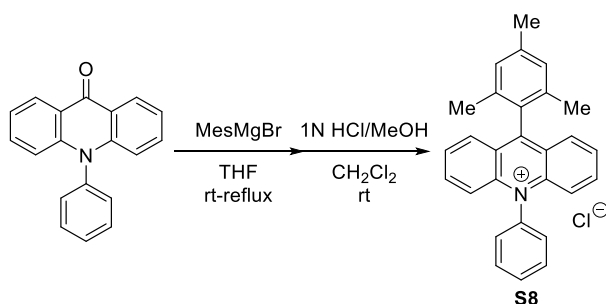
To a mixture of **S7** (337.7 mg, 0.9 mmol) and 4-*tert*-butylpyridine (161.7 μL , 1.1 mmol) in the test tube was added acetonitrile (0.9 mL) and the solution was stirred at 80 $^\circ\text{C}$ for 1 h. After cooling to rt, the mixture was concentrated and 1 N HCl/MeOH (20.0 mL) was introduced slowly. The reaction mixture was then stirred at 50 $^\circ\text{C}$ for 6 h. The concentrated crude material was purified by column chromatography on silica gel (H/EA = 1:1 then $\text{CH}_2\text{Cl}_2/\text{MeOH} = 1:0.5:1$ as eluent) to give **betaine·HCl** (265.8 mg, 0.6 mmol, 70%). **betaine·HCl**: $^1\text{H NMR}$ (600 MHz, CD_3OD) δ 8.35 (2H, d, $J = 6.9$ Hz), 7.89 (2H, d, $J = 6.9$ Hz), 7.62 (1H, d, $J = 8.4$ Hz), 7.60-7.51 (3H, m), 7.30 (1H, dd, $J = 7.2, 1.5$ Hz), 7.07 (1H, d, $J = 1.5$ Hz), 7.06 (1H, t, $J = 8.4$ Hz), 5.76 (1H, d, $J = 14.7$ Hz), 5.72 (1H, d, $J = 14.7$ Hz), 1.36 (9H, s); $^{13}\text{C NMR}$ (151 MHz, CD_3OD) δ 173.0, 158.6, 145.0, 140.0, 133.2, 131.9, 131.5, 130.1, 128.9 (q, $J_{\text{C-F}} = 4.2$ Hz), 128.3, 128.1 (q, $J_{\text{C-F}} = 2.9$ Hz), 126.0, 125.7 (q, $J_{\text{C-F}} = 270.4$ Hz), 124.8, 123.0 (q, $J_{\text{C-F}} = 32.8$ Hz), 117.3, 64.1, 37.5, 30.1; $^{19}\text{F NMR}$ (373 MHz, CD_3OD) δ -62.3; IR (film) 2970, 1638, 1614, 1458, 1373, 1331, 1279, 1260, 1163, 1111, 1074, 1053 cm^{-1} ; HRMS (ESI) Calcd for $\text{C}_{23}\text{H}_{23}\text{ONF}_3$ ($[\text{M}-\text{Cl}]^+$) 386.1726. Found 386.1724.



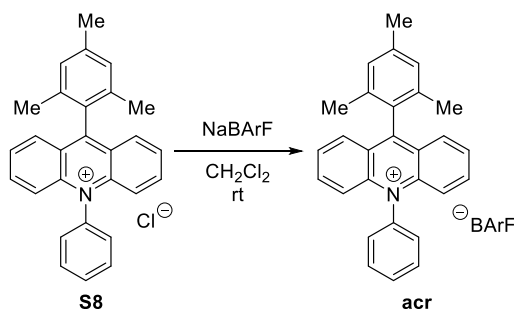
Betaine was prepared by passage of a methanolic solution of **betaine·HCl** through a column of ion exchange resin (Amberlyst A-26, OH form).⁸ The solution was concentrated by rotary evaporation and the residual solid was washed with Et_2O on a funnel. The solid thus obtained was dried under reduced pressure to afford the **betaine** as a yellow solid, and **betaine** was used for the homo-coupling reaction of oxindoles without further purification. **betaine**: $^1\text{H NMR}$ (400 MHz, CD_3OD) δ 8.29 (2H, d, $J = 5.6$ Hz), 7.77 (2H, d, $J = 5.6$ Hz), 7.49 (2H,

br), 7.43 (1H, t, $J = 7.4$ Hz), 7.27 (1H, d, $J = 7.4$ Hz), 7.21 (1H, d, $J = 8.8$ Hz), 6.69-6.60 (2H, m), 6.04 (1H, d, $J = 14.4$ Hz), 5.59 (1H, d, $J = 14.4$ Hz), 1.33 (9H, s); ^{13}C NMR (100 MHz, CD_3OD) δ 172.2, 170.0, 149.9, 144.9, 143.6, 134.1, 133.0, 131.4, 131.1, 130.1, 128.6, 128.5, 127.4 (q, $J_{\text{C-F}} = 2.9$ Hz), 127.0 (q, $J_{\text{C-F}} = 270.2$ Hz), 125.5, 121.4, 114.6 (q, $J_{\text{C-F}} = 32.2$ Hz), 65.0, 37.3, 30.0; ^{19}F NMR (373 MHz, CD_3OD) δ -60.7; IR (film) 2968, 1639, 1603, 1522, 1487, 1450, 1339, 1321, 1300, 1254, 1121, 1088, 1065 cm^{-1} ; HRMS (ESI) Calcd for $\text{C}_{23}\text{H}_{23}\text{ONF}_3^+$ ($[\text{M}+\text{H}]^+$) 386.1726. Found 386.1721.

Preparation and Characterization of *N*-Phenyl Acridinium BArF:



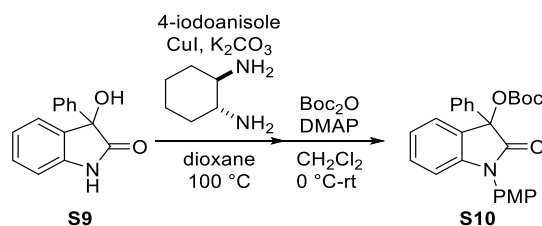
N-Phenyl acridone was prepared by following the literature procedure.¹⁰ A solution of *N*-Phenyl acridone (1.04 g, 3.8 mmol) in THF (3.8 mL) were introduced to a THF solution of 2-mesitylmagnesium bromide (ca. 1 M, 38.0 mL, 38.0 mmol) at rt and the reaction mixture was stirred for 6 h under reflux. The resulting mixture was cooled to room temperature, diluted with saturated aqueous solution of NaHCO_3 . The aqueous phase was extracted with EA twice and the combined organic extracts were washed with brine. After drying over Na_2SO_4 and filtration, the organic phase was concentrated under reduced pressure. The crude residue was dissolved into CH_2Cl_2 (20.0 mL) and added 1N HCl/MeOH (20.0 mL) was added slowly to the mixture. After being stirred for 30 min at rt, the residual solid was purified by column chromatography on silica gel ($\text{H}/\text{EA} = 1:1$ then $\text{CH}_2\text{Cl}_2/\text{MeOH} = 1:0-5:1$ as eluent) to give **S8** (1.19 g, 2.90 mmol, 77%). **S8**: ^1H NMR (600 MHz, CDCl_3) δ 8.26 (2H, ddd, $J = 9.0, 6.6, 1.8$ Hz), 8.00 (2H, t, $J = 7.8$ Hz), 7.94 (2H, d, $J = 7.8$ Hz), 7.91 (1H, t, $J = 7.8$ Hz), 7.88 (2H, d, $J = 6.6$ Hz), 7.86 (2H, t, $J = 9.0$ Hz), 7.66 (2H, d, $J = 9.0$ Hz), 7.20 (2H, s), 2.50 (3H, s), 1.86 (6H, s); ^{13}C NMR (151 MHz, CDCl_3) δ 164.9, 142.0, 140.8, 139.5, 136.8, 136.2, 132.3, 132.0, 129.3, 129.2, 129.1, 129.0, 128.3, 126.0, 120.4, 21.4, 20.6; IR (film): 3082, 2995, 2893, 1607, 1578, 1535, 1487, 1437, 1383, 1285, 1254, 893 cm^{-1} ; HRMS (ESI) Calcd for $\text{C}_{28}\text{H}_{24}\text{N}^+$ ($[\text{M}-\text{Cl}]^+$) 374.1903. Found 374.1908.



S8 (164.0 mg, 0.40 mmol) and Na[B(3,5-(CF₃)₂C₆H₃)₄] (NaBArF) (354.5 mg, 0.40 mmol) were dissolved into CH₂Cl₂ (2.0 mL). The reaction mixture was stirred for 10 min at room temperature and diluted with water. The aqueous phase was extracted with CH₂Cl₂ three times and the organic extracts were dried over Na₂SO₄. Concentration and subsequent purification of the residue by column chromatography on silica gel (H/CH₂Cl₂ = 1:1-0:1 as eluent) gave **acr** (415.9 mg, 0.34 mmol, 84%) as yellow solid. **acr**: ¹H NMR (400 MHz, CDCl₃) δ 8.02 (2H, t, *J* = 8.4 Hz), 7.97 (2H, d, *J* = 8.4 Hz), 7.84-7.71 (5H, m), 7.69 (8H, s), 7.54 (2H, d, *J* = 8.4 Hz), 7.49-7.41 (6H, m), 7.19 (2H, s), 2.48 (3H, s), 1.74 (6H, s); ¹³C NMR (100 MHz, CDCl₃) δ 166.1, 161.9 (q, *J*_{C-B} = 49.8 Hz), 141.8, 141.4, 139.5, 136.5, 135.6, 134.9, 132.6, 132.0, 129.5, 129.4, 129.1 (q, *J*_{C-F} = 31.6 Hz), 129.0, 127.4, 124.6 (q, *J*_{C-F} = 274.0 Hz), 119.8, 117.6, 21.3, 20.0, two carbon atoms were not found provably due to overlapping; ¹⁹F NMR (373 MHz, CDCl₃) δ -62.4; IR (film): 2814, 2635, 1609, 1580, 1491, 1460, 1439, 1354, 1283, 1269, 1167, 1155, 1101, 887 cm⁻¹; HRMS (ESI) Calcd for C₂₈H₂₄N⁺ ([M-BArF]⁺) 374.1903. Found 374.1906.

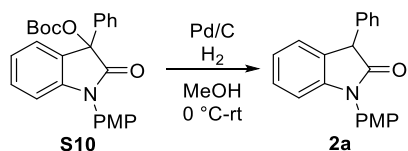
Preparation and Characterization of Oxindoles 2:

Compound **S9** was prepared from isatin by following the literature procedure²⁰, and *N*-PMP oxindoles **2**²¹ was prepared by following the literature procedure.



S9 (2.25 g, 10.0 mmol), 4-iodoaniline (3.51 g, 15.0 mmol), CuI (952 mg, 5.0 mmol), and K₂CO₃ (3.04 g, 22.0 mmol) were placed in a two-necked flask equipped with a condenser. After introducing 1,4-dioxane (33.3 mL), *trans*-cyclohexane-1,2-diamine (1.2 mL, 10.0 mmol) was added, and evacuation and refill with argon were repeated three times. The reaction mixture was stirred at 100 °C for 12 h and was cooled to rt. After addition of 1 N hydrochloric acid, the mixture was filtered through a pad of Celite. The concentrated filtrate was extracted with CH₂Cl₂. The organic extract was washed with H₂O twice and brine, and dried over Na₂SO₄. After filtration and concentration, DMAP (610.9 mg, 5.0 mmol) and CH₂Cl₂ (33.3 mL) were added to the residue. Boc₂O (4.6 mL, 20.0 mmol) was then added slowly to the solution at 0 °C and the reaction mixture was stirred for 3 h at rt. The resulting mixture was diluted with H₂O and extracted with CH₂Cl₂ twice. The combined organic extracts were washed with brine, filtered, and concentrated. Subsequent purification of the residue by column chromatography on silica gel (H/EA = 20:1-3:1 as eluent) afforded **S10** (3.05 g, 7.06 mmol, 71%) as a white solid. **S10**: ¹H NMR (600 MHz, CDCl₃) δ 7.46 (2H, m), 7.37-7.28 (7H, m), 7.12 (1H, t, *J* = 7.6 Hz), 7.00 (2H, d, *J* = 9.0 Hz), 6.79 (1H, d, *J* = 7.6 Hz), 3.83 (3H, s), 1.43 (9H, s); ¹³C NMR (151 MHz, CDCl₃) δ 173.9, 159.4, 151.4, 145.5, 136.6, 130.1, 129.0, 128.7, 128.3, 127.4, 126.6, 124.6, 123.4, 115.0, 109.8, 83.5, 82.0, 55.7, 27.9, one carbon atom was not found probably

due to overlapping; IR (film): 3059, 1738, 1614, 1512, 1483, 1464, 1369, 1283, 1248, 1152, 1105, 824 cm^{-1} ; HRMS (ESI) Calcd for $\text{C}_{26}\text{H}_{25}\text{O}_5\text{NNa}^+$ ($[\text{M}+\text{Na}]^+$) 454.1625. Found 454.1622.



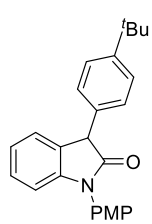
S10 (3.05 g, 7.06 mmol) was dissolved in methanol (22.9 mL) and EA (7.1 mL) under argon atmosphere. The solution was cooled to 0 °C and 10% palladium on carbon (Pd/C) (1.44 g) was added. Atmosphere of the reaction was exchanged with hydrogen and the mixture was stirred at rt overnight. The reaction mixture was passed through a pad of Celite with the aid of CH_2Cl_2 to remove Pd/C. After removal of the solvents, the crude residue was purified by column chromatography on silica gel (H/EA = 5:1-1:1 as eluent) to afford **2a** (2.00 g, 6.35 mmol, 90%) as a white solid. **2a**: ^1H NMR (600 MHz, CDCl_3) δ 7.37-7.32 (4H, m), 7.31-7.27 (3H, m), 7.24 (1H, t, $J = 8.4$ Hz), 7.21 (1H, d, $J = 7.2$ Hz), 7.07 (1H, t, $J = 7.2$ Hz), 7.03 (2H, d, $J = 9.0$ Hz), 6.81 (1H, d, $J = 8.4$ Hz), 4.77 (1H, s), 3.85 (3H, s); ^{13}C NMR (151 MHz, CDCl_3) δ 175.6, 159.3, 145.0, 137.0, 129.1, 128.8, 128.6, 128.4, 128.2, 127.7, 127.3, 125.4, 123.1, 115.0, 109.5, 55.7, 52.3; IR (film) 3059, 1717, 1611, 1510, 1462, 1371, 1298, 1246, 1217, 1163, 1030, 910, 831 cm^{-1} ; HRMS (ESI) Calcd for $\text{C}_{21}\text{H}_{17}\text{O}_2\text{NNa}^+$ ($[\text{M}+\text{Na}]^+$) 338.1152. Found 338.1148.

2b: ^1H NMR (600 MHz, CDCl_3) δ 7.33 (2H, dt, $J = 9.0, 3.0$ Hz), 7.23 (1H, t, $J = 8.1$ Hz), 7.22-7.19 (3H, m), 7.07 (1H, t, $J = 8.1$ Hz), 7.03 (2H, dt, $J = 9.0, 3.0$ Hz), 6.89 (2H, dt, $J = 9.0, 3.0$ Hz), 6.81 (1H, d, $J = 8.1$ Hz), 4.72 (1H, s), 3.86 (3H, s), 3.80 (3H, s); ^{13}C NMR (151 MHz, CDCl_3) δ 176.0, 159.2₈, 159.2₅, 145.0, 129.7, 129.0₃, 128.9₆, 128.3, 128.2, 127.4, 125.4, 123.1, 115.0, 114.5, 109.5, 55.7, 55.5, 51.5; IR (film) 1717, 1609, 1510, 1441, 1371, 1300, 1248, 1219, 1177, 1163, 1096, 1030, 815 cm^{-1} ; HRMS (ESI) Calcd for $\text{C}_{22}\text{H}_{19}\text{O}_3\text{NNa}^+$ ($[\text{M}+\text{Na}]^+$) 368.1257. Found 368.1252.

2c: ^1H NMR (600 MHz, CDCl_3) δ 7.33 (2H, d, $J = 9.0$ Hz), 7.23 (1H, t, $J = 7.8$ Hz), 7.20 (1H, d, $J = 7.2$ Hz), 7.18-7.15 (4H, m), 7.07 (1H, t, $J = 7.8$ Hz), 7.02 (2H, d, $J = 9.0$ Hz), 6.80 (1H, d, $J = 7.8$ Hz), 4.73 (1H, s), 3.85 (3H, s), 2.34 (3H, s); ^{13}C NMR (151 MHz, CDCl_3) δ 175.8, 159.3, 145.0, 137.5, 134.0, 129.8, 129.0, 128.5, 128.3, 128.2, 127.4, 125.4, 123.1, 115.0, 109.5, 55.7, 51.9, 21.3; IR (neat) 2924, 1717, 1609, 1508, 1462, 1373, 1298, 1248, 1163, 1096, 1030 cm^{-1} ; HRMS (ESI) Calcd for $\text{C}_{22}\text{H}_{19}\text{O}_2\text{NNa}^+$ ($[\text{M}+\text{Na}]^+$) 352.1308. Found 352.1304.

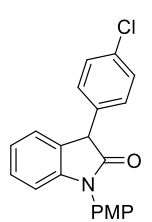
2d: ^1H NMR (600 MHz, CDCl_3) δ 7.33 (2H, d, $J = 9.0$ Hz), 7.23 (1H, t, $J = 7.8$ Hz), 7.25-7.20 (2H, m), 7.19 (1H, d, $J = 7.8$ Hz), 7.16 (1H, d, $J = 7.8$ Hz), 7.07 (1H, t, $J = 7.5$ Hz), 7.02 (2H, d, $J = 9.0$ Hz), 6.81 (2H, d, $J = 7.8$ Hz), 4.74 (1H, s), 3.85 (3H, s), 2.59 (2H, t, $J = 7.2$ Hz), 1.58 (2H, tt, $J = 7.8, 7.2$ Hz), 1.35 (2H, tq, $J = 7.8, 7.2$ Hz), 0.92 (3H, t, $J = 7.2$ Hz); ^{13}C NMR (151 MHz, CDCl_3) δ 175.9, 159.3, 145.0, 142.4, 134.1, 129.1, 129.0, 128.4, 128.3, 128.2, 127.4, 125.5, 123.1, 115.0, 109.5, 55.7, 51.9, 35.5, 33.7, 22.5, 14.1; IR (film) 2928, 1719, 1609, 1512, 1462, 1373, 1298, 1248, 1217, 1163, 1230, 827 cm^{-1} ;

HRMS (ESI) Calcd for $C_{25}H_{26}NO_2^+$ ($[M+H]^+$) 372.1958. Found 372.1959.

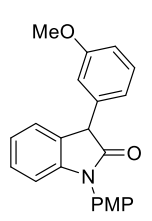


2e: 1H NMR (600 MHz, $CDCl_3$) δ 7.37 (2H, d, $J = 8.4$ Hz), 7.33 (2H, d, $J = 8.4$ Hz), 7.25-7.20 (4H, m), 7.07 (1H, t, $J = 8.1$ Hz), 7.02 (2H, d, $J = 8.4$ Hz), 6.81 (1H, d, $J = 8.1$ Hz), 4.75 (1H, s), 3.85 (3H, s), 1.31 (9H, s); ^{13}C NMR (151 MHz, $CDCl_3$) δ 175.9, 159.3, 150.6, 145.1, 133.8, 128.9, 128.3, 128.2, 127.4, 126.0, 125.5, 123.1, 115.0, 109.5, 55.7, 51.8, 34.7, 31.5, one carbon was not found probably due to overlapping; IR (film) 2961, 1717, 1609, 1512, 1462, 1369, 1298, 1248, 1217, 1163, 1026,

910, 824 cm^{-1} ; HRMS (ESI) Calcd for $C_{25}H_{25}NO_2Na^+$ ($[M+Na]^+$) 394.1778. Found 394.1775.

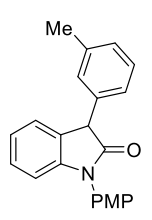


2f: 1H NMR (600 MHz, $CDCl_3$) δ 7.33 (2H, d, $J = 7.8$ Hz), 7.32 (2H, d, $J = 8.4$ Hz), 7.28-7.21 (3H, m), 7.20 (1H, d, $J = 7.8$ Hz), 7.09 (1H, t, $J = 7.8$ Hz), 7.03 (2H, d, $J = 8.4$ Hz), 6.82 (1H, d, $J = 7.8$ Hz), 4.74 (1H, s), 3.86 (3H, s); ^{13}C NMR (151 MHz, $CDCl_3$) δ 175.2, 159.4, 145.1, 135.4, 133.8, 130.0, 129.2, 128.7, 128.2, 128.1, 127.1, 125.4, 123.3, 115.1, 109.7, 55.7, 51.6; IR (film) 1713, 1609, 1518, 1491, 1460, 1371, 1325, 1254, 1169, 1219, 1088, 1016, 818 cm^{-1} ; HRMS (ESI) Calcd for $C_{21}H_{16}O_2NClNa^+$ ($[M+Na]^+$) 372.0762. Found 372.0764.



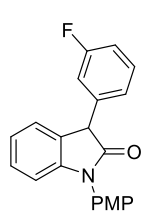
2g: 1H NMR (600 MHz, $CDCl_3$) δ 7.33 (2H, dt, $J = 9.0, 3.6$ Hz), 7.29-7.21 (3H, m), 7.07 (1H, t, $J = 7.8$ Hz), 7.03 (2H, dt, $J = 9.0, 3.6$ Hz), 6.87 (1H, d, $J = 8.4$ Hz), 6.86-6.83 (2H, m), 6.81 (1H, d, $J = 8.4$ Hz), 4.74 (1H, s), 3.86 (3H, s), 3.80 (3H, s); ^{13}C NMR (151 MHz, $CDCl_3$) δ 175.5, 160.1, 159.3, 145.0, 138.4, 130.0, 128.6, 128.5, 128.2, 127.3, 125.5, 123.2, 121.0, 115.1, 114.7, 113.0, 109.5, 55.7, 55.4, 52.2; IR (film) 2922, 1717, 1609, 1512, 1485, 1462, 1371, 1298, 1246, 1213, 1163, 1032, 833

cm^{-1} ; HRMS (ESI) Calcd for $C_{22}H_{19}O_3NNa^+$ ($[M+Na]^+$) 368.1257. Found 368.1253.



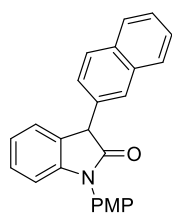
2h: 1H NMR (600 MHz, $CDCl_3$) δ 7.34 (2H, d, $J = 9.0$ Hz), 7.24 (2H, t, $J = 7.5$ Hz), 7.21 (1H, d, $J = 7.5$ Hz), 7.11 (1H, d, $J = 7.5$ Hz), 7.10 (1H, s), 7.08 (1H, t, $J = 7.5$ Hz), 7.06 (1H, d, $J = 7.5$ Hz), 7.03 (2H, d, $J = 9.0$ Hz), 6.82 (1H, d, $J = 7.5$ Hz), 4.73 (1H, s), 3.86 (3H, s), 2.34 (3H, s); ^{13}C NMR (151 MHz, $CDCl_3$) δ 175.8, 159.3, 145.0, 138.8, 136.9, 129.4, 129.0, 128.9, 128.6, 128.4, 128.2, 127.4, 125.7, 125.4, 123.1, 115.0, 109.5, 55.7, 52.3, 21.6; IR (film) 2924, 1717, 1611, 1512, 1483, 1462,

1371, 1298, 1248, 1163, 1096, 1030, 833 cm^{-1} ; HRMS (ESI) Calcd for $C_{22}H_{19}O_2NNa^+$ ($[M+Na]^+$) 352.1308. Found 352.1303.

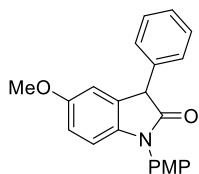


2i: 1H NMR (600 MHz, $CDCl_3$) δ 7.36-7.30 (3H, m), 7.26 (1H, t, $J = 7.8$ Hz), 7.22 (1H, d, $J = 7.8$ Hz), 7.12 (1H, d, $J = 7.8$ Hz), 7.10 (1H, t, $J = 7.8$ Hz), 7.03 (2H, d, $J = 9.0$ Hz), 7.01-6.96 (2H, m), 6.82 (1H, d, $J = 7.8$ Hz), 4.77 (1H, s), 3.86 (3H, s); ^{13}C NMR (151 MHz, $CDCl_3$) δ 175.0, 163.2 (d, $J_{C-F} = 247.3$ Hz), 159.4, 145.0, 139.2 (d, $J_{C-F} = 7.1$ Hz), 130.5 (d, $J_{C-F} = 7.2$ Hz), 128.7, 128.1, 128.0, 127.1, 125.5, 124.5, 123.3, 115.6 (d, $J_{C-F} = 21.6$ Hz), 115.1, 114.8 (d, $J_{C-F} = 21.6$ Hz), 109.7, 55.7, 51.8; ^{19}F

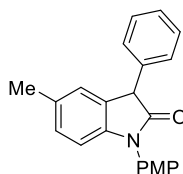
NMR (471 MHz, $CDCl_3$) δ -112.3; IR (film) 2928, 1717, 1611, 1512, 1485, 1464, 1371, 1298, 1248, 1163, 1036, 833 cm^{-1} ; HRMS (ESI) Calcd for $C_{21}H_{16}O_2NFNa^+$ ($[M+Na]^+$) 356.1057. Found 356.1052.



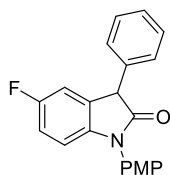
2j: ^1H NMR (600 MHz, CDCl_3) δ 7.84-7.79 (3H, m), 7.78 (1H, s), 7.49-7.45 (2H, m), 7.39-7.34 (3H, m), 7.27 (1H, t, $J = 7.5$ Hz), 7.24 (1H, d, $J = 7.5$ Hz), 7.09 (1H, t, $J = 7.5$ Hz), 7.04 (2H, d, $J = 9.0$ Hz), 6.86 (1H, d, $J = 7.5$ Hz), 4.94 (1H, s), 3.86 (3H, s); ^{13}C NMR (151 MHz, CDCl_3) δ 175.6, 159.4, 145.1, 134.4, 133.7, 133.0, 129.0, 128.8, 128.5, 128.2, 128.0, 127.8₃, 127.7₇, 127.3, 126.4, 126.3, 126.2, 125.5, 123.2, 115.1, 109.6, 55.7, 52.5; IR (film) 2932, 1715, 1611, 1510, 1483, 1462, 1371, 1298, 1246, 1163, 1030, 908, 806 cm^{-1} ; HRMS (ESI) Calcd for $\text{C}_{25}\text{H}_{19}\text{O}_2\text{NNa}^+$ ($[\text{M}+\text{Na}]^+$) 388.1308. Found 388.1303.



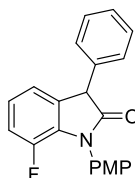
2k: ^1H NMR (600 MHz, CDCl_3) δ 7.36 (1H, t, $J = 7.8$ Hz), 7.34 (1H, d, $J = 7.8$ Hz), 7.33 (2H, d, $J = 9.0$ Hz), 7.32-7.27 (3H, m), 7.02 (2H, d, $J = 9.0$ Hz), 6.82 (1H, d, $J = 2.4$ Hz), 6.77 (1H, dd, $J = 7.8, 2.1$ Hz), 6.74 (1H, d, $J = 7.8$ Hz), 4.74 (1H, s), 3.85 (3H, s), 3.75 (3H, s); ^{13}C NMR (151 MHz, CDCl_3) δ 175.3, 159.2, 156.4, 138.6, 137.0, 130.0, 129.1, 128.7, 128.0, 127.8, 127.6, 115.0, 113.2, 113.0, 110.0, 56.0, 55.7, 52.7; IR (film) 2938, 1715, 1607, 1512, 1487, 1456, 1364, 1246, 1175, 1163, 1030 cm^{-1} ; HRMS (ESI) Calcd for $\text{C}_{22}\text{H}_{19}\text{O}_3\text{NNa}^+$ ($[\text{M}+\text{Na}]^+$) 368.1257. Found 368.1252.



2l: ^1H NMR (600 MHz, CDCl_3) δ 7.36 (1H, t, $J = 7.8$ Hz), 7.35 (1H, d, $J = 7.8$ Hz), 7.33 (2H, d, $J = 9.0$ Hz), 7.30 (1H, t, $J = 7.8$ Hz), 7.28 (2H, d, $J = 7.8$ Hz), 7.05-7.01 (4H, m), 6.71 (1H, d, $J = 7.8$ Hz), 4.73 (1H, s), 3.85 (3H, s), 2.31 (3H, s); ^{13}C NMR (151 MHz, CDCl_3) δ 175.6, 159.2, 142.6, 137.2, 132.8, 129.1, 128.9, 128.7, 128.1, 127.7, 127.6, 126.1, 115.0, 109.3, 55.7, 52.4, 21.2, one carbon atom was not found provably due to overlapping; IR (film) 2918, 1717, 1616, 1512, 1489, 1362, 1248, 1163, 1030, 810 cm^{-1} ; HRMS (ESI) Calcd for $\text{C}_{22}\text{H}_{19}\text{O}_2\text{NNa}^+$ ($[\text{M}+\text{Na}]^+$) 352.1308. Found 352.1304.

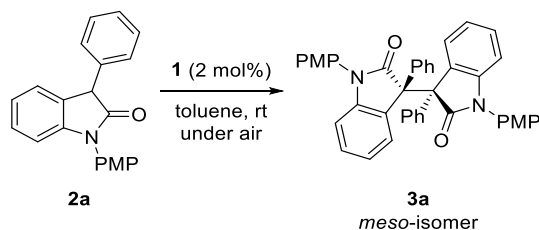


2m: ^1H NMR (600 MHz, CDCl_3) δ 7.37 (2H, t, $J = 7.8$ Hz), 7.34-7.30 (3H, m), 7.27 (2H, d, $J = 7.8$ Hz), 7.03 (2H, d, $J = 9.0$ Hz), 6.97-6.91 (2H, m), 6.74 (1H, dd, $J = 7.8, 4.2$ Hz), 4.75 (1H, s), 3.82 (3H, s); ^{13}C NMR (151 MHz, CDCl_3) δ 175.3, 159.5 (d, $J_{\text{C-F}} = 241.4$ Hz), 159.4, 141.0, 136.4, 130.3 (d, $J_{\text{C-F}} = 8.6$ Hz), 129.2, 128.5, 128.1, 128.0, 127.2, 115.1, 114.8 (d, $J_{\text{C-F}} = 23.1$ Hz), 113.3 (d, $J_{\text{C-F}} = 24.6$ Hz), 110.1 (d, $J_{\text{C-F}} = 8.8$ Hz), 55.7, 52.5; ^{19}F NMR (471 MHz, CDCl_3) δ -119.9; IR (film) 3063, 1717, 1607, 1510, 1483, 1454, 1366, 1296, 1246, 1198, 1163, 1030, 810 cm^{-1} ; HRMS (ESI) Calcd for $\text{C}_{21}\text{H}_{16}\text{O}_2\text{NFNa}^+$ ($[\text{M}+\text{Na}]^+$) 356.1057. Found 356.1052.

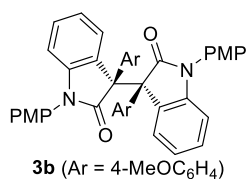


2n: ^1H NMR (600 MHz, CDCl_3) δ 7.37 (1H, t, $J = 7.0$ Hz), 7.36 (1H, d, $J = 8.4$ Hz), 7.35-7.29 (3H, m), 7.27 (2H, d, $J = 9.0$ Hz), 7.03-6.99 (3H, m), 6.98 (2H, d, $J = 9.0$ Hz), 4.79 (1H, s), 3.85 (3H, s); ^{13}C NMR (151 MHz, CDCl_3) δ 175.4, 159.4, 147.5 (d, $J_{\text{C-F}} = 247.3$ Hz), 136.5, 131.6, 131.4 (d, $J_{\text{C-F}} = 7.1$ Hz), 129.2, 128.6, 128.4, 128.0, 123.6 (d, $J_{\text{C-F}} = 7.2$ Hz), 121.2 (d, $J_{\text{C-F}} = 2.9$ Hz), 116.8 (d, $J_{\text{C-F}} = 20.2$ Hz), 114.3, 55.6, 52.4, one carbon atom was not found provably due to overlapping; ^{19}F NMR (471 MHz, CDCl_3) δ -129.3; IR (film) 3009, 1722, 1715, 1512, 1483, 1470, 1456, 1298, 1246, 1200, 1161, 1130, 833 cm^{-1} ; HRMS (ESI) Calcd for $\text{C}_{21}\text{H}_{16}\text{O}_2\text{NFNa}^+$ ($[\text{M}+\text{Na}]^+$) 356.1057. Found 356.1053.

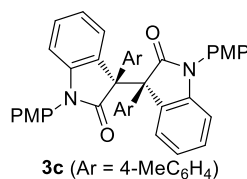
Representative Procedure for Catalytic Homo-Dimerization of Oxindole 2:



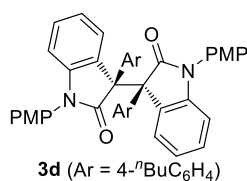
Oxindole **2a** (31.5 mg, 0.1 mmol) and air-saturated toluene (1.0 mL) were added to a test tube successively at rt. After addition of **1** (1.07 mg, 0.002 mmol) as solid, the reaction mixture was stirred for 24 h under air and then, a 0.5 M solution of trifluoroacetic acid in toluene (4.0 μ L) was introduced. The whole mixture was concentrated and purified by silica gel column chromatography (H/EA = 10:1-3:1 as eluent) to afford **3a** (53.4 mg, 0.089 mmol) in 88% yield. Absolute configuration was assigned by X-ray diffraction analysis (see Figure S10). Rotational isomer (~10%) was observed in ^1H NMR but only major isomer was assigned below.^{14d} **3a**: ^1H NMR (600 MHz, CDCl_3 , 50 $^\circ\text{C}$) δ 7.59 (2H, br), 7.33 (2H, t, $J = 7.8$ Hz), 7.31-7.20 (8H, m), 7.16 (2H, t, $J = 7.8$ Hz), 6.91 (8H, br), 6.63 (2H, br), 6.42 (2H, br), 3.80 (6H, s); ^{13}C NMR (151 MHz, CDCl_3 , 50 $^\circ\text{C}$) δ 174.6, 159.5, 145.8, 131.7, 128.9₄, 128.8₇, 128.5₂, 128.4₈, 128.1, 127.8, 127.5, 127.2, 121.4, 115.1, 109.7, 55.7, 55.6; IR (film): 3007, 2837, 1715, 1607, 1512, 1462, 1375, 1323, 1298, 1248, 1163, 1105, 1032, 835, 810 cm^{-1} ; HRMS (ESI) Calcd for $\text{C}_{42}\text{H}_{33}\text{O}_4\text{N}_2^+$ ($[\text{M}+\text{H}]^+$) 629.2435. Found 629.2432.



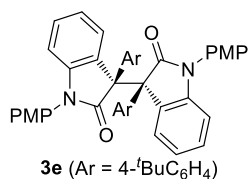
3b: ^1H NMR (600 MHz, CDCl_3 , 50 $^\circ\text{C}$) δ 7.69 (2H, br), 7.37 (4H, br), 7.21 (2H, t, $J = 7.8$ Hz), 6.90 (6H, br), 6.80 (4H, br), 6.61 (4H, br), 6.10 (2H, br), 3.81 (6H, s), 3.79 (6H, s); ^{13}C NMR (151 MHz, CDCl_3 , 50 $^\circ\text{C}$) δ 174.6, 159.4₄, 159.3₆, 145.7, 132.8, 128.7, 128.4, 128.2, 127.4, 127.3, 121.3, 114.9, 112.5, 109.5, 55.6, 55.5, 55.2, one carbon atom was not found provably due to overlapping or broadening; IR (film): 2934, 2837, 1717, 1607, 1510, 1443, 1375, 1298, 1248, 1188, 1163, 1032, 831, 804 cm^{-1} ; HRMS (ESI) Calcd for $\text{C}_{44}\text{H}_{36}\text{O}_6\text{N}_2\text{Na}^+$ ($[\text{M}+\text{Na}]^+$) 711.2466. Found 711.2461.



3c: ^1H NMR (600 MHz, CDCl_3 , 50 $^\circ\text{C}$) δ 7.36 (4H, br), 7.21 (2H, t, $J = 7.8$ Hz), 7.18-7.10 (4H, m), 6.90 (8H, br), 6.62 (4H, br), 6.50 (2H, br), 3.79 (6H, s), 2.26 (6H, s); ^{13}C NMR (151 MHz, CDCl_3 , 50 $^\circ\text{C}$) δ 174.5, 159.5, 145.8, 136.4, 132.6, 128.8, 128.7, 128.5, 128.3, 127.9, 127.5, 126.9, 121.3, 115.0, 109.6, 55.7, 55.6, 21.8; IR (film): 3009, 2932, 2837, 1713, 1612, 1512, 1489, 1369, 1323, 1298, 1246, 1215, 1163, 1032, 835, 818 cm^{-1} ; HRMS (ESI) Calcd for $\text{C}_{44}\text{H}_{37}\text{O}_4\text{N}_2^+$ ($[\text{M}+\text{H}]^+$) 657.2748. Found 657.2745.

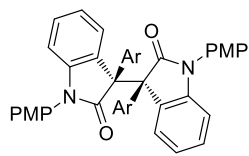


3d: ^1H NMR (500 MHz, CDCl_3 , 50 $^\circ\text{C}$) δ 7.44 (4H, br), 7.21 (2H, t, $J = 7.5$ Hz), 7.06 (4H, d, $J = 7.5$ Hz), 6.89 (8H, br), 6.60 (4H, br), 6.10 (2H, br), 3.78 (6H, s), 2.62 (4H, t, $J = 7.5$ Hz), 1.61 (4H, tt, $J = 7.5, 7.0$ Hz), 1.37 (4H, tq, $J = 7.5, 7.0$ Hz), 0.93 (6H, t, $J = 7.5$ Hz); ^{13}C NMR (126 MHz, CDCl_3 , 50 $^\circ\text{C}$) δ 174.7, 159.5, 145.8, 142.7, 131.5, 128.9, 128.8, 128.6, 128.3, 127.8, 127.5, 127.2, 121.1, 115.0, 109.6, 55.7, 55.6, 35.3, 33.5, 22.5, 14.0; IR (film): 2928, 2857, 1715, 1605, 1510, 1462, 1375, 1323, 1298, 1246, 1163, 1103, 1032, 833, 800 cm^{-1} ; HRMS (ESI) Calcd for $\text{C}_{50}\text{H}_{49}\text{O}_4\text{N}_2^+$ ($[\text{M}+\text{H}]^+$) 741.3687. Found 741.3689.



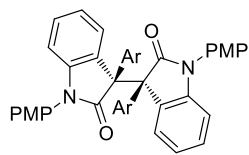
3e (Ar = 4-^tBuC₆H₄)

3e: ¹H NMR (600 MHz, CDCl₃, 50 °C) δ 7.45 (6H, br), 7.28 (4H, br), 7.21 (2H, t, *J* = 7.8 Hz), 6.91 (8H, br), 6.61 (4H, br), 3.80 (6H, s), 1.34 (18H, s); ¹³C NMR (151 MHz, CDCl₃, 50 °C) δ 174.8, 159.5, 150.9, 145.8, 131.3, 128.9, 128.7, 128.6, 128.3, 127.8, 127.5, 124.1, 121.3, 115.0, 109.5, 55.7, 55.6, 34.6, 31.5; IR (film): 2961, 1721, 1607, 1514, 1464, 1375, 1298, 1248, 1163, 1034, 833, 804 cm⁻¹; HRMS (ESI) Calcd for C₅₀H₄₈O₄N₂Na⁺ ([M+Na]⁺) 763.3506. Found 763.3507.



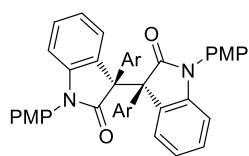
3f (Ar = 4-ClC₆H₄)

3f: ¹H NMR (600 MHz, CDCl₃, 50 °C) δ 7.49 (6H, br), 7.25 (8H, br), 6.91 (6H, br), 6.64 (4H, br), 3.80 (6H, s); ¹³C NMR (151 MHz, CDCl₃, 50 °C) δ 174.2, 159.7, 145.8, 134.7, 132.9, 129.4, 129.0, 128.8, 128.3, 127.7, 127.5, 127.2, 121.7, 115.2, 110.0, 55.8, 55.7; IR (film): 2936, 2913, 1713, 1607, 1512, 1462, 1375, 1325, 1298, 1246, 1163, 1096, 1030, 1015, 835, 800 cm⁻¹; HRMS (ESI) Calcd for C₄₂H₃₁O₄N₂³⁵Cl₂⁺ ([M+H]⁺) 697.1655. Found 697.1652.



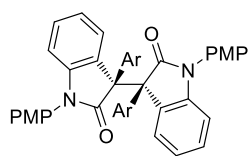
3g (Ar = 3-MeOC₆H₄)

3g: ¹H NMR (600 MHz, CDCl₃, 50 °C) δ 7.30 (4H, br), 7.22 (4H, t, *J* = 7.8 Hz), 7.20-7.12 (4H, m), 6.90 (4H, br), 6.91-6.84 (4H, m), 6.62 (4H, br), 3.79 (6H, s), 3.62 (6H, br); ¹³C NMR (151 MHz, CDCl₃, 50 °C) δ 174.4, 159.6, 158.6, 145.7, 129.2, 129.0, 128.9, 128.6, 128.5, 128.4, 127.8, 125.5, 124.0, 121.8, 121.5, 115.1, 109.7, 55.7₁, 55.6₆, 55.1; IR (film): 3007, 2936, 2835, 1715, 1605, 1512, 1464, 1375, 1323, 1296, 1248, 1163, 1105, 1034, 829 cm⁻¹; HRMS (ESI) Calcd for C₄₄H₃₇O₆N₂⁺ ([M+H]⁺) 689.2646. Found 689.2646.



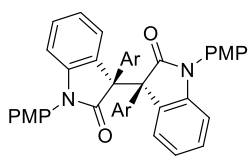
3h (Ar = 3-MeC₆H₄)

3h: ¹H NMR (600 MHz, CDCl₃, 50 °C) δ 7.35 (4H, br), 7.22 (2H, t, *J* = 7.8 Hz), 7.20-7.12 (4H, m), 6.91 (8H, br), 6.63 (4H, br), 6.50 (2H, br), 3.80 (6H, s), 2.27 (6H, s); ¹³C NMR (151 MHz, CDCl₃, 50 °C) δ 174.5, 159.5, 145.8, 136.4, 132.6, 128.8, 128.7, 128.6, 128.5, 128.3, 128.0, 127.5, 126.9, 121.3, 115.0, 109.6, 55.7, 55.6, 21.8, one carbon atom was not found provably due to overlapping or broadening; IR (film): 3009, 2837, 1715, 1607, 1512, 1464, 1375, 1325, 1298, 1248, 1163, 1105, 1032, 829 cm⁻¹; HRMS (ESI) Calcd for C₄₄H₃₆O₄N₂Na⁺ ([M+Na]⁺) 679.2567. Found 679.2566.



3i (Ar = 3-FC₆H₄)

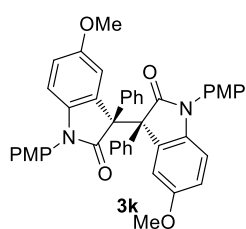
3i: ¹H NMR (500 MHz, CDCl₃, 50 °C) δ 7.35 (6H, br), 7.27-7.20 (4H, m), 7.04 (2H, td, *J* = 8.5, 2.5 Hz), 6.91 (8H, br), 6.64 (2H, br), 6.40 (2H, br), 3.80 (6H, s); ¹³C NMR (126 MHz, CDCl₃, 50 °C) δ 173.8, 161.9 (d, *J*_{C-F} = 245.4 Hz), 159.5, 145.6, 135.6, 129.2, 128.8, 128.6, 128.3 (d, *J*_{C-F} = 10.8 Hz), 127.5, 127.1, 121.6, 118.7 (d, *J*_{C-F} = 25.5 Hz), 115.1, 115.0, 109.8, 55.6, 55.5, one carbon atom was not found provably due to overlapping or broadening; ¹⁹F NMR (471 MHz, CDCl₃, 50 °C) δ -113.0; IR (film): 3013, 2936, 2841, 1715, 1607, 1584, 1512, 1464, 1375, 1298, 1248, 1163, 1105, 1032, 831 cm⁻¹; HRMS (ESI) Calcd for C₄₂H₃₁O₂N₂F₂⁺ ([M+H]⁺) 665.2246. Found 665.2242.



3j (Ar = 2-naphthyl)

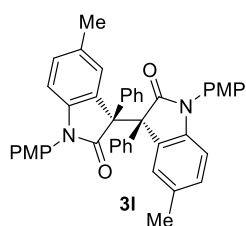
3j: ¹H NMR (600 MHz, CDCl₃, 50 °C) δ 7.98 (2H, br), 7.82 (4H, d, *J* = 7.0 Hz), 7.70 (2H, br), 7.61 (2H, br), 7.47 (2H, t, *J* = 7.0 Hz), 7.39 (2H, t, *J* = 7.0 Hz), 7.25 (2H, t, *J* = 7.0 Hz), 6.91 (8H, br), 6.66 (4H, br), 6.50 (2H, br), 3.80 (6H, s); ¹³C NMR (151 MHz, CDCl₃, 50 °C) δ 174.5, 159.6, 145.9, 133.1, 132.6, 131.7, 129.1, 129.0, 128.9, 128.6, 127.9, 127.4, 126.6, 126.3, 125.8, 121.6, 115.1, 109.8, 55.7₃, 55.6₆, three carbon atoms were not found provably due to overlapping or broadening; IR (film): 3011, 2837, 1715, 1607, 1512, 1462, 1375, 1298, 1248, 1163, 804 cm⁻¹; HRMS (ESI) Calcd

for $C_{50}H_{37}O_4N_2^+$ ($[M+H]^+$) 729.2748. Found 729.2746.



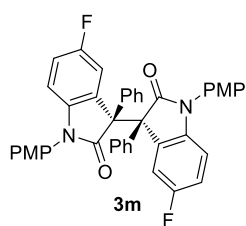
3k: 1H NMR (600 MHz, $CDCl_3$, 50 °C) δ 7.60 (6H, br), 7.33 (2H, t, $J = 7.8$ Hz), 7.27 (4H, t, $J = 7.2$ Hz), 6.90 (6H, br), 6.79 (2H, dd, $J = 7.8, 1.8$ Hz), 6.56 (2H, br), 6.05 (2H, br), 3.79 (6H, s), 3.58 (6H, s); ^{13}C NMR (151 MHz, $CDCl_3$, 50 °C) δ 174.2, 159.4, 155.0, 139.6, 131.6, 131.5, 128.7, 128.6, 128.1, 127.8, 127.2, 115.0, 114.9, 114.6, 110.0, 56.0, 55.6, one carbon atom was not found provably due to overlapping or broadening; IR (film): 3003, 2936, 2839,

1713, 1597, 1514, 1487, 1464, 1369, 1281, 1248, 1211, 1163, 1034, 820 cm^{-1} ; HRMS (ESI) Calcd for $C_{44}H_{37}O_6N_2^+$ ($[M+H]^+$) 689.2646. Found 689.2642.



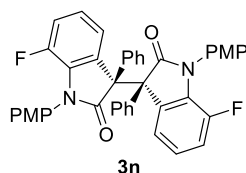
3l: 1H NMR (600 MHz, $CDCl_3$, 50 °C) δ 7.58 (6H, br), 7.33 (2H, t, $J = 7.8$ Hz), 7.26 (4H, t, $J = 7.2$ Hz), 7.03 (2H, d, $J = 7.8$ Hz), 6.90 (6H, br), 6.51 (2H, br), 6.09 (2H, br), 3.78 (6H, s), 2.17 (6H, s); ^{13}C NMR (151 MHz, $CDCl_3$, 50 °C) δ 174.5, 159.4, 143.6, 131.7, 130.7, 129.0, 128.8, 128.4, 128.0, 127.8, 127.6, 127.1, 126.9, 115.0, 109.2, 55.7, 55.6, 21.3; IR (film): 3007, 2922, 2837, 1713, 1612, 1512, 1491, 1369, 1323, 1298, 1248, 1215, 1163, 1032, 818

cm^{-1} ; HRMS (ESI) Calcd for $C_{44}H_{36}O_4N_2Na^+$ ($[M+Na]^+$) 679.2567. Found 679.2568.



3m: 1H NMR (500 MHz, $CDCl_3$, 50 °C) δ 7.54 (6H, br), 7.35 (2H, t, $J = 8.0$ Hz), 7.28 (4H, t, $J = 8.0$ Hz), 7.00 (4H, br), 7.00-6.90 (6H, m), 6.57 (2H, dd, $J = 8.0, 5.0$ Hz), 6.80 (6H, s); ^{13}C NMR (126 MHz, $CDCl_3$, 50 °C) δ 174.2, 159.7, 158.3 (d, $J_{C-F} = 240.7$ Hz), 141.7, 131.2, 129.3, 128.7, 128.5, 127.5, 127.2, 115.9, 115.5 (d, $J_{C-F} = 23.1$ Hz), 115.3, 110.1 (d, $J_{C-F} = 7.3$ Hz), 55.74, 55.69, one carbon atom was not found provably due to overlapping or broadening;

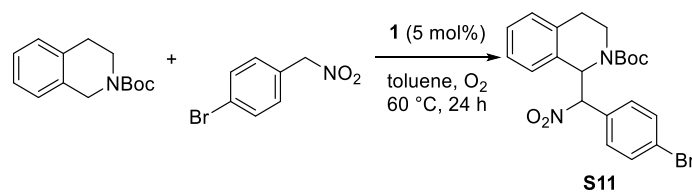
^{19}F NMR (471 MHz, $CDCl_3$, 50 °C) δ -120.8; IR (film): 3007, 2934, 2839, 1717, 1605, 1514, 1485, 1371, 1298, 1250, 1182, 1032, 822 cm^{-1} ; HRMS (ESI) Calcd for $C_{42}H_{31}O_4N_2F_2^+$ ($[M+H]^+$) 665.2246. Found 665.2242.



3n: 1H NMR (500 MHz, $CDCl_3$, 50 °C) δ 7.50 (6H, br), 7.33 (2H, t, $J = 7.5$ Hz), 7.25 (4H, t, $J = 7.5$ Hz), 7.01 (2H, dd, $J = 11.0, 7.5$ Hz), 6.92-6.83 (8H, m), 6.29 (2H, br), 3.79 (6H, s); ^{13}C NMR (126 MHz, $CDCl_3$, 50 °C) δ 174.4, 159.7, 148.0 (d, $J_{C-F} = 248.0$ Hz), 132.5, 131.5, 131.0, 128.9, 128.5, 128.4, 128.2, 127.4, 123.6, 121.7, 117.4 (d, $J_{C-F} = 19.3$ Hz), 114.4, 55.7,

55.6; ^{19}F NMR (471 MHz, $CDCl_3$, 50 °C) δ -129.1; IR (film): 3011, 2837, 1721, 1624, 1512, 1485, 1466, 1371, 1298, 1248, 1215, 1161, 1032, 831, 806 cm^{-1} ; HRMS (ESI) Calcd for $C_{42}H_{31}O_4N_2F_2^+$ ($[M+H]^+$) 665.2246. Found 665.2244.

Procedure for Coupling Reaction of *N*-Boc 1,2,3,4-Tetrahydroisoquinoline with α -Aryl Nitromethane



N-Boc 1,2,3,4-tetrahydro-isoquinoline (23.3 mg, 0.1 mmol), 1-bromo-4-(nitromethyl)benzene (43.2 mg, 0.2 mmol) and toluene (1.0 mL) were added to a test tube successively at rt. After addition of **1** (2.67 mg, 0.005 mmol) as solid, the reaction mixture was stirred at 60 °C for 24 h under O₂ atmosphere. After cooling to rt, a 0.5 M solution of trifluoroacetic acid in toluene (10.0 μL) was introduced. The whole mixture was concentrated and purified by silica gel column chromatography (toluene/EA = 1:0-20:1 as eluent) to afford **S11** as a mixture of diastereomers (36.7 mg, 0.082 mmol). **S11**: ¹H NMR (400 MHz, CD₃CN, 70 °C) major diastereomer δ 7.71-7.54 (4H, m), 7.36-7.14 (3H, m), 7.12 (1H, d, *J* = 7.2 Hz), 6.10 (1H, br), 5.83 (1H, d, *J* = 10.0 Hz), 3.73 (1H, br), 3.21 (1H, dt, *J* = 13.2, 6.8 Hz), 2.93 (2H, t, *J* = 6.8 Hz), 1.31 (9H, s); ¹³C NMR (100 MHz, CD₃CN, 70 °C) major diastereomer δ 136.3, 134.5, 133.1, 132.9, 132.1, 130.6, 129.8, 128.4, 127.7, 125.1, 95.6, 81.6, 79.3, 40.3, 28.6, 28.2, one carbon atom was not found probably due to broadening; IR (film): 2978, 2930, 2359, 2342, 1690, 1555, 1491, 1418, 1391, 1364, 1325, 1292, 1242, 1161, 1123 cm⁻¹; HRMS (ESI) Calcd for C₂₁H₂₃O₄N₂⁷⁹BrNa⁺ ([M+Na]⁺) 469.0733. Found 469.0736.

p*K*_a Determination for Acridinium Betaine in MeCN:

p*K*_a value of acridinium betaine **1** was determined by following the literature procedure.²² In the titration of **1** with acetic acid (AcOH, p*K*_{a,AcOH} = 23.51 in MeCN²³), betaine·H⁺ and AcO⁻ forms in equilibrium. To a 0.10 mM solution of **1** in MeCN (2.0 mL) was added 0-120 μL of a MeCN solution of AcOH (1.0 mM) and 200-80 μL of MeCN (total volume = 2200 μL). The changes in the UV-Vis spectra were monitored at 361 nm after each addition (Fig S1) and corrected for volume additions. The concentrations of **1** ([Betaine]) and **1**·H ([BetaineH]) were determined from the UV-Vis spectra using eq 1, where A is the absorbance at 361 nm over the course of the titration and *l* = 1.0 cm is the path length. The mass balance (eq 2) and ε were determined by the UV-Vis spectra of **1** or **1**·HOAc. (ε_{Betaine} = 13814 M⁻¹cm⁻¹, ε_{BetaineH} = 12164 M⁻¹cm⁻¹). The calculated concentrations are [Betaine]_{calc} = {A - ε_{BetaineH}[Betaine]_{total}}/(ε_{Betaine} - ε_{BetaineH}), and [BetaineH]_{calc} = {A - ε_{Betaine}[Betaine]_{total}}/(ε_{BetaineH} - ε_{Betaine}).

$$A = l \times \{(\epsilon_{\text{betaine}}[\text{Betaine}]) + (\epsilon_{\text{betaineH}}[\text{BetaineH}])\} \quad (1)$$

$$[\text{Betaine}]_{\text{total}} = [\text{Betaine}]_{\text{initial}} = [\text{Betaine}] + [\text{BetaineH}] \quad (2)$$

$$K_{eq} = \frac{[\text{BetaineH}][\text{OAc}]}{[\text{Betaine}][\text{AcOH}]} \quad (3)$$

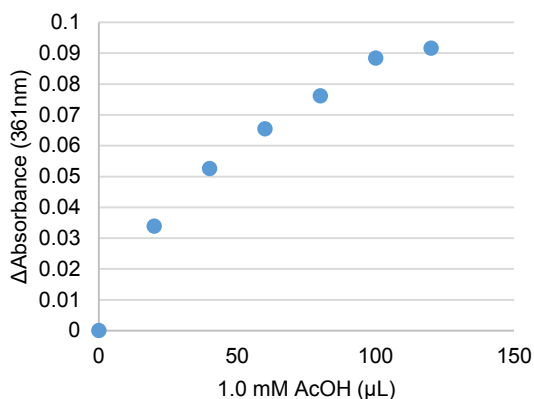


Figure S1. Change in absorbance at 361 nm upon addition of AcOH to a 0.10 mM solution of betaine in MeCN.

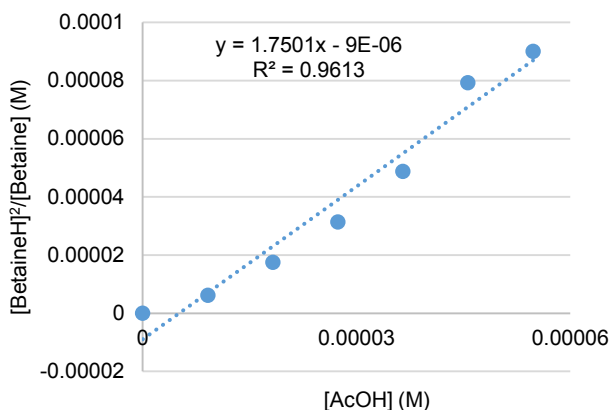
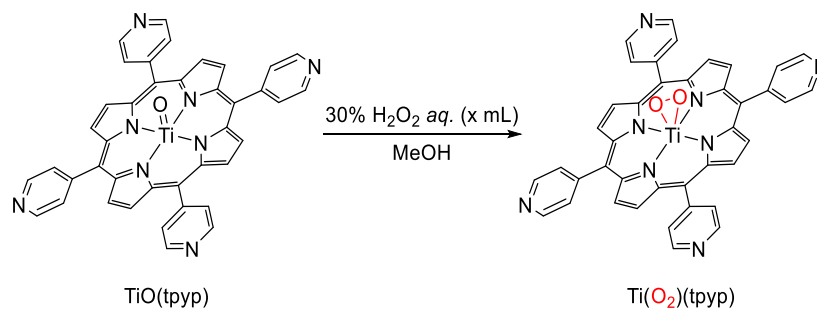


Figure S2. Plot of $[\text{BetaineH}]^2/[\text{Betaine}]$ vs. $[\text{AcOH}]$ for the equilibrium titration. The slope of the plot is K_{eq} .

Because $[\text{BetaineH}]$ is assumed to be equal to $[\text{OAc}]$, K_{eq} (eq 3) was calculated by the plot of $[\text{BetaineH}]^2/[\text{Betaine}]$ vs. $[\text{AcOH}]$ giving $K_{\text{eq}} = 1.75 \pm 0.16$ (Fig S2). The $\text{p}K_{\text{a}}$ of BetaineH in MeCN equals $\{\text{p}K_{\text{a,AcOH}} - [-\log(K_{\text{eq}})]\}$ giving $\text{p}K_{\text{a,BetaineH}} = 23.7 \pm 0.1$. This value was verified by titrations of 0.10 mM betaine · HCl with DBU (1.0 mM in MeCN) using a similar procedure, yielding $K_{\text{eq}} = 0.17 \pm 0.04$. Using the $\text{p}K_{\text{a,DBU-H}}$ (24.34²⁴), this gives $\text{p}K_{\text{a,BetaineH}} = 23.6 \pm 0.1$.

Detection of Hydrogen Peroxide:



Hydrogen peroxide (H_2O_2) was detected upon treatment with oxo[5,10,15,20-*tetra*-(4-pyridyl)porphyrinato]titanium(IV) ($\text{TiO}(\text{tpyp})$), which is known to rapidly react with even trace amounts of H_2O_2 .¹⁷ To a $50 \mu\text{M}$ solution of $\text{TiO}(\text{tpyp})$ in MeOH (2.0 mL) was added 0-800 μL of a 30% aqueous solution of H_2O_2 . After being stirred for 5 min at rt, the mixture was analyzed by UV-Vis measurement (A). A blank solution was prepared in a similar manner except for using distilled water instead of the sample solution and its absorbance was designated as A_B . The difference in absorbance was determined as follows: $\Delta A = A_B - A$. An increasing peak at 442 nm suggests the generation of the $\text{Ti}(\text{O}_2)(\text{tpyp})$ complex (Fig S3).

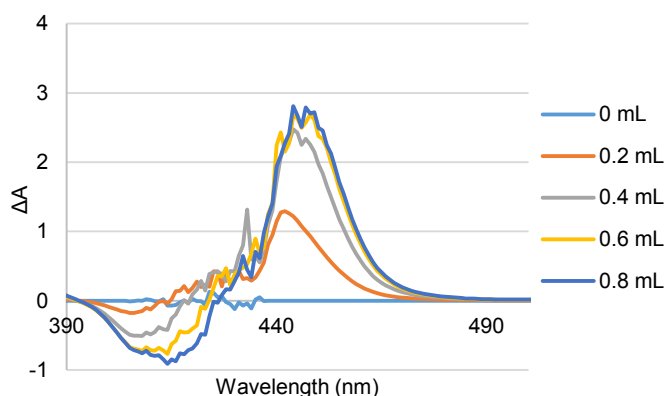
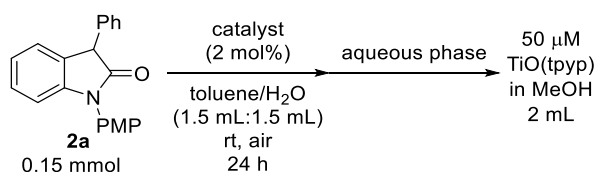


Figure S3. The difference in absorbance spectrum of the $\text{TiO}(\text{tpyp})$ in MeOH and 30% $\text{H}_2\text{O}_2\text{aq.}$ (x mL)



To a solution of oxindole **2a** (47.3 mg, 0.15 mmol) in toluene (1.5 mL) and distilled water (1.5 mL) were added acridinium betaine **1** (1.60 mg, 0.003 mmol) as solid and the resulting reaction mixture was stirred for 24 h under air. The aqueous and organic layers were separated. The aqueous phase (0-800 μL) was introduced to a solution of $50 \mu\text{M}$ $\text{TiO}(\text{tpyp})$ in MeOH (2 mL). After being stirred for 5 min at rt, the solution was analyzed by UV-Vis measurement (Fig S4).

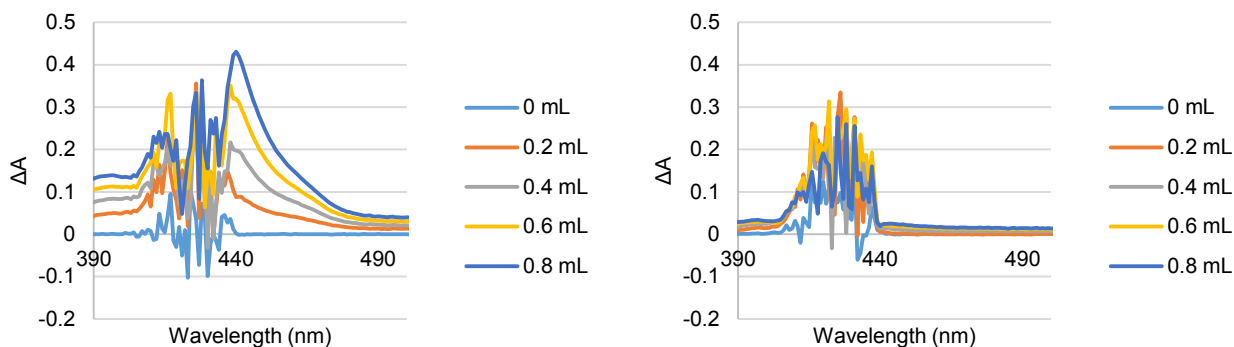
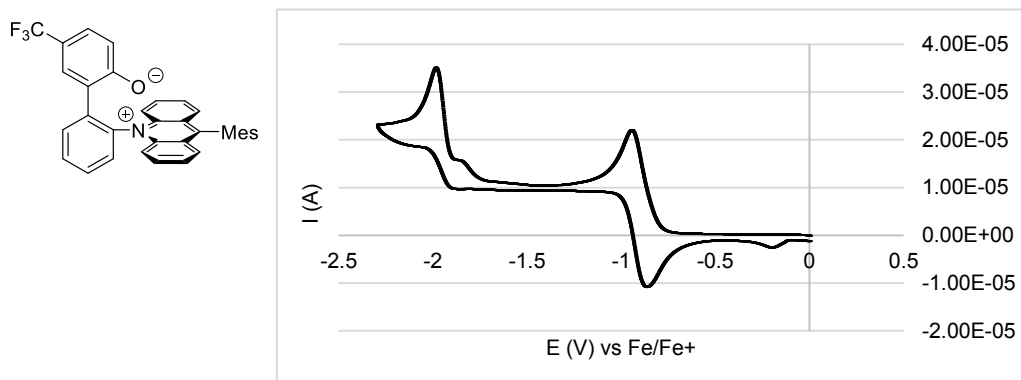


Figure S4 UV-Vis Difference Spectra of the TiO(tpy) in MeOH. Left: Acridinium betaine **1** as a catalyst. Right: Pyridinium betaine as a catalyst.

Electrochemical Studies:

Cyclic voltammetry was performed on an ALS/chi-617A electrochemical analyzer. The voltammetric cell consisting of a glassy carbon electrode, a Pt wire counter electrode, and an Ag/AgNO₃ reference electrode. The measurements were carried out under N₂ using a solution of a sample with a concentration of 1.0 mM in MeCN containing tetrabutylammonium perchlorate as a supporting electrolyte (0.10 M). The scan rate was 100 mV/s. Nitrogen was passed through the sample during the measurements to avoid the deleterious influence of oxygen. The redox potentials were calibrated to the SCE scale with a ferrocene/ferrocenium ion couple.



General Procedure for Monitoring Conversion of Oxindole:

Oxindole **2e** (55.7 mg, 0.15 mmol) was dissolved into air-saturated toluene (1.0 mL) at 25 °C in the presence of 1,3,5-trimethoxybenzene (25.2 mg, 0.15 mmol) as an internal standard for HPLC analysis. A solution of **1** in toluene (0.5 mL) was introduced to the mixture at 25 °C under air in order to start the reaction and consumption of **2e** was monitored by ReactIR analysis at 1219 cm⁻¹. The reaction was quenched with addition of a 0.5 M solution of trifluoroacetic acid in toluene and overall conversion of **2e** was determined by HPLC analysis (Mightysil, RP =

18, GP 250-6.0, 5 μm ; Kanto Chemical Co., Inc., a 70% aqueous of THF as eluent), in which a peak area of **2e** was compared with that of 1,3,5-trimethoxybenzene. Delta in IR absorption was calibrated to estimated conversion of **2e** by using linear relationship to concentration change in HPLC to plot conversion vs reaction time (Fig. S5).

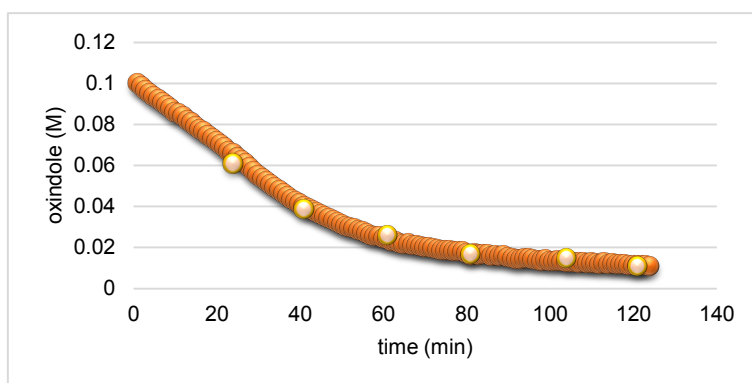


Figure S5 Conversion of Oxindole Determined by ReactIR (red) and ^1H NMR Analysis (pink)

Monitoring of the Reaction Rate:

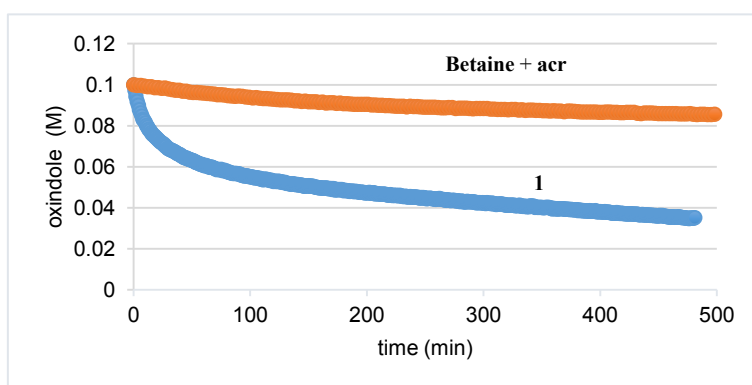


Figure S6 Initial Rate Difference **1** (blue) vs. **betaine + acr** (red). Reaction conditions: $[\mathbf{2e}] = 0.1$ M, catalyst = 0.0005 M under air.

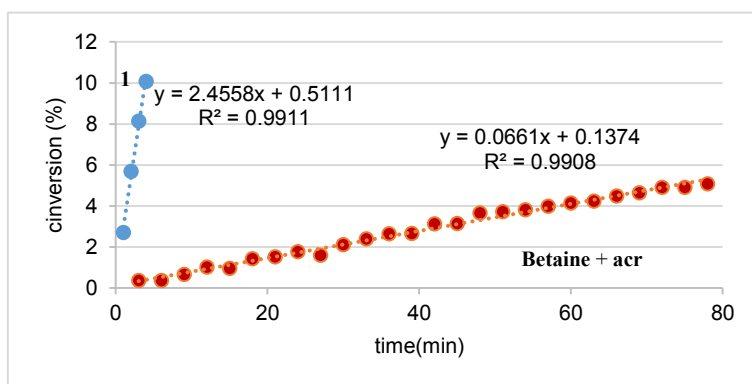


Figure S7 Initial conversion of oxindole **1** (blue) vs. **betaine + acr** (red). Reaction conditions: $[\mathbf{2e}] = 0.1$ M, catalyst = 0.0005 M under air.

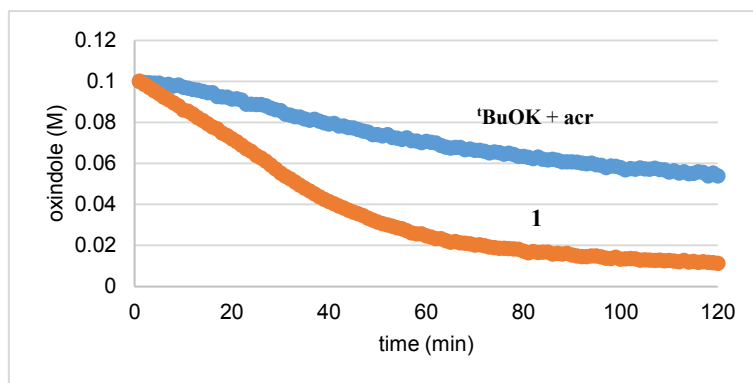
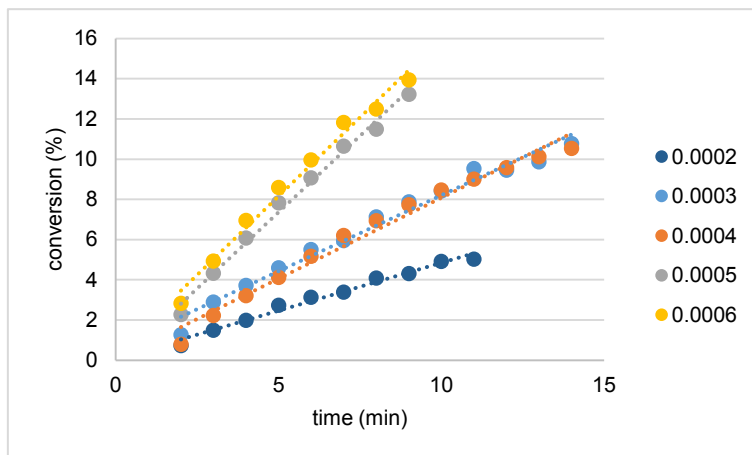


Figure S8 Initial Rate Difference of **1** (red) vs. **tBuOK + acr** (blue). Reaction conditions: $[2e] = 0.1$ M, $[1] = 0.002$ M $[tBuOK] = [acr] = 0.006$ M under air.

Kinetic Order Data

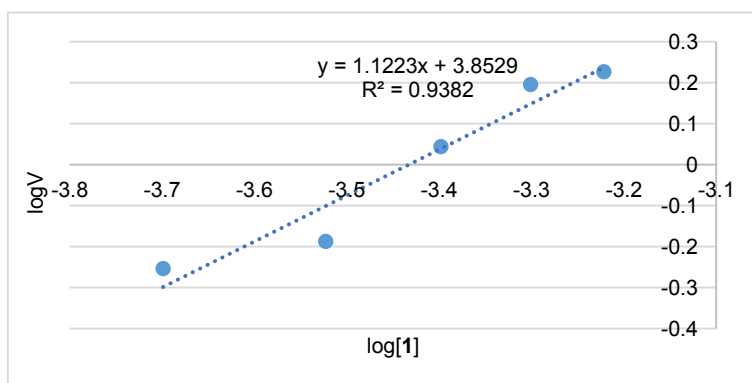
Kinetic Order on Acridinium Betaine

[1] = 0.0002 ~ 0.0006 M, [2e] = 0.1 M. Under air atmosphere.



[1]	v(1st)	v(2nd)	average	log[1]	logV
0.0002	0.4761	0.6393	0.5577	-3.69897	-0.2536
0.0003	0.7549	0.5456	0.65025	-3.52288	-0.18692
0.0004	0.8034	1.4092	1.1063	-3.39794	0.043873
0.0005	1.5187	1.6177	1.5682	-3.30103	0.195401
0.0006	1.5654	1.8046	1.685	-3.22185	0.2266

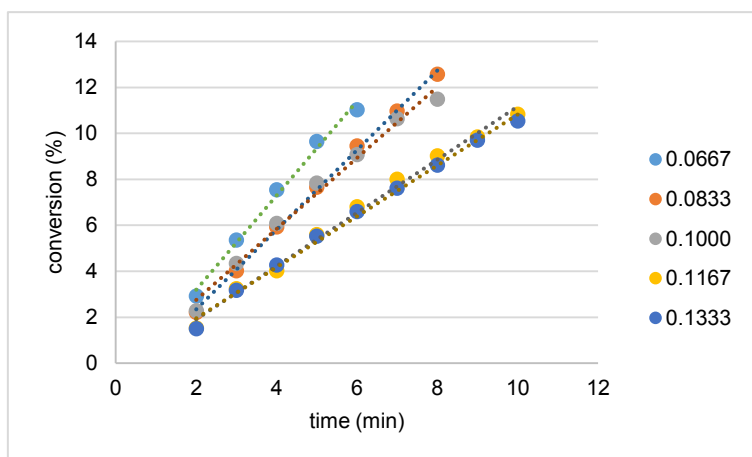
v = Initial rate kinetics. Kinetic order was determined by using average of Initial rate kinetics



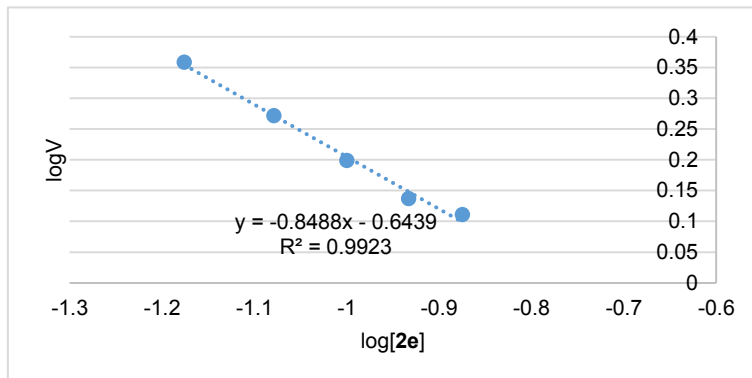
1.1th order dependence on acridinium betaine 7.

Kinetic Order on Oxindole

[1] = 0.0005 M, [2e] = 0.0667 ~ 0.133M. Under air atmosphere.



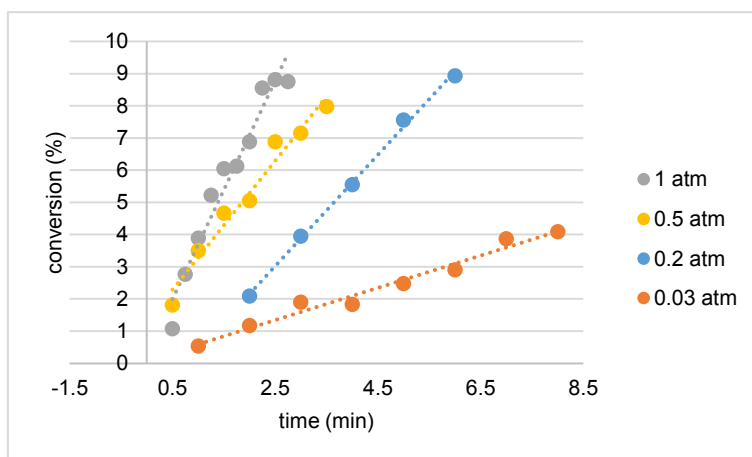
[2e]	v(1st)	v(2nd)	average	log[2e]	logV
0.0667	2.0511	2.5181	2.2846	-1.17609	0.35881
0.0833	1.7521	1.9909	1.8715	-1.07918	0.27219
0.1000	1.5448	1.6177	1.58125	-1	0.199001
0.1167	1.1578	1.5861	1.37195	-0.93305	0.137338
0.1333	1.1087	1.4734	1.29105	-0.87506	0.110943



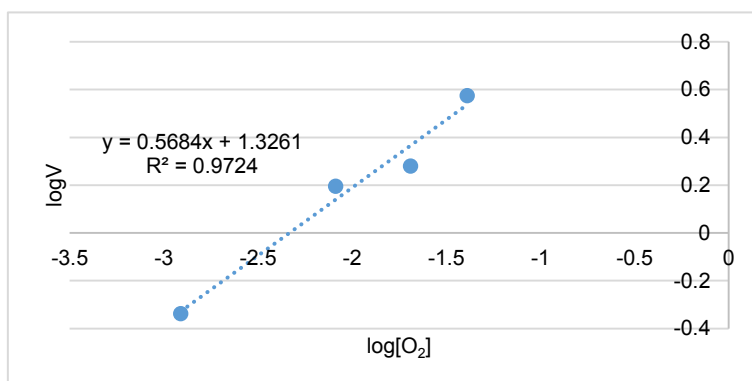
-0.85^{th} order dependence on oxindole 2e.

Kinetic Order on Oxygen

[1] = 0.0005 M, [2e] = 0.1M. Concentration of oxygen was calculated by ideal gas law ($PV = nRT$).



O ₂ (atm)	[O ₂]	v(1st)	v(2nd)	average	log[O ₂]	logV
1	0.040871	3.3924	4.1295	3.76095	-1.38858	0.575298
0.5	0.020436	2.0018	1.8105	1.90615	-1.68961	0.280157
0.2	0.008174	1.5187	1.6177	1.5682	-2.08755	0.195401
0.03	0.001226	0.501	0.4186	0.4598	-2.91146	-0.33743

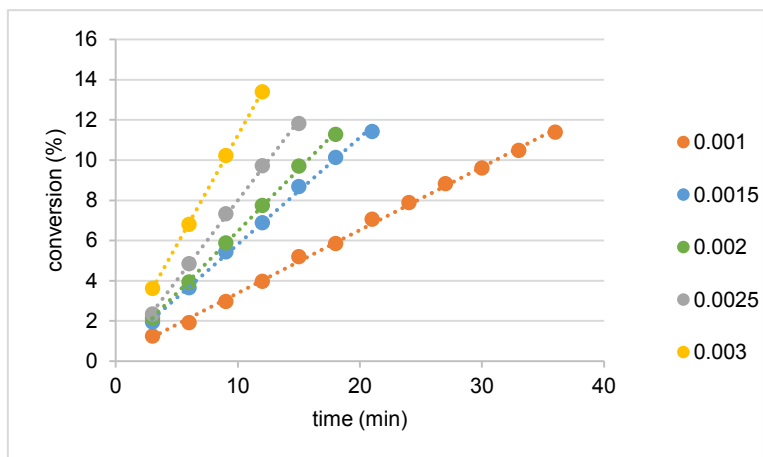


0.57th order dependence on oxygen

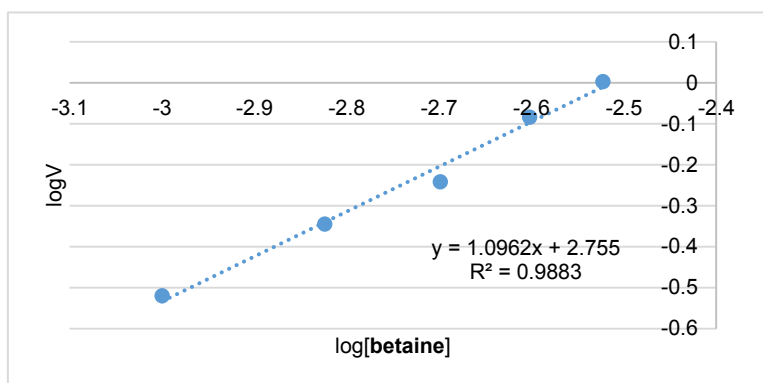
Kinetic Orders for the Binary Catalyst System:

Kinetic Order on Betaine

[betaine] = 0.001 ~ 0.003 M, [acr] = 0.002 M, [2e] = 0.1M. Under air atmosphere.



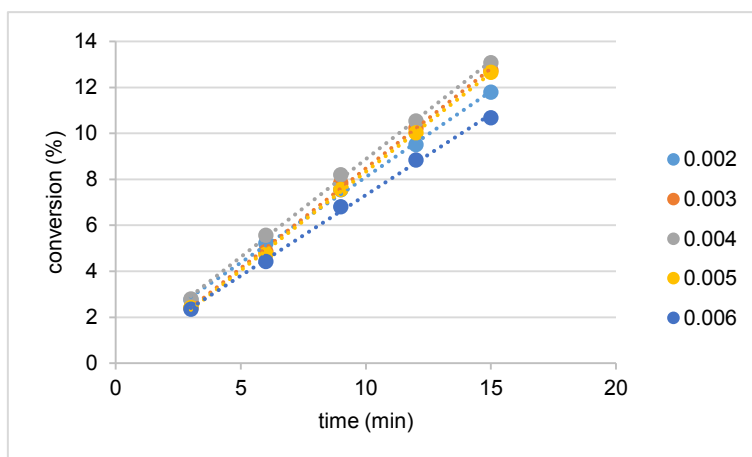
[betaine]	v(1st)	v(2nd)	average	log[betaine]	logV
0.001	0.2918	0.3131	0.30245	-3	-0.51935
0.0015	0.3734	0.5313	0.45235	-2.8239087	-0.34453
0.002	0.5315	0.6162	0.57385	-2.69897	-0.2412
0.0025	0.855	0.7942	0.8246	-2.60206	-0.08376
0.003	0.9245	1.0913	1.0079	-2.5228787	0.003417



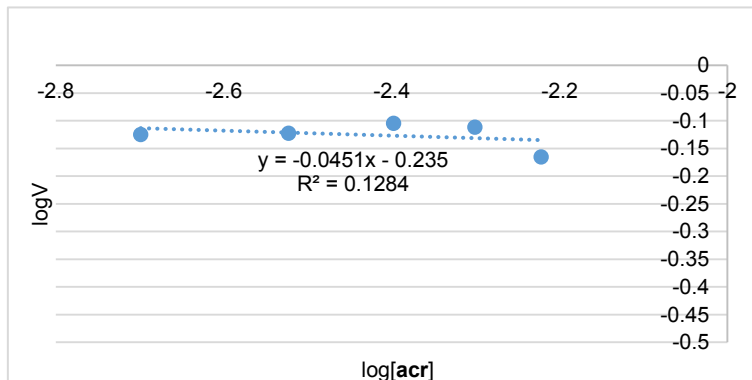
1.1th order dependence on **betaine**

Kinetic Order on the Acridinium Salt

[betaine] = 0.002 M, [acr] = 0.002 ~ 0.006M, [11e] = 0.1M. Under air atmosphere.



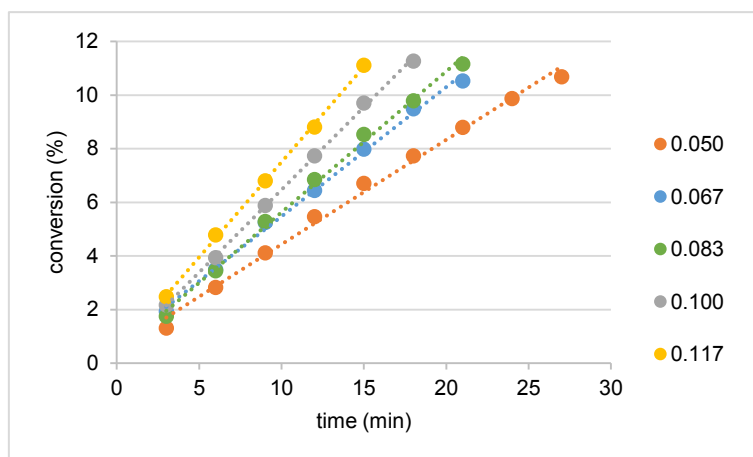
[acr]	v(1st)	v(2nd)	average	log[acr]	logV
0.002	0.7453	0.7564	0.75085	-2.69897	-0.12445
0.003	0.8683	0.6415	0.7549	-2.522879	-0.12211
0.004	0.8515	0.7203	0.7859	-2.39794	-0.10463
0.005	0.8585	0.6896	0.77405	-2.30103	-0.11123
0.006	0.7024	0.6641	0.68325	-2.221849	-0.16542



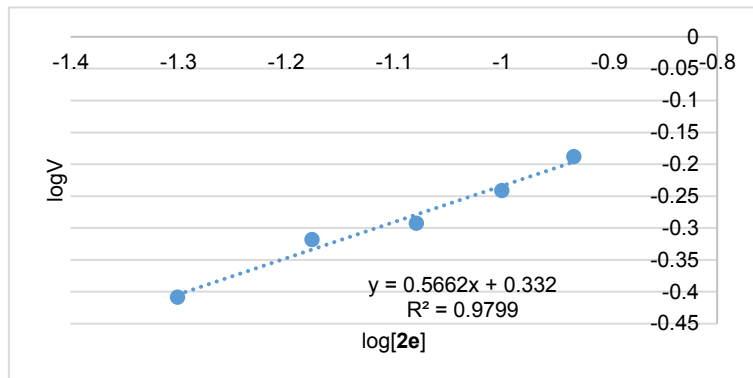
0th order dependence on the acridinium salt

Kinetic Order on Oxindole

[betaine] = 0.002 M, [acr] = 0.002 M, [2e] = 0.05 ~ 0.117 M. Under air atmosphere.



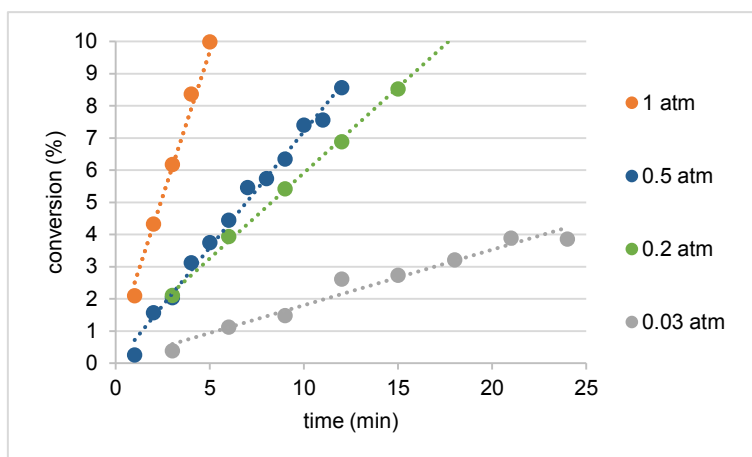
[2e]	v(1st)	v(2nd)	avarage	log[2e]	logV
0.0500	0.3907	0.3901	0.3904	-1.30103	-0.40849
0.0667	0.4789	0.4824	0.48065	-1.17609	-0.31817
0.0833	0.4948	0.5257	0.51025	-1.07918	-0.29222
0.1000	0.5314	0.6162	0.5738	-1	-0.24124
0.1167	0.5876	0.71	0.6488	-0.93305	-0.18789



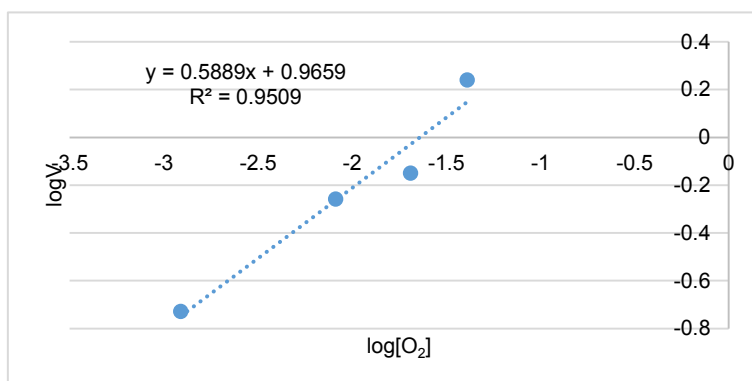
0.57th order dependence on oxindole 2e.

Kinetic Order on Oxygen

[betaine] = 0.002 M, [acr] = 0.002 M, [2e] = 0.1 M.



O ₂ (atm)	[O ₂]	v(1st)	v(2nd)	average	log[O ₂]	logV
1	0.040871	1.7986	1.6847	1.74165	-1.38858	0.240961
0.5	0.020436	0.7203	0.6993	0.7098	-1.68961	-0.14886
0.2	0.008174	0.5315	0.57385	0.552675	-2.08755	-0.25753
0.03	0.001226	0.1725	0.2018	0.18715	-2.91146	-0.72781



0.59th order dependence on oxygen

Crystallographic Structure Determination: The single crystal, obtained by the procedure described below, was mounted on MicroMesh. Data of X-ray diffraction were collected at 123 K on a Rigaku FR-X with Pilatus 200K with fine-focus sealed tube Mo/K α radiation ($\lambda = 0.71075 \text{ \AA}$). An absorption correction was made using Crystal Structure. The structure was solved by direct methods and Fourier syntheses, and refined by full-matrix least squares on F^2 by using SHELXL-2014.²⁵ All non-hydrogen atoms were refined with anisotropic displacement parameters. A hydrogen atom bonded to a nitrogen atom was located from a difference synthesis and their coordinates and isotropic thermal parameters refined. The other hydrogen atoms were placed in calculated positions and isotropic thermal parameters refined.

Recrystallization of 1: Recrystallization of **1** was performed by using benzene as a solvent at rt.

Recrystallization of 3a: Recrystallization of **3a** was performed by using a toluene/H solvent system at rt.

Table S1. Crystal data and structure refinement for **1**.

Empirical formula	C ₃₈ H ₂₉ F ₃ N O
Formula weight	572.62
Temperature	123(2) K
Wavelength	0.71075 Å
Crystal system	Orthorhombic
Space group	P b c n
Unit cell dimensions	a = 15.083(2) Å α = 90° b = 14.7314(19) Å β = 90° c = 26.284(4) Å γ = 90°
Volume	5840.1(14) Å ³
Z	8
Density (calculated)	1.303 Mg/m ³
Absorption coefficient	0.091 mm ⁻¹
F(000)	2392
Crystal size	0.400 x 0.400 x 0.100 mm ³
Theta range for data collection	3.024 to 25.499°.
Index ranges	-18 ≤ h ≤ 18, -17 ≤ k ≤ 17, -29 ≤ l ≤ 31
Reflections collected	35390
Independent reflections	5433 [R _{int} = 0.1422]
Completeness to theta = 25.242°	99.8 %
Absorption correction	Semi-empirical from equivalents
Max. and min. transmission	1.000 and 0.685
Refinement method	Full-matrix least-squares on F ²
Data / restraints / parameters	5433 / 0 / 391
Goodness-of-fit on F ²	0.913
Final R indices [I > 2σ(I)]	R ₁ = 0.0489, wR ₂ = 0.1163
R indices (all data)	R ₁ = 0.0618, wR ₂ = 0.1188
Extinction coefficient	0
Largest diff. peak and hole	0.264 and -0.289 e.Å ⁻³

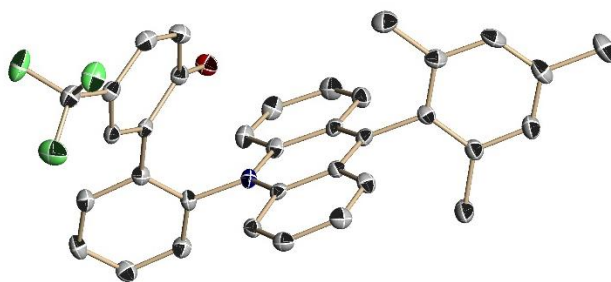
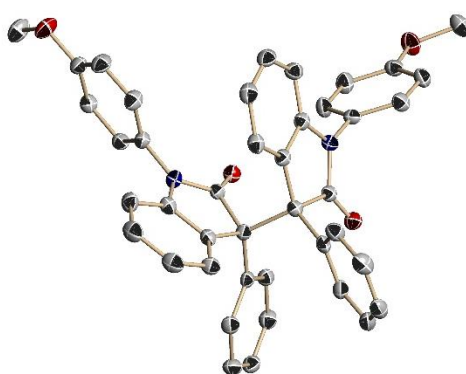
**Figure S9.** Molecular structure of **1**. The thermal ellipsoids of non-hydrogen atoms are shown at the 50% probability level. Calculated hydrogen atoms and solvent molecules were omitted for clarity. Gray: carbon, red: oxygen, blue: nitrogen, green: fluorine.

Table S2. Crystal data and structure refinement for **3a**.

Empirical formula	C ₄₉ H ₄₀ N ₂ O ₄	
Formula weight	720.83	
Temperature	123(2) K	
Wavelength	0.71075 Å	
Crystal system	Triclinic	
Space group	P-1	
Unit cell dimensions	a = 11.4060(15) Å	$\alpha = 89.519(6)^\circ$
	b = 12.0431(15) Å	$\beta = 88.399(6)^\circ$
	c = 13.804(2) Å	$\gamma = 75.619(6)^\circ$
Volume	1836.0(4) Å ³	
Z	2	
Density (calculated)	1.304 Mg/ m ³	
Absorption coefficient	0.083 mm ⁻¹	
F(000)	760	
Crystal size	0.250 x 0.150 x 0.050 mm ³	
Theta range for data collection	3.177 to 25.500°.	
Index ranges	-13<=h<=13, -14<=k<=14, -16<=l<=16	
Reflections collected	12883	
Independent reflections	6564 [R _{int} = 0.0245]	
Completeness to theta = 25.242°	96.1 %	
Absorption correction	Semi-empirical from equivalents	
Max. and min. transmission	1.000 and 0.870	
Refinement method	Full-matrix least-squares on F ²	
Data / restraints / parameters	6564 / 0 / 499	
Goodness-of-fit on F ²	1.079	
Final R indices [I>2sigma(I)]	R ₁ = 0.0376, wR ₂ = 0.1044	
R indices (all data)	R ₁ = 0.0458, wR ₂ = 0.1072	
Extinction coefficient	0	
Largest diff. peak and hole	0.297 and -0.240 e.Å ⁻³	

**Figure S10.** Molecular structure of **3a**. The thermal ellipsoids of non-hydrogen atoms are shown at the 50% probability level. Calculated hydrogen atoms and solvent molecules were omitted for clarity. Gray: carbon, red: oxygen, blue: nitrogen.

Reference and Note

- (1) (a) Ashby, E. C. *Acc. Chem. Res.* **1988**, *21*, 414. (b) Tuck, D. G. *Coord. Chem. Rev.* **1992**, *112*, 215. (c) Wakselman, C. J. *Fluorine Chem.* **1992**, *59*, 367. (d) Eisch, J. J. *Res. Chem. Intermed.* **1996**, *22*, 145. (e) Connelly, N. G.; Geiger, W. E. *Chem. Rev.* **1996**, *96*, 877. (f) Mikami, T.; Narasaka, K. In *Advances in Free Radical Chemistry*; Zard, S. Z., Ed.; JAI: Stamford, CT, 1999; Vol. 2, p 45. (g) Fokin, A. A.; Schreiner, P. R. *Chem. Rev.* **2002**, *102*, 1551. (h) Schreiner, P. R.; Fokin, A. A. *Chem. Rec.* **2004**, *3*, 247. (i) Rosen, B. M.; Percec, V. *Chem. Rev.* **2009**, *109*, 5069. (j) Szostak, M.; Spain, M.; Procter, D. J. *Chem. Soc. Rev.* **2013**, *42*, 9155. (k) Zhang, N.; Samanta, S. R.; Rosen, B. M.; Percec, V. *Chem. Rev.* **2014**, *114*, 5848. (l) Jia, X. *Synthesis* **2016**, *48*, 18. (m) Tellis, J. C.; Kelly, C. B.; Primer, D. N.; Jouffroy, M.; Patel, N. R.; Molander, G. A. *Acc. Chem. Res.* **2016**, *49*, 1429.
- (2) Shaw, M. H.; Twilton, J.; MacMillan, D. W. C. *J. Org. Chem.* **2016**, *81*, 6898.
- (3) For reviews on PCET, see: (a) Huynh, M. H. V.; Meyer, T. J. *Chem. Rev.* **2007**, *107*, 5004. (b) Weinberg, D. R.; Gagliardi, C. J.; Hull, J. F.; Murphy, C. F.; Kent, C. A.; Westlake, B. C.; Paul, A.; Ess, D. H.; McCafferty, D. G.; Meyer, T. J. *Chem. Rev.* **2012**, *112*, 4016. (c) Yayla, H. G.; Knowles, R. R. *Synlett* **2014**, *20*, 2819. (d) Gentry, E. C.; Knowles, R. R. *Acc. Chem. Res.* **2016**, *49*, 1546.
- (4) Godemert, J.; Oudeyer, S.; Levacher, V. *ChemCatChem* **2016**, *8*, 74.
- (5) (a) Uraguchi, D.; Koshimoto, K.; Ooi, T. *J. Am. Chem. Soc.* **2008**, *130*, 10878. (b) Uraguchi, D.; Koshimoto, K.; Ooi, T. *Chem. Commun.* **2010**, *46*, 300. (c) Uraguchi, D.; Koshimoto, K.; Sanada, C.; Ooi, T. *Tetrahedron: Asymmetry* **2010**, *21*, 1189. (d) Uraguchi, D.; Oyaizu, K.; Ooi, T. *Chem. Eur.-J.* **2012**, *18*, 8306. (e) Uraguchi, D.; Oyaizu, K.; Noguchi, H.; Ooi, T. *Chem. Asian-J.* **2015**, *10*, 334. (f) Oyaizu, K.; Uraguchi, D.; Ooi, T. *Chem. Commun.* **2015**, *51*, 4437. (g) Torii, M.; Kato, K.; Uraguchi, D.; T. Ooi, *Beilstein J. Org. Chem.* **2016**, *12*, 2099.
- (6) (a) Zhang, W.-Q.; Cheng, L.-F.; Yu, J.; Gong, L.-Z. *Angew. Chem. Int. Ed.* **2012**, *51*, 4085. (b) Claraz, A.; Landelle, G.; Oudeyer, S.; Levacher, V. *Eur. J. Org. Chem.* **2013**, 7693. (c) Zhou, X.; Wu, Y.; Deng, L. *J. Am. Chem. Soc.* **2016**, *138*, 12297.
- (7) (a) Wang, Y.-B.; Sun, D.-S.; Zhou, H.; Zhang, W.-Z.; Lu, X.-B. *Green Chem.* **2014**, *16*, 2266. (b) Tsutsumi, Y.; Yamakawa, K.; Yoshida, M.; Ema, T.; Sakai, T. *Org. Lett.* **2010**, *12*, 5728. (c) Guillerm, B.; Lemaury, V.; Cornil, J.; Lazzaroni, R.; Dubois, P.; Coulembier, O. *Chem. Commun.* **2014**, *50*, 10098.
- (8) (a) Uraguchi, D.; Koshimoto, K.; Miyake, S.; Ooi, T. *Angew. Chem. Int. Ed.* **2010**, *49*, 5567. (b) Uraguchi, D.; Koshimoto, K.; Ooi, T. *J. Am. Chem. Soc.* **2012**, *134*, 6972.
- (9) Satoh, N.; Fukuzumi, S. *Rev. Heteroatom Chem.* **1999**, *20*, 249.
- (10) Wilger, D. J.; Grandjean, J.-M. M.; Lammert, T. R.; Nicewicz, D. A. *Nat. Chem.* **2014**, *6*, 720.
- (11) See SI for experimental details.
- (12) (a) Yayla, H. G.; Wang, H.; Tarantino, K. T.; Orbe, H. S.; Knowles, R. R. *J. Am. Chem. Soc.* **2016**, *138*, 10794. (b) Gentry, E. C.; Knowles, R. R. *Acc. Chem. Res.* **2016**, *49*, 1546.
- (13) Gaussian 09, Revision D.01., Frisch, M. J. et al. Gaussian, Inc.: Wallingford, CT, 2013.
- (14) (a) Lee, H. J.; Lee, S.; Lim, J. W.; Nyoung, J. *Kim Bull. Korean Chem. Soc.* **2013**, *34*, 2446. (b) Ghosh, S.; Chaudhuri, S.; Bisai, A. *Org. Lett.* **2015**, *17*, 1373. (c) Jia, W.-L.; He, J.; Yang, J.-J.; Gao, X.-W.; Liu, Q.; Wu,

- L.-Z. *J. Org. Chem.* **2016**, *81*, 7172. (d) Sohtome, Y.; Sugawara, M.; Hashizume, D.; Hojo, D.; Sawamura, M.; Muranaka, A.; Uchiyama, M.; Sodeoka, M. *Heterocycles* **2017**, DOI: 10.3987/COM-16-S(S)75.
- (15) Because the initial rate of the reaction with 2 mol% of **1** was too fast for tracking by React-IR, the indicated ratio of the initial rate was calculated based on the comparison under the conditions with 0.5 mol% of catalyst loading.
- (16) The reaction rate under the influence of 6 mol% of KO^tBu was comparable to that of binary catalysis. This indicated that the enhancement in the enolate concentration did not lead to accelerate the generation of the radical enolate and subsequent carbon-carbon bond formation.
- (17) Matsubara, C.; Kawamoto, N.; Takamura, K. *Analyst* **1992**, *117*, 1781.
- (18) Yu, J.; Wang, Z.; Zhang, Y.; Su, W. *Tetrahedron* **2015**, *71*, 6116.
- (19) Although the transformation should be initiated from the benzylic radical generation, the detailed mechanism is unclear at present.
- (20) Natarajan, A.; Fan, Y.-H.; Chen, H.; Guo, Y.; Iyasere, J.; Harbinski, F.; Christ, W. J.; Aktas, H.; Halperin, J. A. *J. Med. Chem.* **2004**, *47*, 1882.
- (21) Taylor, A. M.; Altman, R. A.; Buchwald, S. L. *J. Am. Chem. Soc.* **2009**, *131*, 9900.
- (22) Manner, V. W.; DiPasquale, A. G.; Mayer, J. M. *J. Am. Chem. Soc.*, **2008**, *130*, 7210.
- (23) Kütt, A.; Leito, I.; Kaljurand, I.; Sooväli, L.; Vlasov, V. M.; Yagupolskii, L. M.; Koppel, I. A. *J. Org. Chem.* **2006**, *71*, 2829.
- (24) Kaljurand, I.; Kütt, A.; Sooväli, L.; Rodima, T.; Mäemets, V.; Leito, I.; Koppel, I. A. *J. Org. Chem.* **2005**, *70*, 1019.
- (25) Sheldrick, G. M. *Acta Cryst* **2015**, *C71*, 3.

Publication List

Chapter 2: Chiral Ammonium Betaine-Catalyzed Asymmetric Mannich-Type Reaction of Oxindoles

M. Torii, K. Kato, D. Uraguchi, T. Ooi, *Beilstein J. Org. Chem.* **2016**, *12*, 2099.

Chapter 3: Stereoselective Aza-Henry Reaction of 3-Nitro Dihydro-2(3H)-Quinolones with *N*-Boc Aldimines under the Catalysis of Chiral Ammonium Betaines

D. Uraguchi, M. Torii, K. Kato, T. Ooi, *Heterocycle* **2017**, *Accepted*.

Chapter 4: Acridinium Betaines as a Single-Electron-Transfer Catalyst: Molecular Design and Application to the Dimerization of Oxindoles

D. Uraguchi, M. Torii, T. Ooi, *ACS Catal.* **2017**, *Accepted*

Acknowledgements

The author would like to express the deepest appreciation to Professor Takashi Ooi at Nagoya University, for his invaluable guidance and hearty encouragement through the doctoral course research.

He is deeply grateful to my supervisor, Dr. Daisuke Uraguchi for my guidance, encouragement, and excellent discussion about my research.

He is particularly grateful for the assistance given by Dr. Kohsuke Ohmatsu, Dr. Yusuke Ueki, Dr. Tripathi, Chandra Bhushan, Dr. Makoto Sato and Dr. Yoshitaka Aramaki for their valuable discussion and practical advice.

Author would like to express his special thanks to Professor Hiroshi Shinokubo and Professor Yoshihiko Yamamoto for their helpful suggestions and discussion on my dissertation committee.

He would like to thank to Dr. Kenichiro Itami, Dr. Junichiro Yamaguchi and Dr. Kei Muto for advice and permission to use ReactIR for kinetic analysis.

He is particularly grateful for the assistance given by Dr. Junya Ohyama, Dr. Satoru Hiroto and Dr. Jun Kumagai for understanding reaction mechanism.

It is pleasure my appreciation to all colleagues, especially to Dr. Yuichiro Ando and Dr. Ken Yoshioka for his encouragement and discussion, and also to Dr. Kyohei Koshimoto, Dr. Keigo Oyaizu, Mr. Kohsuke Kato for their supports.

He would also like to express my gratitude to the Program for Leading Graduate Schools" Integrative Graduate Education and Research in Green Natural Sciences" and "CREST-JST" for my financial support

Finally, he would like to thank my family, Mr. Kazuyasu Torii, Mrs. Mieko Torii, Mrs. Setsuko Torii, Ms. Yuka Torii, Mr. Toshihiko Sugiura, and Mr. Kakuro Sugiura for their warm encouragement.

Masahiro Torii

Department of Applied Chemistry
Graduate School of Engineering
Nagoya University
2017